Hungarian Geographical Bulletin

Földrajzi Értesítő

Special issue:
Applied Urban Climate and Bioclimate

Edited by
János Unger

Volume 65 Number 2 2016

HAS
Research Centre for Astronomy and Earth Sciences
GEOGRAPHICAL INSTITUTE

HUNGARIAN GEOGRAPHICAL BULLETIN Volume 65 Number 2 2016

HUNGARIAN GEOGRAPHICAL BULLETIN 65 2016 (2)

CONTENT

Applied Urban Climate and Bioclimate

Studies

Book review

Guest editorial address

In the last decades urbanisation accelerated and reached enormous magnitude. The Earth's urban population grows faster than the total population, therefore, more and more people live in urbanised regions. Not only the large cities but also the smaller ones can modify almost all properties of the urban atmospheric environment compared to the natural surroundings. These changes are caused by the artificial building-up, as well as by the emission of heat, moisture and pollution related to human activities resulting changes in radiation, energy and momentum processes. As a result a local climate (*urban climate*) develops in the urbanised areas. The climate modification effect of cities occurs most notably in the temperature increase (*urban heat island*) which influences, on the one hand, the energy demand for heating in winter and air conditioning in summer, and on the other hand, it increases the thermal load of the city dwellers in varying degrees in time and space within the settlement. The heat island affects not only the quality of life and well-being (e.g. human comfort), but in many cases also the health conditions of people living in cities. This can be a problem especially as heat waves are becoming more and more frequent due to climate change.

This special issue of the Hungarian Geographical Bulletin provides some insights into the recent results of research groups of five Central European cities (Brno, Budapest, Cluj-Napoca, Novi Sad and Szeged) from four countries related to this large and diverse topic. Certain parts of their research were linked by joint projects (e.g. URBAN-PATH project – http://en.urban-path.hu/, Urban climate in Central European cities and global climate change project – http://www.klimat.geo.uj.edu.pl/urbanclimate/about.html). The apropos of this thematic issue is given to the session 'Applied urban climate and bioclimate' of the EUGEO-2015 congress in Budapest. The presented results of this session were largely derived from the above mentioned research groups (http://www.eugeo2015.com/sessions/session/3).

The focus of this special issue is the measurement/modelling of thermal patterns and human thermal sensation within urban environments. The first three papers deal with temperature measurements at districts and city scales. The next three ones contribute to our knowledge on human thermal comfort and radiation modification effects of urban environments. The last two studies present modelling tools that can be used to assess and compare the intra-urban thermal conditions both at present and in the future.

János Unger

DOI: 10.15201/hungeobull.65.2.1 Hungarian Geographical Bulletin 65 2016 (2) 93–103.

Analysis of the air temperature and relative humidity measurements in Budapest-Ferencváros

Rita PONGRÁCZ[1], Judit BARTHOLY, Zsuzsanna DEZSŐ and Csenge DIAN

Abstract

Ferencváros (9th district of Budapest) is one of the oldest districts among the 23 ones of the Hungarian capital. It is located near the river Danube in the southern central very heterogeneous part of the city, consisting of three- and four-storey old buildings, block houses with 4 or 8 levels, brownfield industrial areas, and large areas occupied by the railways system. Due to the functional and structural changes of special subsections of the district substantial local climatic changes occurred in the past few decades. The local government made efforts to complete several block rehabilitation programs already starting from the 1980s. Within the framework of these programs inner parts of the blocks were demolished, thus, inside the blocks more public green areas could be created. In order to evaluate the climatic conditions, we have recently initiated an *in situ* urban measurement program in the Inner Ferencváros and the rehabilitation zone. Air temperature and relative humidity where measured along a multi-site measuring path covering the target area, and continuously at a single site representative to the rehabilitation zone. Our measurements are compared to the regular meteorological data available from the Budapest-Pestszentlőrinc synoptic station. Our preliminary results are presented in this paper, which highlights the general characteristics of the urban environmental effects.

Keywords: block rehabilitation, in situ measurements, urban heat island, dew point temperature

Introduction

Concentrated human presence and the associated anthropogenic activities modify the natural environment in various ways. This cause several environmental and socio-economic issues, which should especially be assessed in large urban areas. Since more than half of the global population (and about 70% of the Hungarian population) is living in cities (United Nations, 2012; KSH 2012) these issues affect many people all over the world as well, as in Hungary. The artificial surface cover modifies the radiation budget resulting in higher urban temperature compared to the surrounding rural vicinity. Furthermore, the hydrological cycle is also modified in the urban environment through the lack of natural soil cover, which would serve as additional source of atmospheric humidity.

The complex environmental effect can be summarized as the urban heat island (UHI), which is usually characterized by the intensity, i.e., the temperature difference between the urban area and the rural surroundings. One approach to study the urban temperature surplus uses air temperature measured at regular meteorological stations or moving vehicles for the analysis of UHI (e.g. Oke, T.R. 1973; Unger, J. *et al.* 2000), whereas another approach applies surface temperature from satellite or aircraft measurements to analyse the surface UHI (e.g. Price, J.C. 1979; Pongrácz, R. *et al.* 2006; Ben-Dor, E. and Saaroni, H. 1997). Within the framework of the urban climate research at the Department of Meteorology of the Eötvös Loránd University surface UHI effects of several Hungarian and Central European cities have been analysed using remotely sensed

[1] Department of Meteorology, Eötvös Loránd University, H-1117 Budapest, Pázmány Péter sétány 1/a.
E-mails: prita@nimbus.elte.hu, bartholy@caesar.elte.hu, dezsozsuzsi@caesar.elte.hu, diancsenge@gmail.com

surface temperature (Dezső, Zs. *et al.* 2005, Pongrácz, R. *et al.* 2010, 2015).

In order to extend our research focus we have initiated a new ground-based measurement program in Budapest at a smaller spatial scale. To cover the entire 525 km^2 area of the capital city is too ambitious at this point, as a first step we started with one of the 23 districts. The selection of the target district was made according to several aspects: (i) the UHI impacts are significant, (ii) the area is heterogeneous, and (iii) the local government is interested in and willing to build a long-term research cooperation. Among the candidate districts, Ferencváros (the 9th district of Budapest) was finally selected due to the multi-decadal-long block rehabilitation programs supported by the local government.

The total population of Ferencváros is currently about 60,000 (Budapest Capital Local Government, 2011), and the spatial extension is 12.5 km^2, which indicate that this is a medium-size district. It is located at the eastern side along the river Danube, which divides the entire city and the downtown region into two parts. Ferencváros itself is a very heterogeneous part of the city with cultural centres, offices, residential, and industrial areas. The district consists of three- and four-storey old buildings, block houses with 4 or 8 levels, brown industrial areas, and large areas occupied by the railways system. The most inner city part is the Inner Ferencváros (*Figure 1*),

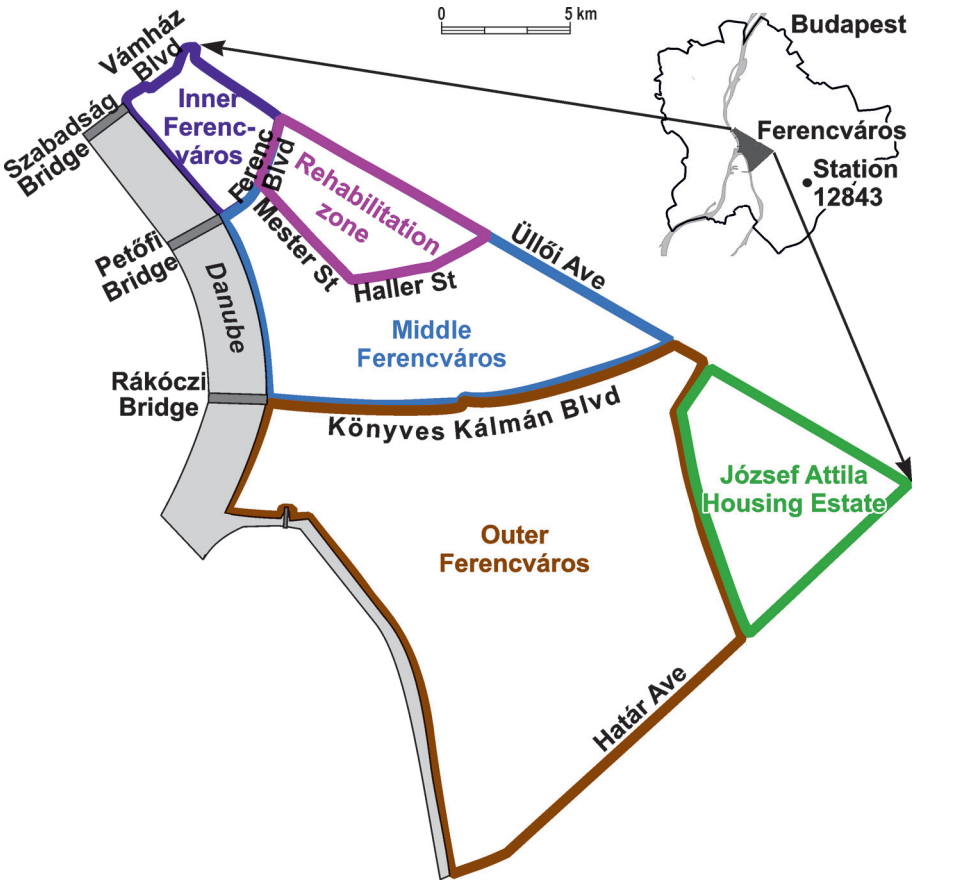

Fig. 1. Location and structure of Ferencváros within Budapest, and location of the reference synoptic station no. 12843 at Pestszentlőrinc, south-eastern part of the city

where mostly offices and multi-residential houses can be found. The past and present (though very decreased) industrial activity is concentrated in the Outer Ferencváros subsection. Residential block houses form the József Attila housing estate, which became quite friendly and green recently. Although this is one of the oldest housung estate of Budapest built in the 1970s, however, the trees planted several decades ago have grown and provide nice environmental conditions to this part of the district.

Partly due to the functional and structural changes of special subsections of the district substantial local climatic changes occurred in the past few decades. The local government made concentrated efforts to improve the environment for the citizens starting from the 1980s. Since 1993 in the most densely built inner part of the district (Inner and Central Ferencváros) entire blocks were renovated and modified. Within the framework of block rehabilitation programs inner parts of the blocks were demolished, thus, inside the renewed blocks more common green spaces could be created. Moreover, several parks have been enlarged, and small green areas have been created along the streets (Local Government of Ferencváros, 2010). The overall increase both in terms of number and spatial extension of green areas is illustrated in *Figure 2*.

In order to describe the climatic conditions of the district, with special focus on the rehabilitation zone, *in situ* measurement program has been introduced. This program consists of two types of measurements: (i) series of measurements in several sites along a predefined path, and (ii) continuous measurements at a single site. For comparison, measurements at another site in Budapest (synoptic station no. 12843 at Pestszentlőrinc) are used. In this study, details of the measurement program are discussed together with preliminary results for both types of measurements. Then, the main conclusions are summarized at the end of the paper.

Measurements along the predefined measuring path

In our urban climate measurement program in the rehabilitation zone of Ferencváros, air temperature and relative humidity are recorded with two Voltcraft HT-200 instruments along a predefined path consisting of 22 measuring points (*Figure 3, Table 1*), which covers the target area.

The measuring sites are selected at different representative points of the district, such as green parks (*Photo 1*), narrow streets,

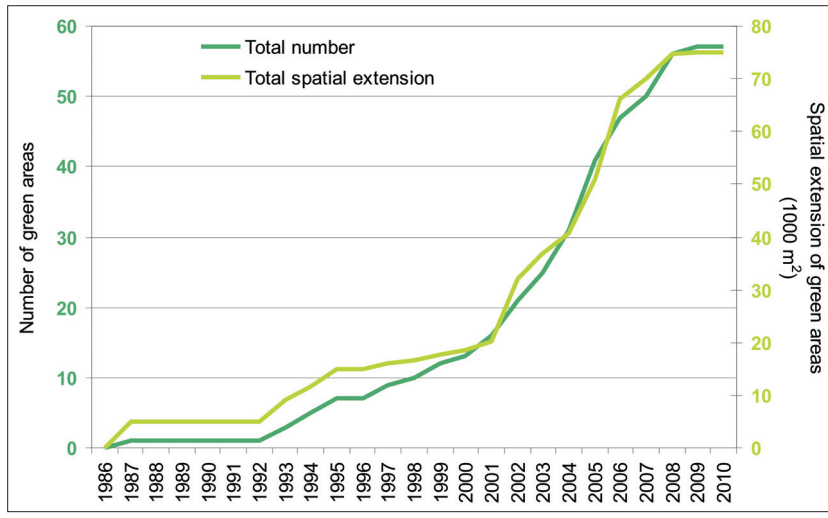

Fig. 2. Increase of the green areas in Budapest-Ferencváros

Fig. 3. Measuring points along the predefined path. Locations of measuring sites are listed in *Table 1.*

Table 1. Location of the measuring sites along the predefined path

Site number: location along the	
northwestern	southeastern
part of the predefined path	
201: Ferenc bld. / Tompa st.	101: Ferenc bld. / Tompa st.
202: Bakáts sq. / Tompa st.	102: Tompa st. / Liliom st.
203: Bakáts sq. / Ráday st.	103: Liliom st. / Tűzoltó st.
204: Ráday st. 42	104: Tűzoltó st. / Bokréta st.
205: Ráday st. / Biblia st.	105: Ferenc sq.
206: Ráday/Erkel st.	106: Balázs Béla st. / Thaly Kálmán st.
207: Kálvin sq.	107: University building (SOTE)
208: Lónyay st. / Gönczy Pál st.	108: Kerekerdő Park
209: Csarnok sq.	109: Márton st./ Gát st.
210: Building Bálna	110: Mester st. /Viola st.
211: Nehru Park	111: Mester st. / Tinódi st.
212: Boráros sq.	112: Boráros sq.

paved squares and roads (*Photo 2*). The whole measuring path is divided into two parts, where the measurements are recorded simultaneously: (i) from 101 to 112, and (ii) from 201 to 212.

The starting and ending sites are identical, i.e. 101 is identical to 201, and 112 is 212. These simultaneous walking tours last about 1–1.5 hours. Then, the measurements are recorded along the same two paths but in

Photo 1 and 2. Measuring sites with completely different surface cover: vegetation cover at Nehru Park (211) (above) and paved cover at Boráros square (112 = 212) (below). Measuring points are indicated by yellow circles

reverse order (i.e. starting from 112/212, and ending at 101/201). Evidently, the measurements cannot be recorded at the same time. Therefore, in order to temporally adjust the measurements, two records from the consequent (and reversed) partial paths are averaged over each site.

This procedure results in average values representative for a virtual time along the whole path. More precisely, since the moving speeds between sites and the distances between sites are not perfectly identical, this virtual time is given as a 10–20 minute time period. For calculating the UHI intensity, temperature measurements are compared to the hourly recorded data of the Budapest synoptic station (ID number: 12843) located in the south-eastern suburb district of the city (Pestszentlőrinc). Similarly, difference between dew point temperature values derived from relative humidity measurements are calculated and analysed.

The measurement program started in early spring of 2015, the measuring dates are listed in *Table 2*. The measurements are scheduled once a week (on Friday), from about noon until the late evening. The on going measurement program involves BSc students specialized in Earth sciences and MSc students specialized in meteorology, therefore, 8 dates were completed in the spring semester of 2015, and another 8 dates in the autumn semester of 2015. During the summer three consecutive days were selected for the measurement program in early July, and the last Friday of August. We are planning to extend further the measurement program at the study area and complete several years of measurements, so the seasonal cycle of temperature and relative humidity differences can be analysed as well, as the inter-annual variability and changes.

Table 2. Measuring dates during 2015

Spring	Summer	Autumn
20 March	6 July	18 September
27 March	7 July	2 October
3 April	8 July	9 October
10 April	28 August	6 November
17 April	–	13 November
24 April	–	20 November
8 May	–	27 November
15 May	–	4 December

Results from the measurements along the predefined measuring path

Since UHI together with a heat-wave results in excessive heat stress for humans, and thus, significant health consequences, measurements on one of the heat-wave days (i.e. 7 July) occurred in the summer 2015 are discussed in this paper. The entire heat-wave period in the Carpathian Basin was dominated by a strong anticyclone over Central/Eastern Europe with clear sky conditions. The averaged air temperature values and the differences compared to the reference station throughout the day – starting from about 14:00 to 21:00 – are shown in *Figure 4*.

The warmest site was the Boráros square (site no. 112 = 212), which is a large paved square near the river Danube with main stations of the public transportation system and partially surrounded by four-storey buildings (*Photo 2*). The recorded temperature exceeded 38 °C between 14:00 and 16:30. The coolest sites were the greener spaces (i.e. park along the Danube, site no. 211; park in the rehabilitation zone, site no. 105). Towards the evening (starting around 17:30) the cooling rate until the end of the measurements (around 21:00) at all the measuring sites was about 1.5–2.0 °C/h. However, the air temperature remained above 30 °C. As far as the UHI intensity, the largest values occurred at the largely paved Boráros square (112 = 212). The largest temperature difference between our measurements and the reference station exceeded 4 °C.

Similarly to the air temperature, the results of the dew point temperature are shown in *Figure 5.* Dew point temperature values recorded in the afternoon were generally lower than dew point temperature in the evening. The difference relative to the synoptic station decreased from about 3–5 °C (at about 14:00) to about 1–2 °C (by about 21:00).

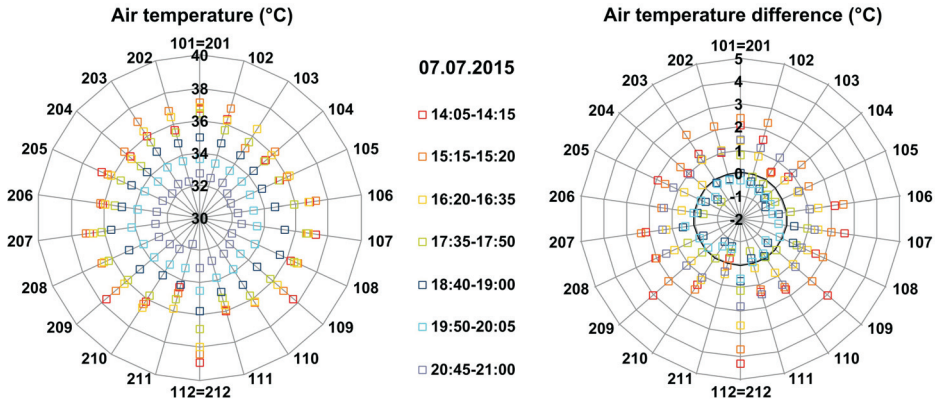

Fig. 4. Averaged temperature and UHI intensity values along the measuring path during the 7 measuring periods, 7 July 2015

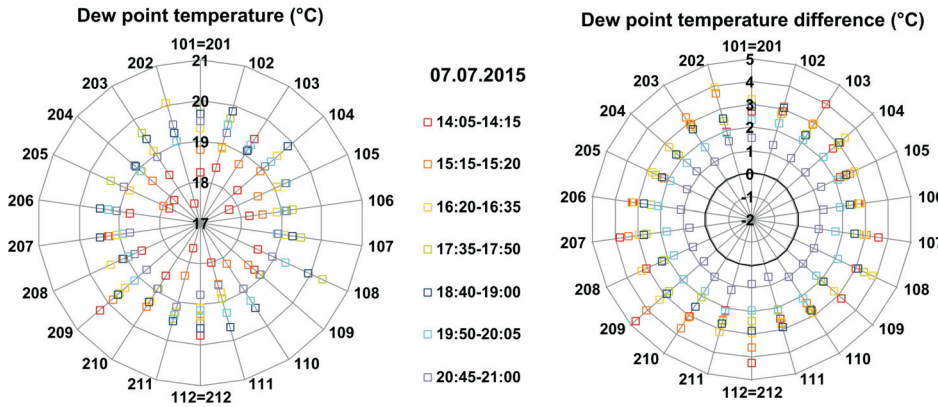

Fig. 5. Averaged dew point temperature values and the difference from the Budapest-Pestszentlőrinc synoptic station along the measuring path during the 7 measuring periods, 7 July 2015

In order to visualise the relationship between the air temperature and dew point temperature differences, the values for the individual sites shown in *Figures 4* and *5* are averaged and plotted in *Figure 6*. It can be clearly seen that the UHI intensity values between 17:30 and 20:00 were quite low, close to zero. This implies that the suburban temperature and the inner-city temperature did not differ significantly in the late afternoon before sunset. Since the last measuring period was already after the sunset (at 20:44), the well-known increase of UHI intensity after the evening (e.g. Oke, T.R. 1982) was clearly detected in our measurements.

The detected higher UHI intensity values in the afternoon period are probably associated with the faster temperature increase of the target urban area compared to the suburban reference station, which is later compensated by the temperature change in the suburban area becoming more similar to the more densely built-up part of the city. Then, in the evening around sunset the suburban area cooled down faster, and the second maximum occurred. Similar results were shown

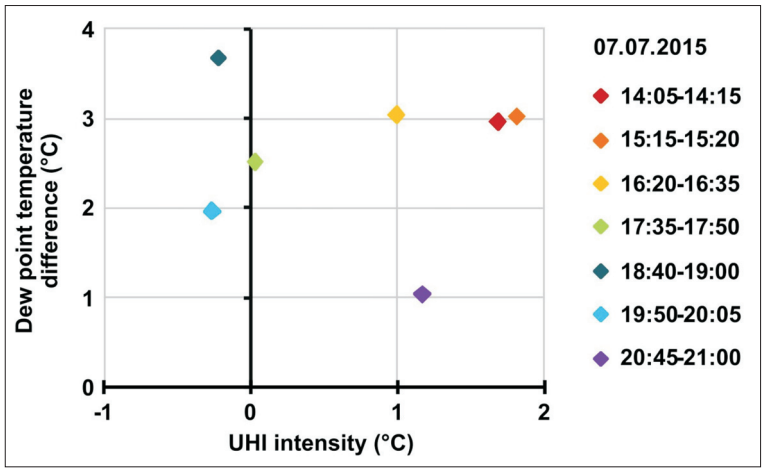

Fig. 6. Relationship between the averaged UHI intensity values and dew point temperature differences relative to Budapest-Pestszentlőrinc synoptic station data during the 7 measuring periods, 7 July 2015 (sunset occurred at 20:44)

for the Polish city Poznań (Półrolniczak, M. *et al.* 2015). However, in order to fully justify the above explanation, longer measurements are needed in Budapest as well, possibly throughout entire 24-hour periods. This is why we are planning to extend our measuring period.

Continuous measurements at a single site

In addition to the moving measurements, air temperature and relative humidity values have been recorded at a permanent site, which is one of the measuring sites along the predefined path, no. 105 located at the Ferenc square *(Photo 3).*

This location has been selected due to its central location within the rehabilitation zone of the district and, moreover, it can be considered as a representative site to the results of the rehabilitation process. The square is surrounded by 4-level houses, and it is covered mainly by vegetation with some paved footpaths for pedestrians. The investigated vegetation consists of several deciduous trees and bushes, and grass can be found on the ground.

For the air temperature measurements Voltcraft DL-141TH is used with 10 minutes recording intervals starting around midday until the evening on the days listed in *Table 2*. These measurements are compared to the regular meteorological measurements recorded at the Budapest synoptic station located at the south-eastern part of the city as a reference (see *Figure 1*).

Results from the measurements at Ferenc square

Among the completed 20 days of our measurement program, 3 summer days are selected here for detailed analysis. Measurements on the third summer day (8 July) were interrupted by a very intense frontal activity with severe thunderstorm and huge amount of precipitation (including hails). Therefore, the previous two heat-wave days (6 and 7 July) are shown together with the warm day at the end of summer (28 August). The day-time temperature at the Ferenc square exceeded 30 °C on all the three days, the heat-wave days were certainly 3–4 °C warmer than the late August day. The maximum measured

Photo 3. Measuring site with continuous recording at Ferenc square (site no. 105)

temperature values are as follows: 37.7 °C, 38.5 °C, and 35.8 °C on 6 July, 7 July, and 28 August, respectively (*Figure 7*).

These warmest periods of the days were measured between 16:30 and 16:50. The overall daily courses of the temperature values are generally similar on the measuring days with the maximum between 16:00 and 17:00. After about 18:00 the measured temperature started to decrease. The temperature difference between the two sites decreased to 0.5–1.5 °C by the time before the sunset, which is probably due to the different speed of temperature change in the central and the outer city areas. Similar results were found for Poznań by Półrolniczak, M. *et al.* (2015). Then, after the sunset temperature difference started to increase again, whereas the measured temperature continued to decrease. The temperature decrease was slower at Ferenc square, in the more densely built-up region of the city than at the suburban reference station resulting in higher UHI intensity values at the late evening.

The temperature difference between Ferenc square and the synoptic reference station was generally larger at the end of August compared to the heat-wave days in early July, which is partly due to the fact that during the heat-wave, all sites are very warm resulting in smaller overall differences.

In order to fully detect the UHI effect and characteristics longer (at least 4–5 hours longer) measurements would be necessary. We plan to extend the measuring period in the summer of 2016.

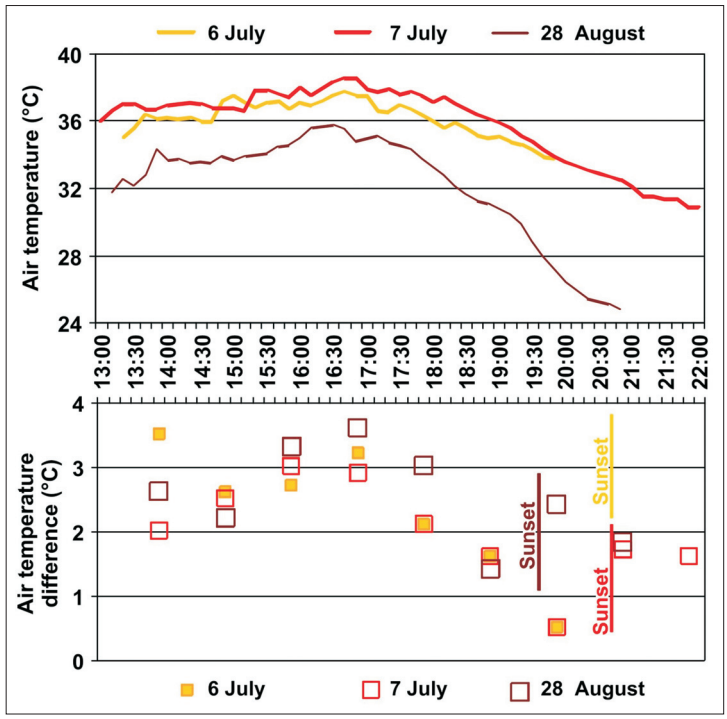

Fig. 7. Recorded air temperature at site no. 105 and the difference from the measurements at the Budapest-Pestszentlőrinc synoptic station on the summer days in 2015. (Times of the sunset are indicated by vertical lines at 20:44, 20:44, and 19:34 on 6 July, 7 July, and 28 August, respectively.

Conclusions

A new *in situ* measurement program has been initiated at the Department of Meteorology of the Eötvös Loránd University. This program has been designed to extend our previous research focus from satellite-based measurements. As a first step we concentrate on a smaller area of the Ferencváros district in Budapest. Since March 2015 air temperature and relative humidity measurements have been regularly recorded along a multi-site path consisting of 22 measuring sites, and at a single measuring site in a representative vegetation covered square within the block rehabilitation zone and the Inner Ferencváros. The measurements available altogether from 20 days (spring, summer and autumn 2015) have been compared to the standard meteorological data from the synoptic station no. 12843 (Budapest-Pestszentlőrinc located at the south-eastern part of the city). Our preliminary results highlight the general characteristics of the UHI effect.

The measurement program has just started, and we are planning to continue throughout 2016 and beyond in order to build year-round datasets for analyzing the seasonal cycle of temperature and relative humidity differences as well, as the diurnal changes and the spatial structure within the study area.

***Acknowledgements*:** The measurements were carried out by involving MSc and BSc students at the Department of Meteorology. Research leading to this paper has been supported by the following sources: Hungarian Scientific Research Fund under grants K-78125, K-83909, K109109, the AGRÁRKLIMA2 project (VKSZ_12-1-2013-0034), and the Bolyai János Fellowship of the Hungarian Academy of Sciences.

REFERENCES

Ben-Dor, E. and Saaroni, H. 1997. Airborne video thermal radiometry as a tool for monitoring microscale scructures of the urban heat island. *International Journal of Remote Sensing* 18. 3039–3053.

Budapest Capital Local Government 2011. *Urban development strategy of Budapest*. Budapest, 287 p. (in Hungarian).

Dezső, Zs., Bartholy, J. and Pongrácz, R. 2005. Satellite-based analysis of the urban heat island effect. *Időjárás – Quarterly Journal of the Hungarian Meteorological Service* 109. 217–232.

KSH 2012. *STADAT Database*. Central Statistical Office, Budapest. http://www.ksh.hu/stadat

Local Government of Ferencváros 2010. *Rehabilitation of Budapest Ferencváros*. Budapest. 80 p.

Oke, T.R. 1973. City size and the urban heat island. *Atmospheric Environment* 7. 769–779.

Oke, T.R. 1982. The energetic basis of the urban heat island. *Quarterly Journal of the Royal Meteorological Society* 108. 1–24.

Półrolniczak, M., Kolendowicz, L., Majkowska, A. and Czernecki, B. 2015. The influence of atmospheric circulation on the intensity of urban heat island and urban cold island in Poznań, Poland. *Theoretical and Applied Climatology*, DOI: 10.1007/s00704-015-1654-0

Pongrácz, R., Bartholy, J. and Dezső, Zs. 2006. Remotely sensed thermal information applied to urban climate analysis. *Advances in Space Research* 37. 2191–2196.

Pongrácz, R., Bartholy, J. and Dezső, Zs. 2010. Application of remotely sensed thermal information to urban climatology of Central European cities. *Physics and Chemistry of the Earth* 35. 95–99.

Pongrácz, R., Bartholy, J., Dezső, Zs. and Dian, Cs. 2015. Analysing the climatic effects of local block rehabilitation programs in Budapest-Ferencváros. *Proceedings of the 9th International Conference on Urban Climate (ICUC9)*, Toulouse, France. 20–24 July 2015. Extended abstract, 6 p.

Price, J.C. 1979. Assessment of the heat island effect through the use of satellite data. *Monthly Weather Review* 107. 1554–1557.

Unger, J., Bottyán, Zs., Sümeghy, Z. and Gulyás, Á. 2000. Urban heat island development affected by urban surface factors. *Időjárás – Quarterly Journal of the Hungarian Meteorological Service* 104. 253–268.

United Nations 2012. *World Urbanization Prospects: The 2011 Revision*. United Nations Population Division, Department of Economic and Social Affairs, http://esa.un.org/unup/index.html

Minsk and Budapest, the two capital cities

Edited by

László Jeney and Dávid Karácsonyi

Department of Economic Geography and Futures Studies, Corvinus University of Budapest; Geographical Institute RCAES MTA; Faculty of Geography, Belarusian State University; Institute for Nature Management, National Academy of Sciences of Belarus

Budapest, 2015. 194 p.

While Budapest used to be the bridge between the West and East in Central Europe, Minsk seems to be in a similar role between the Russian and the EU–Polish influence zones. It means that both capitals are situated on the frontiers between the Euro-Atlantic and the Euro-Asian macro regions. Besides their situations, their similarity in size renders the comparison and the cooperation obvious to proceed. This book is based on the mutual co-operation of Hungarian and Belarussian geographers and gives a scientific outlook not only on the socio-economic development of the two cities but on the urban climate, environment and ecology as well. Hungarian authors of the book introduce Budapest as a Central European metropolis with its historical trajectories and the results of the post-socialist transformation. They also demonstrate the main features of large housing estates and the results of their rehabilitation. Authors from Belarus show the major issues of spatial structure planning of Minsk in a similar context, describing the past and the present changes taking place in the spatial structure of the metropolis. The integrated assessment of the state of urban environment in Minsk is examined also focusing on the ecological frame of the environmental planning in urban agglomerations. The volume serves as a good starting point of a fruitful co-operation between Belarussian and Hungarian geographers dealing with a social and physical urban environment, the state of which deserves extra attention especially in East Central and Eastern Europe.

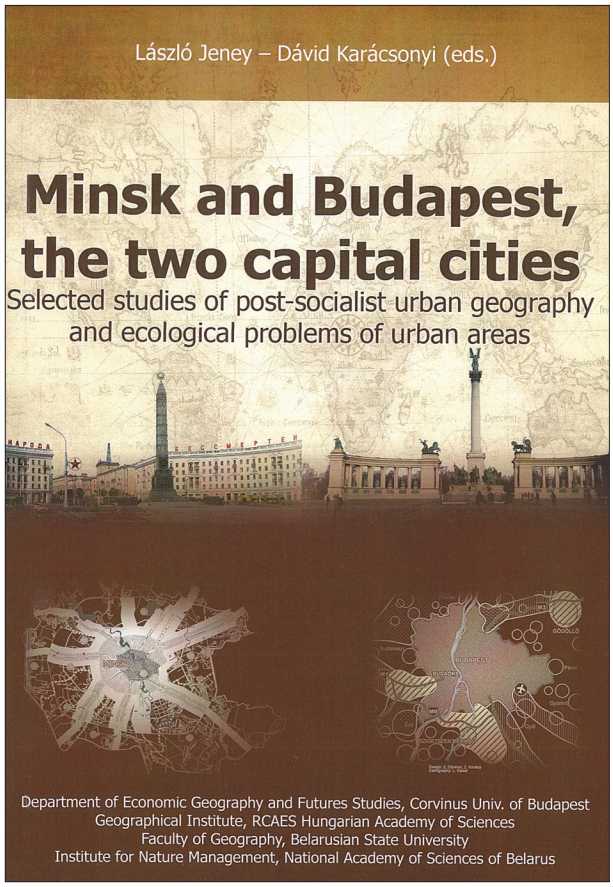

Copies are available:
Library, Geographical Institute of RCAES MTA, H-1112 Budapest, Budaörsi u. 44.
E-mail: magyar.arpad@csfk.mta.hu

DOI: 10.15201/hungeobull.65.2.2 Hungarian Geographical Bulletin 65 2016 (2) 105–116.

Urban heat island patterns and their dynamics based on an urban climate measurement network

Tamás GÁL, Nóra SKARBIT and János UNGER[1]

Abstract

In this paper the spatial pattern of Urban Heat Island (UHI) and its dynamical background are analysed. Furthermore, we examined the annual, seasonal and diurnal characteristics of UHI according to the Local Climate Zones (LCZs). The analysis was performed using one year (between June 2014 and May 2015) dataset from the measurement network of Szeged (Hungary). This network consists of 24 stations measuring air temperature and relative humidity. In the installation of the network the representativeness played an important role in order to that the stations represents their LCZs. We examined the thermal reactions during average and ideal conditions using the so-called weather factor. Our results show that the UHI is stronger in the compactly built zones and there are great differences between the zones. The greatest values appear in summer, while the difference is small in winter. The UHI starts to develop at sunset and exists through approximately 9–10 hours and differences are about 2 °C larger in case of ideal days, when the conditions (wind, cloud cover) are appropriate to the strong development of the UHI. The cooling rates show that the first few hours after sunset are determinative for the developing of UHI. In addition, the effect of UHI on annual mean temperature is also significant.

Keywords: measurement network, Szeged, Urban Heat Island, Local Climate Zones, cooling rate

Introduction

High number of people lives in urban environments. These areas have a specific landscape and their complex surface results characteristic climate modifications. Within these modified climate the excess urban heat in the middle latitudes has primarily economic and health risk. This thermal modification nowadays has been recognized noticeably by the citizens, especially during heat waves, but, generally, it is connected with the climate change. It is not a question that the studies evaluating the global scale changes causing higher frequency of heat waves are important, but analyzing the climatic effect of the urban areas is as important.

The urban climate is defined as a local climate that is modified by the interactions between built-up area and regional climate (World Meteorological Organization 1983). In this context, the elevated urban temperature (urban heat island, UHI) and its magnitude (UHI intensity) is defined as the temperature difference between rural and urban measurement sites.

The most reliable way to study the urban climate is the evaluation of urban scale measurements. There are several examples for this kind of measurements, but the problem is the findings of these studies are hard to adapt to different cities with different size, built-up characteristics and climatic background. To solve this discrepancy Stewart, I.D. and Oke, T.R. (2012) developed the Local Climate Zone (LCZ) system which is a climate-based classification of the surroundings of the urban and rural measuring sites which is applicable universally and relatively easily to local temperature studies using screen-level observations. Usage of this classification can help to

[1] Department of Climatology and Landscape Ecology, University of Szeged. H-6722 Szeged, Egyetem u. 2. E-mails: tgal@geo.u-szeged.hu, skarbitn@geo.u-szeged.hu, unger@geo.u-szeged.hu

generalise the obtained results and it helps to adapt and compare the results to other but urban areas with similar features.

In this study, we present the results of an urban measurement network which was deployed using the concept of the Local Climate Zones, in order to reveal the differences in the thermal reactions of these different general zones. In addition, the novelty of this network representing the different LCZs is the high temporal and spatial resolution. Furthermore, the obtained data give the opportunity to analyse the temporal dynamics and spatial patterns of UHI.

Aims of this study are (i) to present briefly this measurement network, (ii) to evaluate some data of its first operational year in order to investigate the thermal reactions of different LCZs in annual, seasonal and daily timescale, and (iii) to analyze the spatial pattern and temporal dynamics of the UHI and nocturnal cooling rate. Also an important question is (iv) the magnitude of the urban effects for the mean annual temperature of the study area.

Study area and measurement network

Szeged is a medium sized city with a population of approximately 170,000. It is located at a nearly flat terrain in the south-eastern part of Hungary as part of the Great Hungarian Plain. Szeged is divided into two parts by the Tisza River. As far as the climate of Szeged is concerned it is in the Cfb climate type according to Köppen climate classification system (Kottek, M. *et al.* 2006). The city centre is densely built-up, the northern part consist of mostly 5–10 storey residential buildings and family houses are located at the outskirts (Unger, J. *et al.* 2001).

An automatic GIS-method was used to determine the existing LCZs and their extensions in the study area (Lelovics, E. *et al.* 2014). According to this method seven built-up LCZs can be found in and around Szeged and our study area covers six of them (*Figure 1*). The compact zones (LCZs 2 and 3) are found in the downtown, while the open and large low-rise and sparsely built zones are mainly in the outskirts. However, the open midrise zone appears in the centre and in the north-northeast parts of the city too.

A monitoring network was established in Szeged within the framework of an EU project (URBAN-PATH 2016). 24 stations were installed measuring air temperature and relative humidity. The locations of the stations are selected to fulfil two criteria: (I) stations have to be representative for the LCZs within the city, (II) spatial pattern of the network have to be capable to reveal the spatial structure of the UHI. The location process is presented by Lelovics, E. *et al.* (2014) and Unger, J. *et al.* (2015).

The purpose of this network was the examination of excess heat and its intra-urban patterns in the city with appropriate spatial and temporal resolution. The spatial resolution ensures the accurate differences between the particular neighbourhoods, while the temporal resolution provides appropriate dataset for diurnal analysis. From the processed data graphs and high-resolution maps where drawn and presented on the Internet and a public screen thus useful information is provided for the general public (Unger, J. *et al.* 2015).

The data are provided by a Sensirion SHT25 sensor in a radiation protection screen (220 x 310 mm) at the end of a 60 cm console (*Photos 1–3*). The shield is the same as the model used by the Hungarian Meteorological Service (HMS). The accuracy of the sensor is 0.4 °C and 3% for the temperature and humidity, respectively.

The consoles are mounted on lamp posts at a height of 4 m above the ground for security reasons. As the air in the urban canyon is well-mixed, the temperature measured at this height is representative for the lower air layers too (Nakamura, Y. and Oke, T.R. 1988). The stations send the readings to a server in every 10 minute, so this database can be a basis of further analysis with 10 minute time resolution. For further technical details about the sensors, logging, transmission, and online displaying of the data see Unger, J. *et al.* (2015).

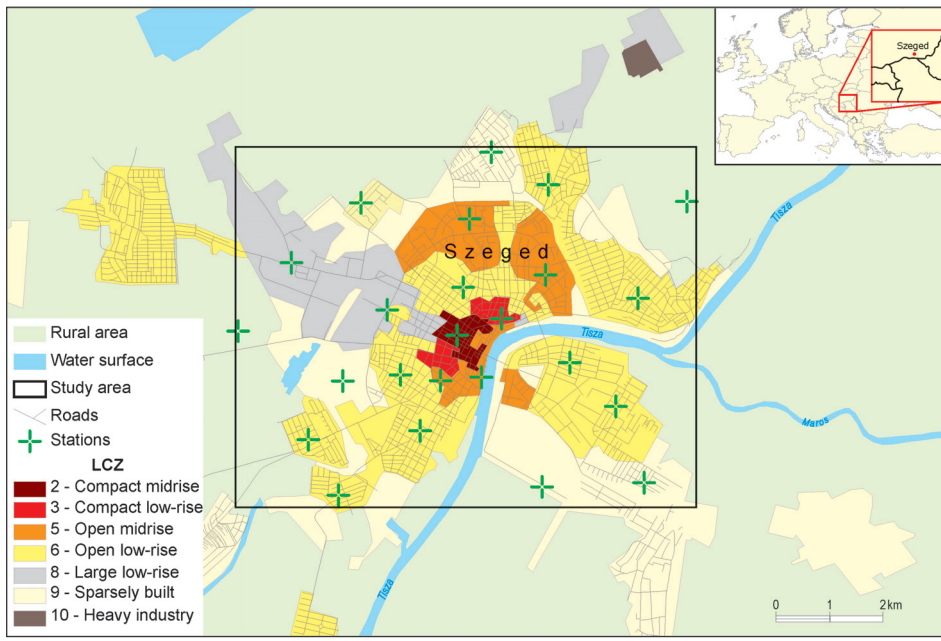

Fig. 1. LCZ map and station locations of the urban monitoring network in Szeged

The extent of the study area is determined by the locations of stations and it covers an 8.6 km x 6.7 km rectangle (see *Figure 1*). For this study we used a one-year period (from June 1, 2014 to May 31, 2015) temperature dataset of the monitoring network.

For the analysis spatial and temporal mean values were calculated in order to represent the different aspects of UHI. In case of spatial mean values the stations data within a given LCZ type were averaged. By temporal aspect first we calculated the sunset in each day. Time of sunset assigned as the beginning of a relative timescale, and using it we calculated the hourly mean temperature for each station. In this timescale 0 hour is the time of sunset, negative and positive hours are before and after the sunset, respectively. Using this approach the long term (seasonal, yearly) mean temperature or UHI intensity development as a result of cooling process can be calculated and compared as the effect of the different time of sunset is filtered out.

For evaluation of UHI and nocturnal cooling a selection of days with ideal conditions is helpful. Ideal weather conditions help to reveal the urban effect on the thermal environment. The selection of the ideal days is based on the weather factor, Φ_w (Oke, T.R. 1998) which is calculated as:

$$\Phi_w = u^{-\frac{1}{2}} (1–kn^2),$$

where u is the wind speed (m/s), k is the Bolz correction factor for cloud height (Bolz, H.M. 1949), n is the cloud amount in tenths. In our case, the Φ_w values calculated for one-hour intervals using the data from the HMS (Hungarian Meteorological Service) station in Szeged. The obtained values were averaged from sunrise to the next sunrise (about 24 hours) as the weather conditions in daylight hours prior to the night and during the night affect mostly the nocturnal air temperature differences above the varied surfaces.

In order to isolate the very specific weather conditions that promote microclimate formation the days with average $\Phi_w > 0.7$ were regarded as ideal days, similar to Stewart, I.D. *et al.* (2014).

Photos 1–3. Typical setup of monitoring stations

Results

Annual, seasonal and diurnal characteristics of UHI

Figure 2 presents the annual and seasonal mean maximum nocturnal temperature differences from station HMS in each LCZ zone. It can be generally established that the highest values appear in summer except in LCZ 9 and are followed by the values of spring. The second lowest temperature differences are in autumn and the smallest values can be found in the winter season. The average annual differences are between the means of spring and autumn.

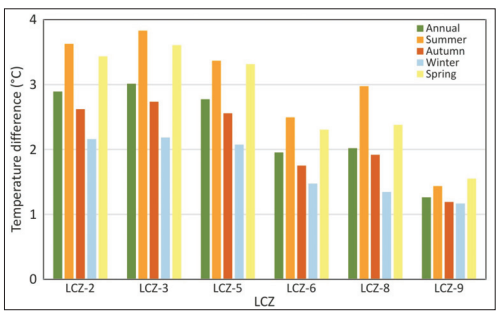

Fig. 2. Annual and seasonal mean maximum nocturnal temperature differences from HMS station by LCZ types (Szeged, June 2014 – May 2015)

If we see the differences among the LCZs the sequence is the same in each season and also annually except from a small deviation. The highest values are in the compact zones and among them the LCZ 3 has the larger differences. In this compact midrise zone, the maximum value is 3.8 °C, while the minimum is 2.2 °C. In LCZ 2 the minimum value is the same, but the maximum is lower by 0.2 °C. They are followed by LCZ 5, where the values range from 2.1 °C to 3.4 °C. In case of winter, LCZ 6 is the next warmest zone, which is followed by LCZ 8. In the other seasons and annual basis, LCZ 6 follows LCZ 8. The maximum value in LCZ 8 is 3.0 °C and the minimum is 1.3 °C, while for LCZ 6 there are 2.5 °C and 1.5 °C, respectively. The minimal temperature differences are in LCZ 9 in every case and they range from 1.2 °C to 1.6 °C.

Investigating the extent of the difference among the zones the biggest deviation, namely, the difference occurs between LCZs 3 and 9: it is approximately 2.4 °C is in summer and 2.1 °C for spring. They are followed by the annual value of 1.8 °C and the smallest differences are in autumn (1.5 °C) and in winter (1.0 °C).

On ideal days, the annual and seasonal mean maximum nocturnal temperature differences from the HMS station in each LCZ zone are presented in *Figure 3*. In this case, the summer values are not the highest in each case. In LCZs 3, 5 and 9 the values of autumn are higher and in LCZ 8 the spring value exceeds both of them. The winter season shows the minimal values except for LCZ 9, where the average spring temperature difference is only 0.1 °C. The annual values follow the summer and autumn differences aside from LCZ 8, where the spring season exceeds it too.

Aside from summer and spring, the maximum differences appear in LCZ 3. In this zone the values range from 3.3 °C to 4.7 °C. In summer and spring, LCZ 2 has larger values, where the maximum is 4.8 °C and the minimum is 3.3 °C. In autumn the second warmest zone is LCZ 5 instead of LCZ 2, while in the other periods it is on the third place. In this zone, the values range from 3.2 °C to 4.7 °C. The sequence of the other zones is the same in every season and annually. The next is the large low-rise zone with values between 2.0 °C and 3.4 °C. It is followed by LCZ 6, where the maximum is 2.9 °C and the minimum is 1.9 °C. As expected, the minimal temperature differences are in LCZ 9 where the values range from 0.1 °C to 1.4 °C. Because of the low values in LCZ 9 the differences between the zones is the highest in spring when the deviation approaches 4.2 °C. The second biggest deviation appears in summer with a value of 3.6 °C. It is followed by the annual (3.4 °C) and autumn (3.3 °C) differences, which are almost the same. The smallest difference is in winter (approximately 2 °C).

In *Figure 4*, the combined annual and diurnal variations of average temperature difference of LCZs from station HMS are presented. The separation of the nocturnal and daily hours and the seasonal changes are obvious and clearly seen except LCZ 9, where the differences are small and there is no unequivocal tendency. This separation is the most noticeable in case of the compact zones and open midrise zone and becomes less characteristic in LCZ 6 and 8.

In the compact zones a much more characteristic temperature difference develops in summer than in the other zones. The difference is around 4–6 °C and it exists through several days. In case of LCZ 9, there is no clear tendency of temperature, so this built-up type affects the temperature in the least.

Other important phenomenon the urban cool island also appears in *Figure 4*. At daytime in all seasons except winter the urban built-up types have lower temperatures than the rural ones as the daytime warming is slower because of the shading effect of buildings. This cool island effect clearly observable in types with dense built-up characteristics (LCZs 2, 3, 5) and less obvious in the case of large low-rise and almost completely disappears in case of LCZs 6 and 9.

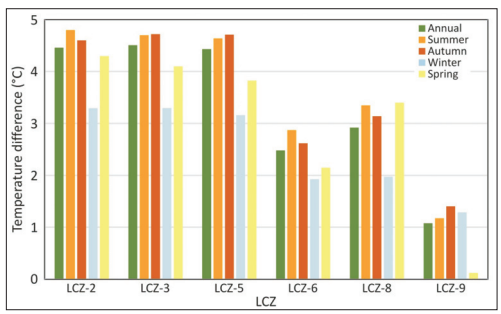

Fig. 3. Annual and seasonal mean maximum nocturnal temperature differences from HMS station by LCZ types on ideal days (Szeged, June 2014 – May 2015)

Spatial pattern and night-time dynamics of UHI

The nocturnal changes of the spatial patterns of UHI are also important to analyze. We examined the nocturnal dynamics of the average UHI intensity from 1 hour before sunset to 13 hours after sunset regarding the HMS station as rural one (*Figure 5*). These maps represent the yearly mean values in the given times, so these maps contain every weather situation including the unfavourable ones too when the urban thermal modification effect is weak.

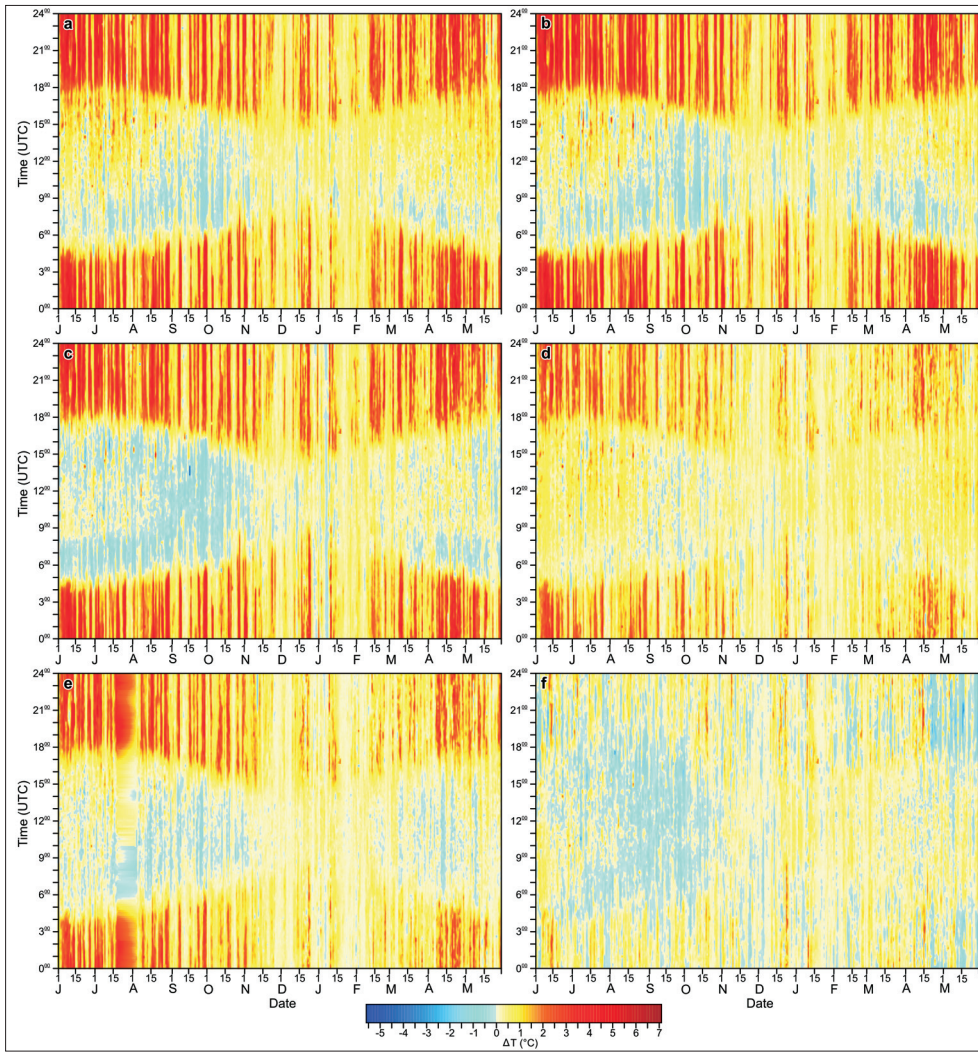

Fig. 4. Annual and diurnal variations of average temperature difference (ΔT) of LCZs from HMS station. – a = LCZ 2 – HMS, b = LCZ 3 – HMS, c = LCZ 5 – HMS, d = LCZ 6 – HMS, e = LCZ 8 – HMS, f = LCZ 9 – HMS) (Szeged, June 2014 – May 2015)

Before sunset there is no characteristic pattern, the UHI starts to develop at sunset and it reaches rapidly its maximum development in the next two hours (*Figure 5*). Under these average conditions, only a relatively weak UHI develops as its maximum intensity is around 2 °C and it is mostly observable in city centre. At the first few hours (until +3 hours) negative values can be found in a small area in the western part of the city. The reason for this is the microclimatic background of these areas (small lakes).

The UHI remains relatively strong during the rest of the nocturnal hours and it starts to decrease rapidly at 10–11 hours after sunset. The shape of the 1 °C isotherm is almost the same from 1 hour until 8 hour after sunset. The pattern of the area with minimum 1 °C

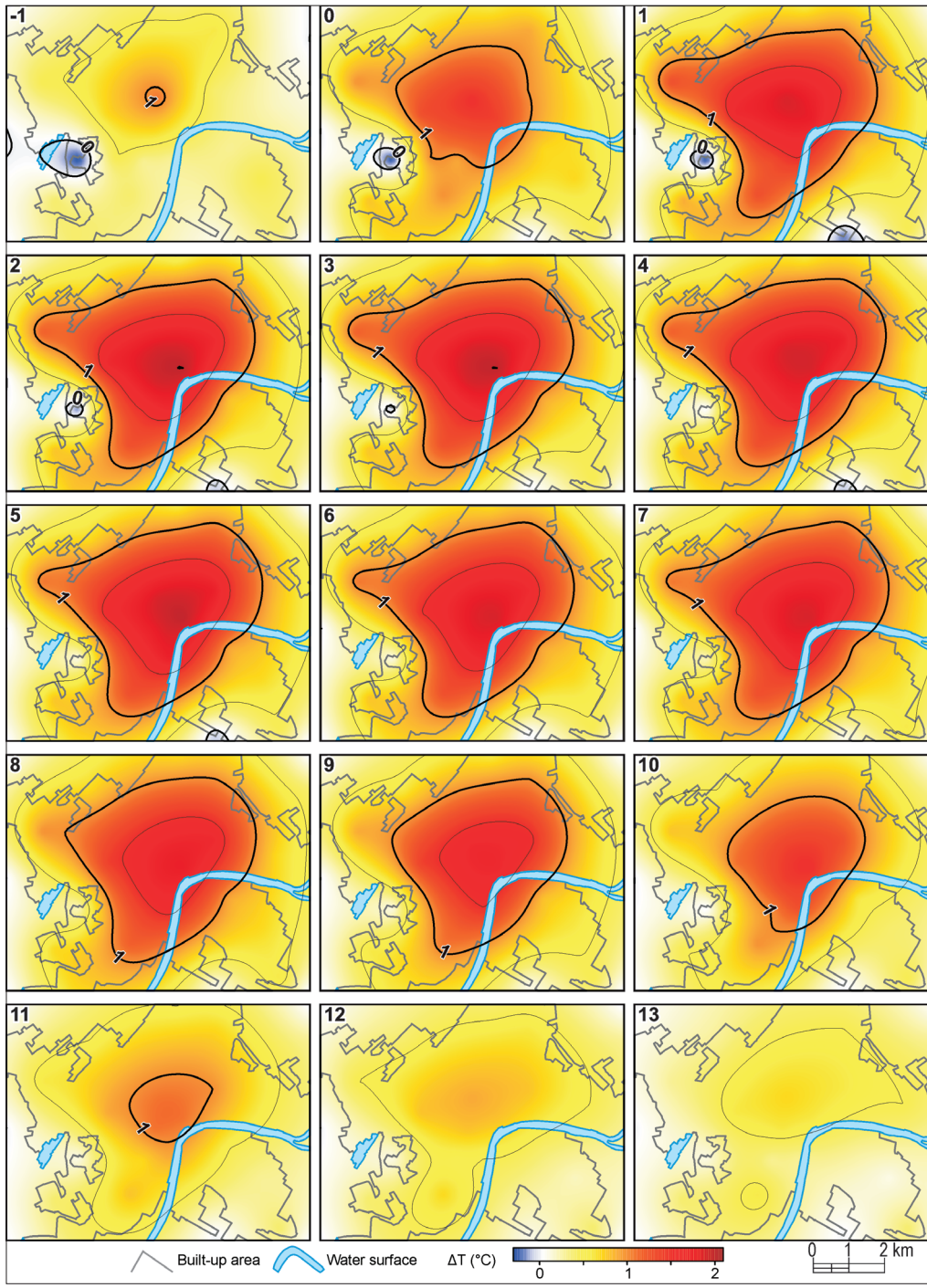

Fig. 5. Patterns of building up and down of average annual UHI intensity (ΔT) (from sunset -1h to sunset+13h) (Szeged, June 2014 – May 2015)

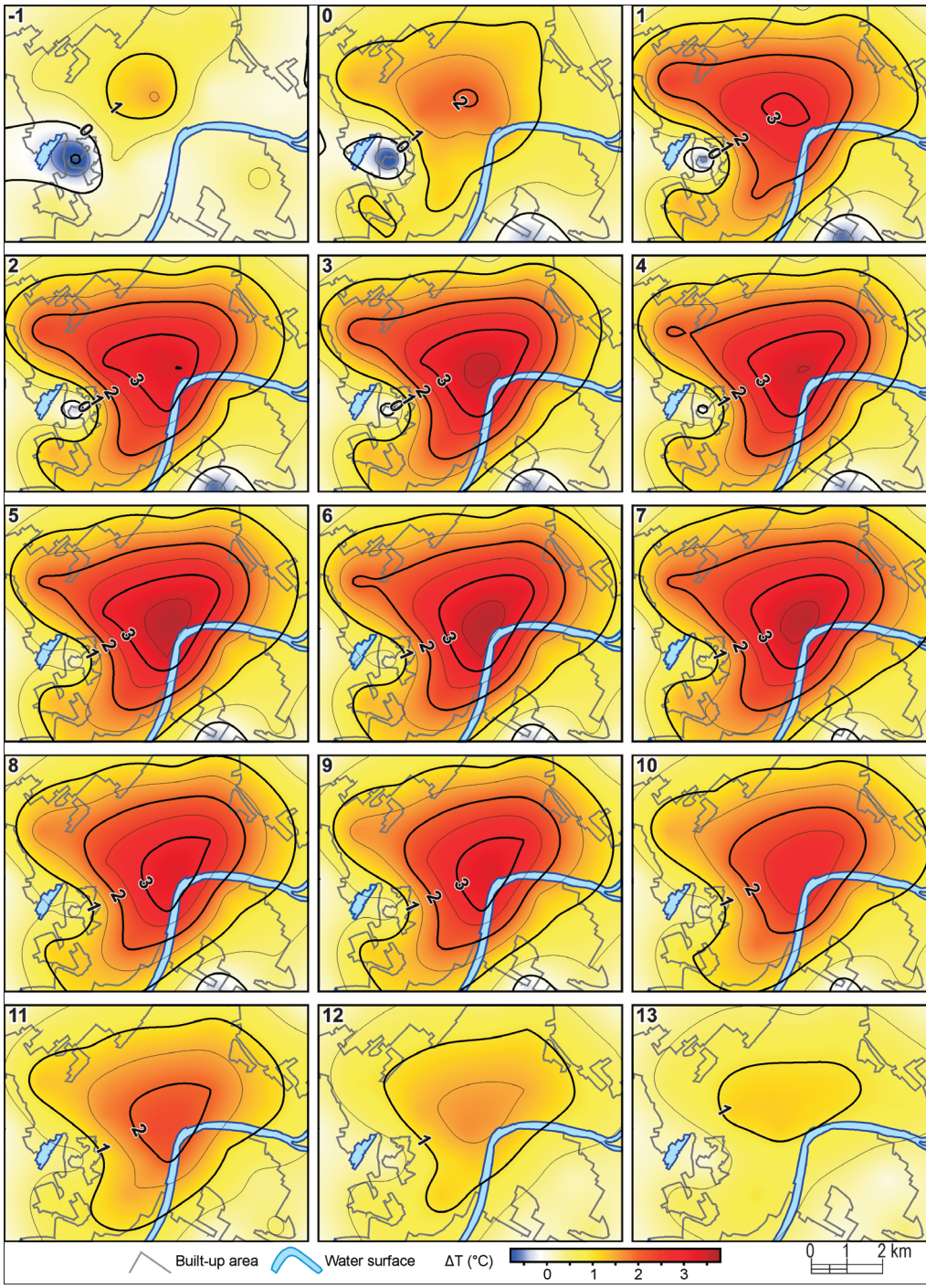

Fig. 6. Patterns of building up and down of average annual UHI (ΔT) on the selected ideal days (from sunset-1h to sunset+13h) in Szeged (June 2014 – May 2015)

difference stretch northwest and southwest directions and dominates the largest part of the city. It reflects the spatial pattern of the different LCZ types (see *Figure 1*), namely the most dense local climate zones has larger temperature surplus.

In the inner parts of the city (basically the city core) the magnitude of UHI reaches at least 1.5 °C. It appears at 1 hour after sunset and last +9 hours. Its extension is slightly changed during the night and it starts to decrease about 8 hours after sunset. Around 10 hours after sunset the UHI starts to collapse and around +12 or 13 hours it completely disappears.

If we concentrate on the favourable weather conditions, then we can found much stronger UHI intensity (*Figure 6*). In this case, the temporal dynamics of the UHI pattern is differs from the case of annual mean values. The maximum intensity is around 4 °C which is almost twice as large as the maximum in *Figure 5*.

The UHI starts to develop at sunset but the temperature difference of 2 °C already appears at this hour. In the next hour the extension of differences over 2 °C increases and values over 3 °C also appear. Later, the UHI becomes more and more extensive and its intensity increases also. The differences over 3 °C dominate the city centre and the remaining parts have values between 1 °C and 2 °C. 3 hours after sunset the intensity exceeds 3.5 °C in the centre and after a small weakening it continuously increases again. The weakening of the UHI starts at 7 hours after sunset when the area with values over 3.5 °C difference decreases and it disappears at +8 hours. For this time, the areas which are delimited by the other isotherms decrease and later gradually disappear. At about +10 hours, there are still some temperature differences, but it decreases continuously and around 12 and 13 hours it is minimal.

The spatial patterns of the UHI from the first hour until the 7th hour are almost identical, thus the temperature surplus develops in the first hours of the night and it is present in the same areas with almost constant values during the night.

Dynamical background of nocturnal UHI at favourable weather conditions

It helps to understand the background of the development of the nocturnal temperature excess if we evaluate the spatial patterns of average hourly cooling rates (*Figure 7*). In order to avoid the drastic temperature changes caused by synoptic scale weather changes, we analyse only the mean hourly cooling/warming rates calculated from the data of ideal days.

The most intensive cooling is at sunset and 1 hour after sunset. At this time, the cooling rate in the city centre is over -1.5 °C and in the largest parts of the city it is over -2 °C. In the rural areas the cooling rate is under -2.5 °C, showing that the rural areas cool faster. These different rates cause the development of UHI and it can be clearly seen that the hours around sunset are crucial for this phenomenon. In the following hours, the cooling rate decreases and there is no significant spatial trend until sunrise. At 10 hours after sunset, the warming process appears and the rate continuously increases. One hour later the warming rate is under 0.5 °C in the city but it is larger in the outskirts and rural areas. In the following periods, the warming reaches 1 °C and 1.5 °C in the city and in the outskirts, respectively. These differences in the warming rates are the reason of the development of the daytime urban cool island presented above.

Effect of the UHI on annual temperatures

In the previous sections we analysed the different aspects of the urban temperature modification: large positive values at night and smaller negative values in the daytime. The crucial question arises whether the nocturnal temperature surplus modifies the spatial pattern of basic climate indices like mean annual temperature. In order to answer this question, we depicted the spatial pattern of this measure (*Figure 8*).

As we can see on *Figure 8*, the effect of UHI is significant. Due to the higher nocturnal temperatures the annual mean temperature

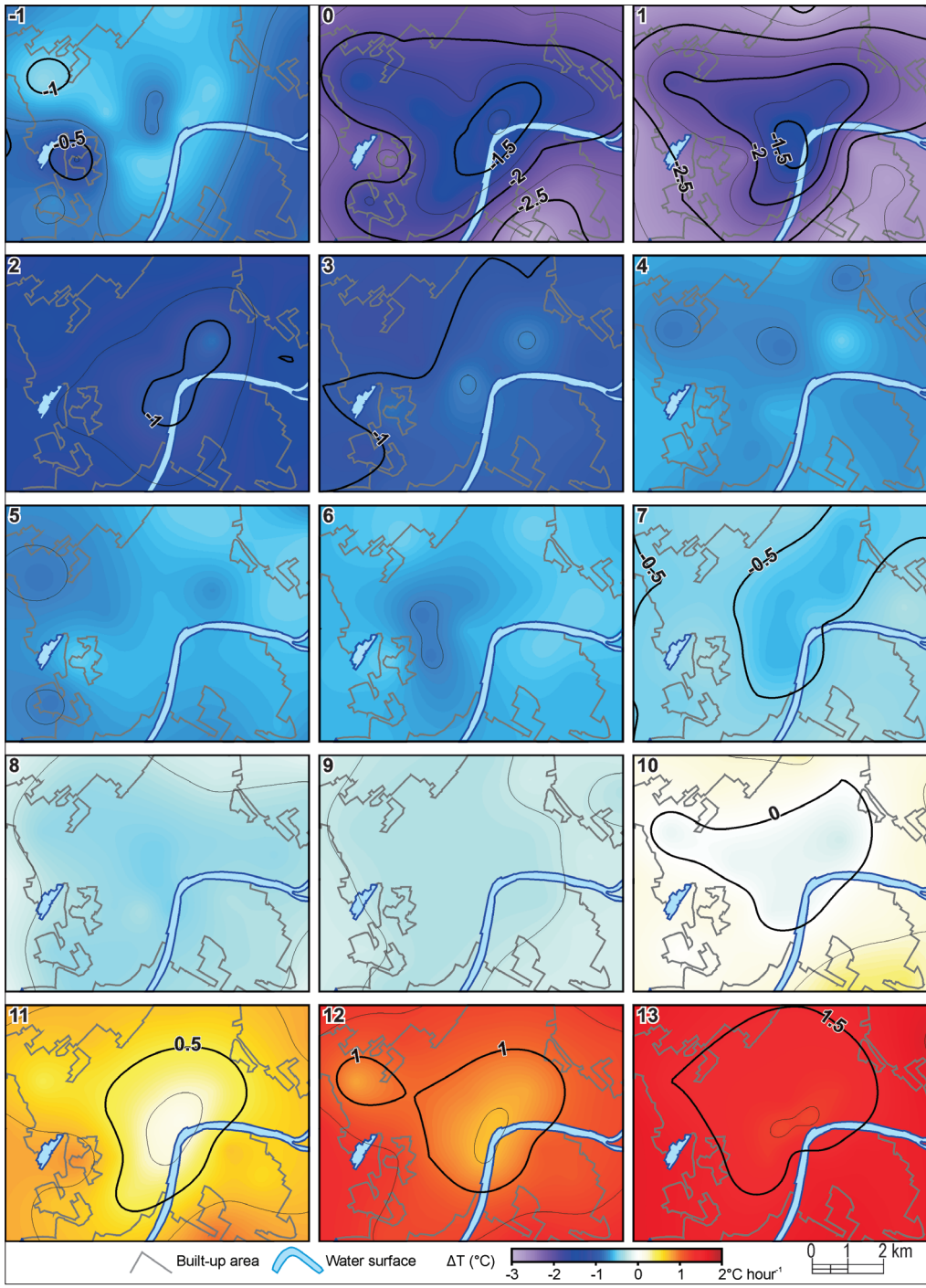

Fig. 7. The average patterns of hourly cooling/warming rates on ideal days (from sunset-1h to sunset+13h) (Szeged, June 2014 – May 2015)

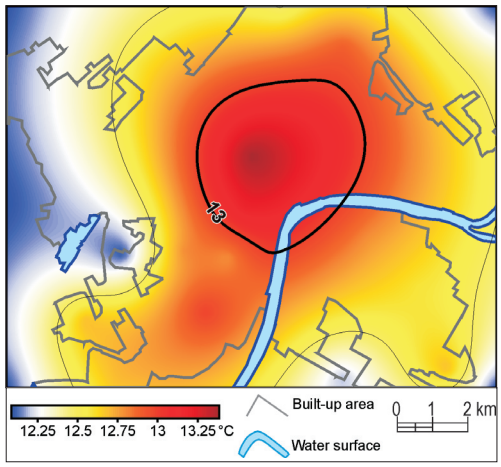

Fig. 8. Annual mean temperature pattern in Szeged (June 2014 – May 2015)

in the inner part of the city is 1 °C higher than the rural one. We have to consider that in this mean value the unfavourable weather conditions and the lower daytime temperatures are also take part.

Conclusions

In this paper, we examined the features of the UHI in Szeged including its annual, seasonal and diurnal characteristics, furthermore its build up and down with the dynamical background. We analysed also the differences between the LCZs in terms of UHI. In the course of this analysis, we investigated the UHI intensity both in average and at ideal conditions. This examination was carried out using 1 year dataset from a 24-station urban measurement network.

From our results, we highlight the following statements. Between the LCZs the greatest urban/rural temperature differences appear in the compact zones. These zones are followed by open midrise and the other low-rise zones, while the smallest differences are in the sparsely built zone. Among the seasons outstanding values are in summer for every LCZ. Considering the ideal conditions, the autumn values are higher in some cases. The strong summer UHI is the most spectacular in LCZs 2, 3 and 5. Furthermore, these zones are cooler than the others relative to the rural area at daytime.

It can be generally noted that the mean annual UHI starts to develop immediately after sunset and exists approximately until 9 hours after sunset. It reaches its maximal intensity about 3 hours after sunset. At ideal conditions a much stronger UHI develops as its intensity approximately 2 °C greater than in average conditions. After sunrise the UHI starts to build down, but on ideal days there is small temperature difference even at this time. Considering the cooling rates the greatest changes appear around sunset and sunrise. The largest cooling is at sunset and 1 hour after sunset: in the rural areas the cooling is more intensive resulting in the urban heat excess. After sunrise the city warms slower than the rural areas, therefore, the urban cool island also occurs.

Finally, we evaluated the annual mean temperature, and we find that the urban temperature modification effect clearly appears in it. That is, the basically nocturnal thermal differences which are significant in case of ideal weather conditions can affect the general climate characteristics of the area. Therefore, any climate assessment or climate modelling work has to take into consideration the urban effect otherwise the results will underestimate the heat load of the urban areas.

***Acknowledgements*:** The study was supported by the Hungarian Scientific Research Fund (OTKA K-111768) and the first author was supported by the János Bolyai Research Scholarship of the Hungarian Academy of Sciences.

REFERENCES

Bolz, H.M. 1949. Die Abhängigkeit der infraroten Gegenstrahlung von der Bewölkung. *Zeitschrift für Meteorologie* 3. 201–203.

Kottek, M., Grieser, J., Beck, C., Rudolf, B. and Rubel, F. 2006. World Map of the Köppen-Geiger climate classification updated. *Meteorologische Zeitschrift* 15. (3): 259–263.

Lelovics, E., Unger, J., Gál, T. and Gál, C.V. 2014. Design of an urban monitoring network based on

Local Climate Zone mapping and temperature pattern modelling. *Climate Research* 60. 51–62.

Nakamura, Y. and Oke, T.R. 1988. Wind, temperature and stability conditions in an east-west oriented urban canyon. *Atmospheric Environment* 22. 2691–2700.

Oke, T.R. 1998. *An algorithmic scheme to estimate hourly heat island magnitude*. In Preprints, 2nd Urban Environment Symposium, 2–6.

Stewart, I.D. and Oke, T.R. 2012. Local Climate Zones for urban temperature studies. *Bulletin of the American Meteorological Society* 93. 1879–1900.

Stewart, I.D., Oke, T.R. and Krayenhoff, E.S. 2014. Evaluation of the 'local climate zone' scheme using temperature observations and model simulations. *International Journal of Climatology* 34. 1062–1080.

Unger, J., Gál, T., Csépe, Z., Lelovics, E. and Gulyás, Á. 2015. Development, data processing and preliminary results of an urban human comfort monitoring and information system. *Időjárás* (Quaterly Journal of Hungarian Meteorological Service) 119. 337–354.

Unger, J., Sümeghy, Z., Gulyás, Á., Bottyán, Z. and Mucsi, L. 2001. Land-use and meteorological aspects of the urban heat island. *Meteorological Applications* 8. 189–194.

URBAN-PATH homepage 2016. http://urban-path.hu/ (last accessed 2016-01-27)

World Meteorological Organization 1983. *Abridged final report, 8th session*. Geneva, Commission for Climatology and Applications of Meteorology (WMO No. 600).

DOI: 10.15201/hungeobull.65.2.3 Hungarian Geographical Bulletin 65 2016 (2) 117–128.

Detection of atmospheric urban heat island through direct measurements in Cluj-Napoca city, Romania

Ioana HERBEL, Adina-Eliza CROITORU, Ionuț RUS, Gabriela Victoria HARPA and Antoniu-Flavius CIUPERTEA[1]

Abstract

In the last decades, cities worldwide have experienced accelerated development, so that continuous urbanization and its impact is presently one of the most important topics in different fields of research. The main aim of this study is to identify the intensity of the atmospheric urban heat island in Cluj-Napoca city, through direct observations campaigns by using fixed points and transect measurements. The data has been collected over a period of 6 months (May–October 2015). The measurements have been performed mainly in anti-cyclonic weather condition, during the night, between 23:00 and 03:00. The profiles trajectories followed the main roads of the city on directions North–South, East–West, and Northwest–Southeast. 8 fixed points have been chosen in order to highlight best the temperature patterns in different Local Climate Zones (LCZs). The main findings of the study are the followings: the direct observations performed in three seasons (spring, summer and autumn) revealed the existence of an atmospheric urban heat island in Cluj-Napoca city; the warmest areas are compact high-rise and compact midrise, located in the eastern half of the city, where the temperature increases by more than 2.0 °C, as average value for all campaigns, but the maximum values, recorded in the summer are higher than 3.0 °C; the coolest areas are sparsely built areas and the large low-rise/water areas, where the temperature is quite similar to that recorded in the nearby rural areas (difference of 0.0–0.1 °C, as average values); local factors, such as mountain breeze and topography have a great impact on the atmospheric urban heat island configuration.

Keywords: atmospheric urban heat island, direct measurements, Cluj-Napoca, Romania

Introduction

In the last decades, cities worldwide have experienced accelerated development, so that continuous urbanization is presently one of the most important dimensions of contemporary global change. Today 54 percent of the world's population lives in urban areas and it is responsible for 76 percent of the energy consumption and greenhouse gas emissions (Grubler, A. *et al.* 2012). Moreover, the urban population is expected to increase to 66 percent by 2050 (United Nations, 2014). This fact implies expanding urban land use and a massive demand for built-up areas should be anticipated in the next few decades (Seto, K.C. *et al.* 2012; Song, X-P. *et al.* 2016). In Europe alone, at present, nearly 73 percent of the population lives in cities and it is projected to reach 82 percent by 2020 (European Environment Agency, 2010; Akbari, H. *et al.* 2016).

Beside the positive aspects of this process, such as increasing the frost-free period or income from better paid jobs, the environmental impact of urbanization is nowadays a major problem discussed in urban planning and development studies. One of the most important consequences of the urbanisation process is the intensification of urban heat island (UHI) (Herbel, I. *et al.* 2015). This phenomenon generates higher air and surface temperatures compared to nearby rural areas and usually

[1] Faculty of Geography, Babeş-Bolyai University. 5–7, Clinicilor Street, 400 006 Cluj-Napoca, Romania. E-mails: ioana.herbel@yahoo.com, croitoru@geografie.ubbcluj.ro, rusionut22@gmail.com, harpa_gabriela@yahoo.com, antonio3088@yahoo.com

causes weather anomalies, a deterioration of the living environment by increasing temperatures and air pollution, by intensifying the heat waves, and even a rise in mortality (Shepherd, J.M. and Burian, S.M. 2003; Memon, R.A. *et al*. 2008; Wong, K.V. *et al.* 2013; Unger, J. *et al*. 2014). During heat waves, inhabitants of urban areas may experience sustained thermal stress both in day-times and night-times whereas in rural areas people get some relief from thermal stress at night (Unger, J. *et al.* 2014). Economically, an increase in energy consumption for cooling is associated to UHI, especially during summer time.

Under these circumstances, in the last years, many researchers in different fields such as climatology, urban planning or remote sensing, focused on urban heat environment and UHI (Li, J. *et al.* 2009; Unger, J. *et al*. 2010; Kumar, D. and Shekhar, S. 2015). The urban environment is a complex system, involving concentrated human activities and integrated ecosystem vulnerabilities that could be seriously affected by the intensity increase of the UHI (Cohen, B. 2006; Hu, L. *et al*. 2015). An UHI can be present at any latitude, may occur during the day or night and can be detected in any season as a function of the local thermal balance. It is more intense on calm and clear days and it is highly affected by wind and precipitation (Santamouris, M. 2015; Akbari, H. *et al*. 2016).

UHIs have been detected in many cities of the world. Thus, by 2011, atmospheric urban heat island (AUHI) observations on 221 cities and towns from all over the world were reported in the literature (Stewart, I.D. 2011). The UHI intensity detected in several European and Mediterranean cities is more significant at night and varies between 1.5 °C and 12.0 °C, while in other cities (e.g. Athens and Parma), maximum UHI intensity occurs during daytime (Santamouris, M. 2007; Founda, D. *et al.* 2015).

The main factors generating and affecting the UHI intensity are the urban architecture, the type of urban materials, the population density, the synoptic and local meteorological conditions as well as the lack or small percentage of green and water surfaces inside the city. Furthermore, artificial heating and cooling of buildings, transportation and industrial processes introduce anthropogenic sources of heat into the urban environment, causing distinct and even enhanced UHIs, their intensities showing an overall increase over the years (Wilby, L.R. 2007; Akbari, H. *et al.* 2016).

Cities with high population density and increased human activities, including intense individual and public transportation, experience a higher UHI intensity during daytime. In some of these cities there is a higher UHI intensity in the summer (e.g. Rome, Madrid) while in others in the winter (e.g. Lisbon). Katoulis, B.D. and Theoharatos, G.A. (1984) and Giannaros, T.M. and Melas, D. (2012) reported a higher UHI intensity in the night time and during the warm period in Thessaloniki and Athens (Greece). Maximum intensity of the daytime UHI in summer was detected in other non-European cities with subtropical or tropical climate, such as Shanghai (Tan, J. *et al*. 2010) or Muscat (Charabi, Y. and Bakhit, A. 2011), while in Szeged (Hungary), during a one-year long measurement campaign, the maximum intensity was found in the night-time (Lelovics, E. *et al*. 2014). It is concluded that reported UHI varies considerably according to existing studies in terms of maximum intensity and season/time of occurrence. In addition to the aforementioned reasons related to different climatic features and thermal balance of the cities, other reasons such as the application of different monitoring protocols or the selection of reference stations could largely influence UHI estimations (Founda, D. *et al*. 2015).

Despite the large number of studies conducted worldwide, in Romania only a few studies have been performed on UHIs until now. For Bucharest, several studies were conducted by using direct measurements data and satellite imagery (Cheval, S. *et al*. 2009; Cheval, S. and Dumitrescu, A. 2009, 2015). For Iaşi, direct measurements were performed in the ‘60s and ‘70s (Gugiuman, I. 1967; Erhan, E. 1971, 1979), while recently the research topic in the same city was re-

assumed by Apostol, L. *et al*. (2012). For Cluj-Napoca only one study focused on the surface urban heat island based on Landsat imagery (Imbroane, A.M. *et al.* 2014).

The main aim of this study is to identify the intensity of atmospheric UHI in Cluj-Napoca city, through direct observations campaigns by using fixed points and transect measurements.

Materials and methods

Study area

Cluj-Napoca is the second most populated city in Romania after the capital city Bucharest and the largest and most populated urban centre in Central Romania (Transylvania). The city is located among three major geographical units (Apuseni Mountains – the northern part of Western Carpathians –, Someşan Plateau and Transylvania Plain). Cluj-Napoca extends over 179.5 km^2 and the population exceeds 320,000 inhabitants.

The city is crossed over from West to East by Someşul Mic River over a length of 16 km. The urban area (located between 300 and 400 m a.s.l.) sprawls along its valley, generating the dominant air flow inside the city. The urban area expansion is limited by the topography which consists mainly of hills up to 1,000 m.

The general climate of the region is continental with western oceanic influences. The dominant concrete and asphalt landscape is the result of the intense urbanization process during the communist era, when neighbourhoods with high-density blocks of flats were built in the peripheral areas of the city. However, this process did not affect the historical centre, dominated by 18th and 19th century buildings with massive baroque architecture.

Data used

The literature on heat islands reports five methods commonly used for the evaluation of this phenomenon: fixed stations/points, mobile transverse, remote sensing, vertical sensing, and energy balances (Gartland, L. 2008). Air temperature is usually measured at about 1.5 meters above the ground. In the areas where measurements in fixed stations are not available, the field campaigns and transects studies involve the use of hand-held measurement devices or mounting measurement equipment on cars (Founda, D. *et al.* 2015).

Since each of the aforementioned methods has its own limitations, we propose a study based on a mixed approach that combines observations in fixed representative points of the city with mobile transects along the street network; then a comparison will be made between the recorded temperature values and those measured in a nearby rural area chosen as a fixed point of reference.

Data collection

Atmospheric urban heat islands are often weak during the late morning and throughout the day and become more pronounced after sunset due to the slow release of heat from urban infrastructure. The timing of this peak depends on the properties of urban and rural surfaces, the season, and prevailing weather conditions (Akbari, H. *et al.* 2015). The great majority of the measurements campaigns were performed during the night, between 23:00 and 03:00 hours, but also a campaign of 24 hours of continuous measurements was conducted.

The data used in this study was collected over a period of 6 months (May–October 2015). Six different measurement campaigns were conducted, two for each season, but only one for each season was chosen to be presented in this study. In order to obtain the highest AUHI intensity, the measurements were performed mainly at higher than normal pressure conditions, clear sky, and calm weather or weak wind.

The mobile transect measurements usually lasted about 3 hours and were performed by car on three different crossing profiles with multiple stops along the routes (*Figure 1*). The profiles trajectories followed the main roads of the city on directions North–South, East–

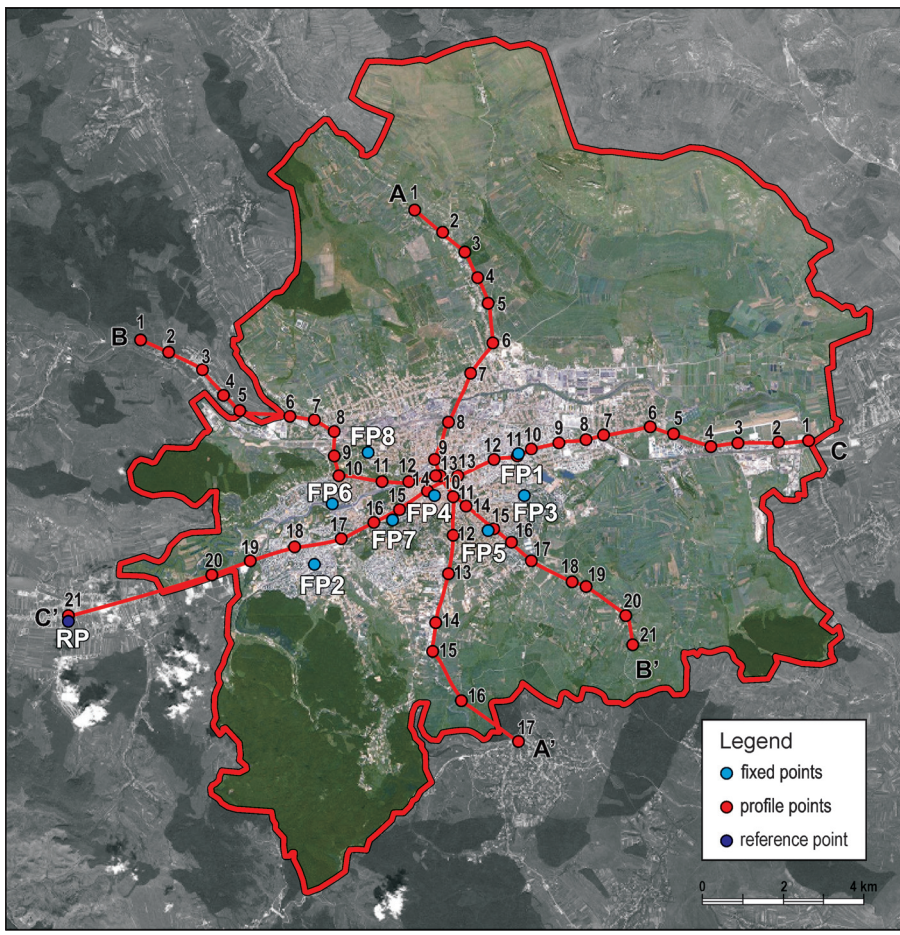

Fig. 1. Profile points, fixed points and reference point used in this study. AA', BB', CC' = explanations are in the text

West, and Northwest–Southeast. The profile points were chosen taking into account different types of the urban tissue in the city and each profile had 17–22 measurement points.

The most representative profile for AUHI detection is CC', as the altitude variation alongside is very low (62 m). Profile AA' is the least representative due to high altitude variation along it (380 m) that could introduce errors in AUHI intensity when no sounding data for lapse rate are available, as is the case in Cluj-Napoca. We chose to use profile AA' because it covers few important urban fabrics and we consider that it is important to have some measurements all over the city, even though the results are not very accurate.

The temperature value was registered simultaneously every 5 minutes in the 7 fixed points located in the urban area, as well as in the fixed point in the nearby rural area.

The fixed points used for observations were chosen in order to best highlight the temperature pattern in different Local Climate Zones (LCZ) (Stewart, I.D. and Oke, T.R. 2012) generated by different urban fabric types and the nearby rural area (RP, Floreşti village). Thus, the code for the fixed points and their corresponding LCZ are listed below:

– FP1 – compact high-rise (Mărăşti Neighbourhood);
– FP2 – compact high-rise (Mănăştur Neighbourhood);

– FP3 – compact midrise (Gheorgheni Neighbourhood);
– FP4 – compact low-rise (city centre, Old Town);
– FP5 – open low-rise (residential area: Andrei Mureşanu Neighbourhood);
– FP6 – large low-rise/water (Babeş Park/ Sports Hall/Someş River side);
– FP7 – scattered trees (park around Faculty of Geography).

In order to improve the spatial resolution of the fixed point network, we also used the data recorded in Cluj-Napoca Weather Station (WMO code: 15120), which is considered representative for sparsely built environment (FP8).

In order to perform measurements, we employed 2 automatic Davis Vantage Pro2™ weather stations (for FP3 and FP7), 3 high precision Dostmann P400 mobile thermo-hygrometers (for mobile transects) and 9 calibrated normal (dry) meteorological thermometers. In order to avoid errors in the measurement process due to wind, a portable meteorological shelter has been used for each point, except for those with automatic weather stations. On transects the data has been collected by using both a Dostmann P400 mobile thermo-hygrometer and a normal mercury thermometer to improve the accuracy of the measurements. The geographical coordinates of each measurement point were recorded by using a GPS logger application (GPS Logger for Android).

Data processing

For data processing the procedure previously described by Herbel, I. *et al.* (2015) was used.

After the data was collected, the altitude corrections were performed for all the temperature values recorded in fixed and transect points, as presented in (1). The mean lapse rate used was 0.65 °C/100 m.

$$T_{Bcor} = T_B + \frac{\Delta H}{100} \text{ x } 0.65, \qquad (1)$$

where T_{Bcor} is corrected temperature in point *B*, located in the urban area (in °C); T_B is the temperature measured in point *B*, located in the urban area (in °C);

$$\Delta H = H_B - H_A, \qquad (2)$$

where H_B is the altitude of the point *B* (m); H_A is the altitude of the reference point (*A*), located in the nearby rural area (m);

In order to use the correct values of the lapse rate for altitude correction, sounding data should be used, but unfortunately this data hasn't been available for Cluj-Napoca weather stations since November 2012. Under these circumstances, we decided to use the mean lapse rate of 0.65 °C/100 m, because during spring and summer campaigns the air pressure was slightly above normal pressure.

For the temperature recorded in fixed points, only altitude corrections were performed, while for transect points a time correction was also necessary.

The primary time deviation was computed as a temperature difference between temperatures recorded in the transect point and those recorded in the reference point (RP) located in Floreşti village.

If the temperature values were recorded at the same time in both points (RP and point on the profile), the primary deviation was obtained using

$$D = T_{PX} - T_R, \qquad (3)$$

where *D* is the difference to be calculated for a point *X* (on the profile); T_{PX} is the temperature measured in point (*X*) of the profile at time t_x; and T_R is temperature measured in RP at time t_x; t_x is the time when the temperature was recorded in point *X* of the profile, given in hours and minutes.

The time corrections were computed only for those points on the profile for which the measurement time did not coincide with the one in RP.

Since the temperature value in the fixed points was collected every 5 minutes, in some cases the temperature data on the profile points was collected between two measure-

ments in RP. In this case, the corresponding RP temperature value was obtained by adding a time correction, calculated by using formula given in (4), to the temperature measured in RP, for each profile point where the measurement time was different from the fixed point measurement time.

$$C_t = (T_2 - T_1)/n \times d, \quad (4)$$

where C_t is the time correction to be added to temperature recorded in RP; the time corrected temperature is needed to get simultaneous values for the profile point and for the RP, in order to calculate the deviation between the two points; T_1 is the temperature measured in RP before the measurement in the point on the profile; T_2 is the temperature measured in RP after the measurement in the point on the profile; n is number of minutes between two consecutive measurements in RP; d is the number of minutes between the measurement in the profile point and the previous measurement in the RP.

After the time correction performed on the reference point value, the deviation of the profile point temperature was calculated by using (3).

Results and discussion

Fixed points measurement

1. Spring measurements

In spring of 2015, the chosen campaign was from May 13, 9:00 a.m. to May 14, 9:00 a.m. The measurements lasted 24 hours in the fixed points. During the data collection where the followings: the sea level pressure (SLP) was slightly above the normal values (1,020 hPa) at the beginning of the interval and decreased below the normal values at the end of the interval. There was variable convective cloudiness, especially during daytime, covering sometimes more than 90 percent of the sky. No clouds were recorded between midnight and 3:00 a.m. Over that interval, the wind blew from Southwest with a speed lower than 2 m/s; at the end of the 24 hour interval precipitation occurred. In the second part of the night, after 4.00 a.m., a cold front affected the area with the end of its squall line, generating important temperature variations and rainfall.

The temperature values recorded in the fixed points is presented in *Figure 2*. The interval of relative thermal stability lasted about 5 hours (from 23:00 to 4:00). As expected, the highest temperature values were recorded in FP1 (compact high-rise), but also in FP3 (compact mid-rise), while the lowest was specific to the RP (Floreşti village) and on the Someş river side (FP6). Between coolest and warmest areas, there was a difference of about 2.0 °C. The city centre is also one of the hot-spots, but more prominent in the daytime as a result of high traffic in the area.

In the night, due to low elevation buildings of the Old City, the deviation from the RP temperature is smaller than the one recorded for the compact high-rise and mid-rise LCZ.

In the daytime, high temperature variations could be observed even for the same point and the data collected in this interval was inappropriate to evaluate the AUHI intensity in Cluj-Napoca city. Therefore, for the next campaigns we focused on the night-time measurements.

2. Summer measurements

For summer of 2015, we chose to present here the results of the first campaign that took place between July 22nd and July 23rd. The temperature values were collected only during the interval of relative thermal stability: 23:00–02:00 h. As general weather conditions, the SLP was slightly above normal (1,017–1,018 hPa), there were no clouds and the wind blew with a speed of 2 m/s from Southwest and South-Southwest.

The temperature values decreased gradually from the beginning until the end of the interval (*Figure 3*). The highest values were identified in FP1 (compact high-rise east), followed by FP3 (compact midrise) and FP4 (compact low-rise), while the lowest ones in the RP. In the interval of relative thermal sta-

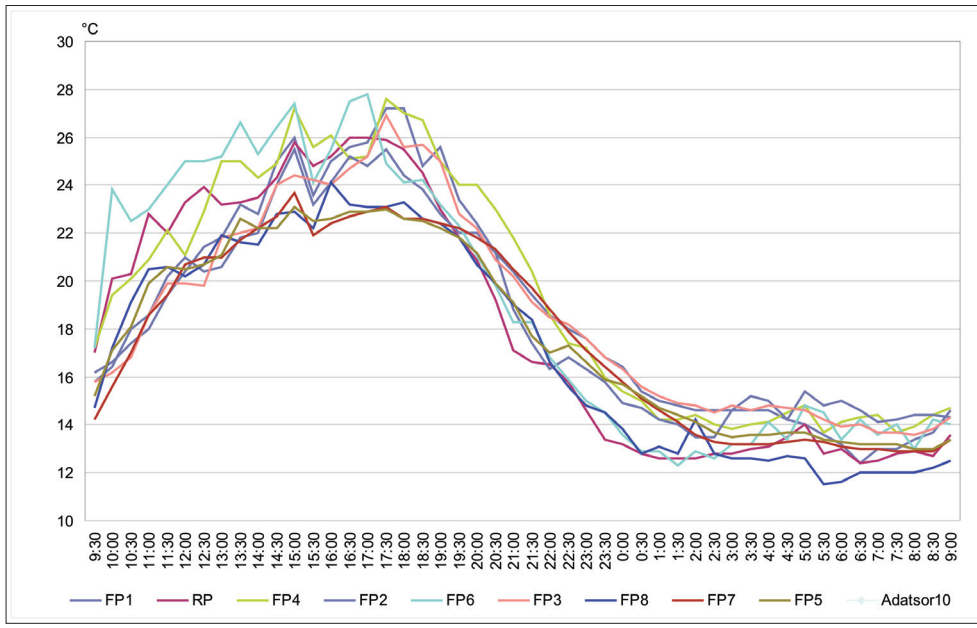

Fig. 2. Temperatures recorded in fixed points during the spring campaign (May 13–14, 2015); hours are given in local time (UTC + 3.00 h)

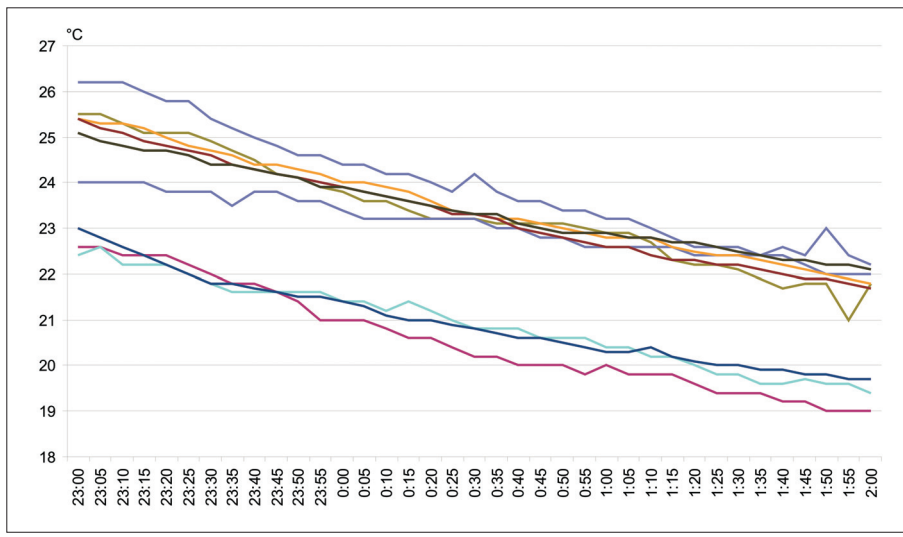

Fig. 3. Temperatures recorded in fixed points during the summer campaign (July 22–23, 2015); hours are given in local time (UTC + 3.00 h)

bility, the differences between the temperatures of the points located in the city area and RP varied from 0.1 °C to 3.2 °C as mean values, and from -0.4 °C to 3.8 °C, in terms of extreme values (*Table 1*).

3. Autumn measurements

From the autumn measurement campaigns for AUHI analysis, we chose to present the one that started on October 24, 23:00 and ended on October 25, 2:00 am. Synoptic con-

Table 1. Altitude corrected deviation in °C compared to the rural area reference point (RP) by seasons

Fix points	Spring (May 13–14) 9:00–9:00 h			Summer (July 22–23) 23:00–02:00 h			Autumn (October 24–25) 23:00–02:00 h			Overall		
	Av.	Min.	Max.	Av.	Min.	Max.	Av.	Min.	Max.	Av.	Min.	Max.
FP1– compact high-rise	1.9	0.9	3.0	3.2	2.8	3.8	1.5	1.1	2.3	2.2	0.9	3.8
FP2 – compact high-rise	1.5	0.5	2.3	2.6	1.5	3.3	1.2	0.8	1.6	1.8	0.5	3.3
FP3 – compact midrise	2.1	0.9	3.0	2.8	2.5	3.1	1.3	0.8	2.0	2.1	0.8	3.1
FP4 – compact low-rise	1.4	0.8	2.0	2.6	1.8	3.0	1.3	0.7	2.3	1.8	0.7	3.0
FP5 – open low-rise	1.5	0.5	2.5	2.8	2.3	3.2	1.4	0.6	2.2	1.9	0.5	3.2
FP6 – large low-rise/water	-0.1	-1.1	0.8	0.1	-0.4	0.6	0.4	-0.2	1.0	0.1	-1.1	1.0
FP7 – scattered trees	1.2	0.1	2.6	2.7	2.4	3.1	1.3	0.4	2.1	1.7	0.1	3.1
FP8 – sparsely built	0.4	-0.5	1.8	0.6	0.0	1.0	-1.0	-1.6	-0.5	0.0	-1.6	1.8

ditions analysis revealed that an anticyclone was dominant in the area with SLP ranging from 1,023 to 1,026 hPa. During the measurements, the cloudiness varied from 80 percent at the beginning of the measurements, to no clouds at the end of the interval. The wind blew from Southwest and South-southwest with an average speed of 2 m/s.

The temperature decreased slowly over the interval (*Figure 4*). The highest temperature values were registered, as in the other measurement campaigns, in FP1 (compact high-rise-east) but overall, the differences between the observation points from the urban area and the RP were smaller than in summer. In FP8 (the sparsely built type), the temperature was lower than in RP, with an average deviation of -1.0 °C. The difference between the warmest point (FP1) and RP was smaller at the beginning (1.1 °C), due to high cloudiness, reaching 2.3 °C at the end of the interval. The mean deviation recorded in FP1 was 1.5 °C (*Table 1*).

It is worth mentioning that we chose two fixed points in different compact high-rise areas with different local air circulation. The first one (FP1), located in the eastern part of the city proved to be constantly the warmest area in the city, situation that corresponds to any theoretical approach. The second one (FP2), located in the western part of the city, is directly exposed to the mountain night breeze blowing over the city from West and Southwest. The cool air descends from Western Carpathians with an almost constant velocity of 2 m/s and it is the most common wind blowing over the city in the night-time, transporting the warmer air eastward. This is the explanation for the fact that the western compact high-rise area is cooler than the eastern one. During our campaigns we recorded temperature differences ranging from 0.4 °C to 1.3 °C between the two compact high-rise areas.

Profile measurements

1. AA' Profile

The first profile used in this study extends from the northern part of the study area to the southern part over a distance of 15 km (*Figure 1*) and the temperature was measured in 17 points. Due to the topography of the city, the altitude of the points ranges from 400 m to higher than 700 m. It is the only profile with such an important altitude difference. The presence of the altitude difference makes this profile the least representative one, as presented at data collection. We should note that the use of the altitude corrections may lead to false UHI intensities in the area of higher altitudes and under these conditions we should be very cautious in interpreting the data. Therefore, we focused more on the segment between points 6 and 14, where the altitude variation was quite small. As can be seen in *Figure 1*, the first five and the last three points of the profile are located outside the built area of the city.

The seasonal variation of real time deviation on AA' Profile compared to the nearby

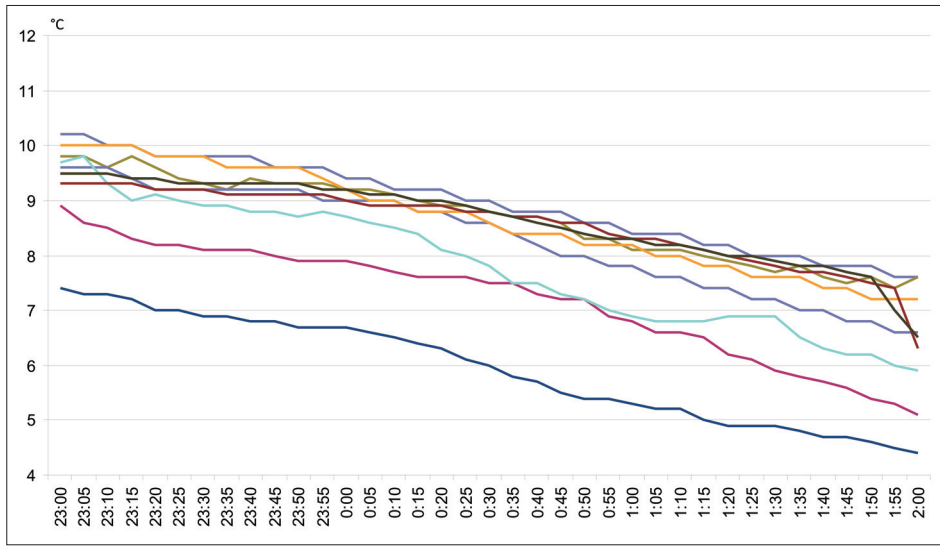

Fig. 4. Temperatures recorded in fixed points during the autumn campaign (October 24–25, 2015); hours are given in local time (UTC + 3.00 h)

rural area is shown in *Figure 5*. The final (southern) part of the profile was usually characterized by thermal inversions.

The shape of the AUHI can only be observed in the first part of the route for the spring and summer measurements. In autumn, thermal inversion occurred at higher altitude. If we ignore the increased temperature values induced by thermal inversions due to the topography and to the weather conditions (and not by the urbanization process) at the last three points of the route, the highest intensity of the AUHI could be observed in the summer (with deviation varying up to 3.0 °C), followed by spring (up to 2.0 °C), and autumn (up to 1.5 °C).

2. BB′ Profile

The second profile has a length of 18 km (*Figure 1*) and lower altitude variations compared to the first one. The average altitude of the profile points is 350 m, except the two final (South-East) points where the altitude increases to more than 450 m. This altitude difference is also associated to thermal inversion phenomena developed between the southern high hills and the city area. They generate higher temperature deviations compared to RP at the end of the route (*Figure 6*) for the campaigns conducted in May and July. The AUHI on BB′ profile can be clearly identified in spring and summer, but not in October, when the temperature recorded in the central part of the city was not much higher compared to that measured in the rural area.

In terms of AUHI intensity on this profile, the highest deviation occurred in the summer with a value reaching up to 3.0 °C in the central area of the city, while the lowest was recorded in the spring (up to 1.3 °C).

3. CC′ Profile

The third route is the most representative for AUHI detection as it has the lowest altitude variations among the points, of only 80 m. The altitude along the profile ranges from 300 m, in the first point of the profile, to 380 m (ASL) in the final point which coincided with the RP.

CC′ Profile extends over 20 km along the most important road trajectory of the city (from East to West), from Cluj-Napoca airport to the RP (*Figure 1*). Its trajectory intersected three fixed points located in the

eastern compact high-rise area (PF1), the compact low-rise area (PF4), and the rural area (RP). Under these circumstances, we used this route also as a quality control of the data measured in the fixed points.

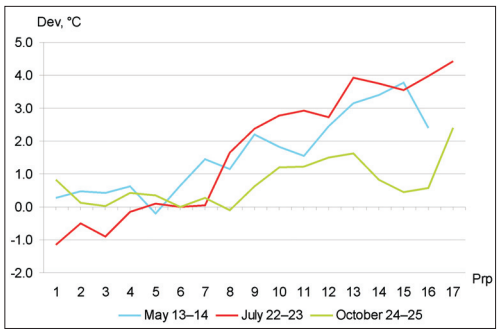

Fig. 5. Temperature deviation compared to RP along AA′ profile. Dev = deviation; Prp = profile point

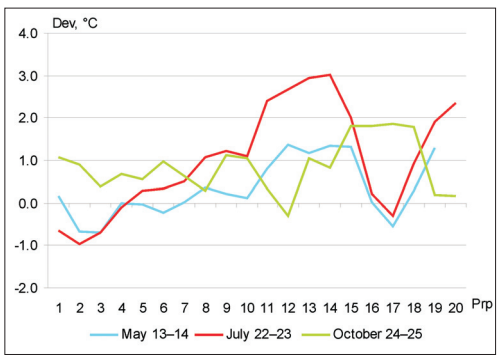

Fig. 6. Temperature deviation compared to RP along BB′ profile. Dev = deviation; Prp = profile point

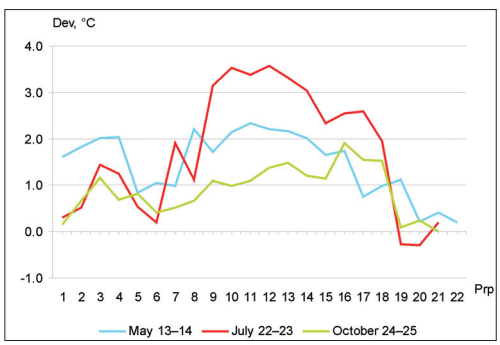

Fig. 7. Temperature deviation compared to RP along CC′ profile. Dev = deviation; Prp = profile point

The AUHI can be very well emphasized on this profile (*Figure 7*) for all seasons considered, but the values for summer are the highest, with more than 3.5°C in the eastern compact high-rise area.

During the campaign conducted in autumn, the most significant deviation could be observed on the second half of the route, denoting the presence of a thermal inversion, as the altitude sharply increases between points 15 and 17.

The high values from the beginning of each CC′ profile correspond to "Avram Iancu" International Airport area (point 3 is in the very front of the airport), which became urbanized enough in the last decade to be considered as a non-rural area. Points 5 and 6 on this profile are located in an open field area, as well as points 19 and 20. The temperature differences recorded in those two similar areas (open field) can be also explained by the air circulation (night breeze), which transports the warm air from the city to the eastern–northeastern areas.

Conclusions

The analysis of direct observations performed in three seasons (spring, summer, and autumn) revealed the existence of an AUHI in Cluj-Napoca city.

The warmest areas are compact high-rise and compact midrise areas located in the eastern half of the city, where the temperature increases by more than 2 °C, as average value for all campaigns, but the maximum values, recorded in summer are more than 3 °C higher. They are followed by compact high-rise areas located in the western part of the city, compact and open low-rise and scattered trees areas, where the temperature as an overall average is 1.7–1.9 °C higher, while the coolest areas are the sparsely built and the large low-rise/water areas, where the temperature is quite similar to that recorded in the nearby rural area (deviations from the RP are between 0.0–0.1 °C, as average values) (*Table 1*).

The profile measurements also emphasized the AUHI dome, for all the campaigns.

Local factors, such as air circulation (mountain breeze descending from Western Carpathians) and topography have a great importance to AUHI configuration. Thus, usually, due to mountain breeze the AUHI at night is elongated eastward, and sometimes isothermia or even thermal inversions can be identified.

***Acknowledgements*:** This work was partially supported by the Sectorial Operational Program for Human Resources Development 2007-2013, co-financed by the European Social Fund, under the project number POSDRU/159/1.5/S/132400 titled Young successful researchers – professional development in an international and interdisciplinary environment.

REFERENCES

Akbari, H., Bell, R., Brazel, T., Cole, D., Estes, M., Heisler, G., Hitchcock, D., Johnson, B., Lewis, M., McPherson, G., Oke, T.R., Parker, D., Perrin, A., Rosenthal, J., Sailor, D., Samenow, J., Taha, S., Voogt, J., Einter, D., Wolf, K. and Zalph, B. 2016. Reducing Urban Heat Islands: Compendium of Strategies. Urban Heat Island Basics, www.epa.gov.

Akbari, H., Cartalis, C., Kolokotsa, D., Muscio, A., Pisello, A.L., Rossi, F., Santamouris, M., Synnefa, A., Wong, N.H. and Zinzi, M. 2015. Local climate change and urban heat island mitigation techniques – The state of the art. *Journal of Civil Engineering and Management* 22. (1): 1–16.

Apostol, L., Alexe, C. and Sfîcă, L. 2012. Thermic differenciations in the Iasi Municipality during a heat wave. Case study July 10-20 2011. *Present Environment and Sustainable Development* 6. (1): 395–404.

Charabi, Y. and Bakhit, A. 2011. Assessment of the canopy urban heat island of a coastal arid tropical city: the case of Muscat, Oman. *Atmospheric Research* 101. 215–227.

Cheval, S. and Dumitrescu, A. 2009. The July urban heat island of Bucharest as derived from MODIS images. *Theoretical and Applied Climatology* 96. (1–2): 145–153.

Cheval, S. and Dumitrescu, A. 2015. The summer surface urban heat island of Bucharest (Romania) retrieved from MODIS images. *Theoretical and Applied Climatology* 121. 631–640.

Cheval, S., Dumitrescu, A. and Bell, A. 2009. The urban heat island of Bucharest during the extreme high temperatures of July 2007. *Theoretical and Applied Climatology* 97. 391–401.

Cohen, B. 2006. Urbanization in developing countries: Current trends, future projections, and key challenges for sustainability. *Technology in Society* 28. (1–2): 63–80.

Erhan, E. 1971. *Climatic differentiations in the urban and surrounding area of Iaşi city*. Lucrări Ştiinţifice Seria Geografie. Oradea, Institutul Pedagogic Oradea.

Erhan, E. 1979. *Climate and microclimates in the area of Iaşi city*. Iaşi, Junimea.

European Environment Agency (EEA) 2010. *European environment state and outlook 2010: urban environment*. SOER Report. 228 p.

Founda, D., Pierros, F., Petrakis, M. and Zerefos, C. 2015. Interdecadal variations and trends of the Urban Heat Island in Athens (Greece) and its response to heat waves. *Atmospheric Research* 161–162. 1–13.

Gartland, L. 2008. *Understanding and mitigating heat in urban areas*. London, Earthscan.

Giannaros, T.M. and Melas, D. 2012. Study of the urban heat island in a coastal Mediterranean City: the case study of Thessaloniki, Greece. *Atmospheric Research* 118. 103–120.

Grubler, A., Bai, X., Buettner, T., Dhakal, S., Fisk, D.J., Ichinose, T. and Weisz, H. 2012. Chapter 18 - Urban Energy Systems. In *Global Energy Assessment – Toward a Sustainable Future.* International Institute for Applied Systems Analysis. Laxenburg, Austria, Cambridge, UK and New York, Cambridge University Press, 1307–1400.

Gugiuman, I. 1967. *A few problems regarding the climatology of the cities in Romania*. ASUCI – GG, Section II, XIII, 27–32.

Herbel, I., Croitoru, A.E., Imbroane, A.M. and Petrea, D. 2015. Methods to detect atmospheric and surface heat islands in urban areas. *Riscuri şi catastrofe* 17. (2): 25–32.

Hu, L., Monaghan, A.J and Brunsell, N.A. 2015. Investigation of urban air temperature and humidity patterns during extreme heat conditions using satellite-derived data. *Journal of Applied Meteorology and Climatology* 54. (11): 2245–2259.

Imbroane, A.M., Croitoru, A.E., Herbel, I., Rus, I. and Petrea, D. 2014. Urban heat island detection by integrating satellite image data and GIS techniques. Case study: Cluj-Napoca city, Romania. In *Proceedings of the 14th International Multidisciplinary Scientific Geoconference SGEM 2014, 17–26 June.* Albena, Bulgaria, 359–366.

Katsoulis, B.D. and Theoharatos, G.A. 1985. Indications on the Urban Heat Island in Athens, Greece. *Journal of Climate and Applied Meteorology* 24. 1296–1302.

Kumar, D. and Shekhar, S. 2015. Statistical analysis of land surface temperature – vegetation indexes

relationship through thermal remote sensing. *Ecotoxicology and Environmental Safety* 121. 39–44.

Lelovics, E., Unger, J., Gál, T. and Gál, C.V. 2014. Design of an urban monitoring network based on Local Climate Zone mapping and temperature pattern modelling. *Climate Research* 60. 51–62.

Li, J., Wang, X., Wang, X., Ma,W. and Zhang, H. 2009. Remote sensing evaluation of urban heat island and its spatial pattern of the Shanghai metropolitan area, China. *Ecological Complexity* 6. (4): 413–420.

Memon, R.A., Leung, D.Y.C. and Liu, C.H. 2008. A review on the generation, determination and mitigation of urban heat island. *Journal of Environmental Sciences-China* 20. (1): 120–128.

Santamouris, M. 2007. Heat island research in Europe – the state of the art. *Journal Advances in Building Energy Research* 1. 123–150.

Santamouris, M. 2015. Analyzing the heat island magnitude and characteristics in one hundred Asian and Australian cities and regions. *Science of the Total Environment* 512–513, 582–598.

Seto, K.C., Guneralp, B. and Hutyra, L.R. 2012. Global forecasts of urban expansion to 2030 and direct impacts on biodiversity and carbon pools. *Proceedings of the National Academy of Sciences of the United States of America* 109. 16083–16088

Shepherd, J.M. and Burian, S.J. 2003. Detection of urban-induced rainfall anomalies in a major coastal city. *Earth Interactions* 7. (4): 1–17.

Song, X.P., Sexton, J.O., Huang, C., Channan, S. and Townshend, J.R. 2016. Characterizing the magnitude, timing and duration of urban growth from time series of Landsat-based estimates of impervious cover. *Remote Sensing of Environment* 175. 1–13.

Stewart, I.D. 2011. A systematic review and scientific critique of methodology in modern Urban Heat Island literature. *International Journal of Climatology* 31. (2): 200–217.

Stewart, I.D. and Oke, T.R. 2012. Local Climate Zones for urban temperature studies. *Bulletin of American Meteorological Society* 93. (12): 1879–1900.

Tan, J., Zheng, Y., Tang, X., Guo, C., Li, L., Song, G., Zhen, X., Yuan, D., Kalkstein, A.J., Li, F. and Chen, H. 2010. The urban heat island and its impact on heat waves and human health in Shanghai. *International Journal of Biometeorology* 54. 75–84.

Unger, J., Savić, S., Gál, T. and Milošević, D. 2014. *Urban Climate and Monitoring Network System in Central European Cities.* Novi Sad–Szeged, University of Novi Sad, Faculty of Sciences (UNSPMF) and University of Szeged, Department of Climatology and Landscape Ecology (SZTE), 101 p.

Unger, J., Sümeghy, Z., Szegedi, S., Kiss, A. and Géczi, R. 2010. Comparison and generalisation of spatial patterns of the urban heat island based on normalized values. *Physics and Chemistry of the Earth* 35. 107–114.

United Nations 2014. *World Urbanization Prospects: The 2014 Revision*. New York: United Nations. http://esa.un.org/unpd/wup/Highlights/WUP2014-Highlights.pdf.

Wilby, R.L. 2007. A review of climate change impacts on the built environment. *Built Environment* 14. 31–45.

Wong, K.V., Paddon, A. and Jimenez, A. 2013. Review of world urban heat islands: Many linked to increased mortality. *Journal of Energy Resources Technology* 135. (2): 022101–022112.

DOI: 10.15201/hungeobull.65.2.4 Hungarian Geographical Bulletin 65 2016 (2) 129–137.

Outdoor human thermal comfort in local climate zones of Novi Sad (Serbia) during heat wave period

Dragan D. MILOŠEVIĆ[1], Stevan M. SAVIĆ[1], Vladimir MARKOVIĆ[2], Daniela ARSENOVIĆ[2] and Ivan ŠEĆEROV[3]

Abstract

Urban climate monitoring system (UCMS) was established in Novi Sad (Serbia) in 2014 based on the Local Climate Zones (LCZs) classification system, GIS model calculations and field work. Seven built and two land cover LCZ types were delineated and 27 stations equipped with air temperature and relative humidity sensors were distributed across all LCZs. Suitability of the developed monitoring system for human outdoor thermal comfort research in different LCZs of the city and its surroundings was investigated during a heat wave period using Physiologically Equivalent Temperature (PET) index. During the daytime (night-time) the highest thermal loads are present in o*pen midrise* (*compact midrise*) LCZ, while the most comfortable is LCZ A (*dense trees*) during the whole day. In general, the highest thermal loads are obtained in *midrise*, followed by *low-rise*, *sparsely built*, *low plants* and *dense trees* LCZs. All LCZs (except LCZ A – *dense trees*) had higher PET when compared to LCZ D (LCZ D – *low plants*) during evening and nocturnal hours with maximum difference of 7.1 °C (00 UTC) between LCZ 2 (*compact midrise*) and LCZ D (*low plants*). Contrary to this, LCZ D (*low plants*) had higher PET compared to the majority of LCZs during the daytime with maximum difference of 8.5 °C (9 UTC) when compared to LCZ A (*dense trees*). Furthermore, the smallest thermal comfort differences during heat wave occurred between LCZs with similar structure (i.e. *open low-rise* and *large low-rise*, *compact midrise* and *compact low-rise*) and cover (i.e. *sparsely built* and *low plants*).

Keywords: urban climate monitoring, local climate zone, thermal comfort, heat wave, Novi Sad, Serbia

Introduction

People living in urban areas are under substantial thermal stress during the extreme temperature events such as heat wave (HW). Thermal discomfort will be exaggerated in the future as climate change scenarios show increase in the intensity and frequency of HWs in Europe in the twenty first century (Christensen, J. *et al.* 2007). Thus, monitoring of outdoor human thermal comfort conditions will provide important data for urban planners and decision-makers in order to create lively urban areas for its residents in the future (Milošević, D.D. *et al.* 2015a).

Development of urban climate monitoring system (UCMS) is needed in order to comprehensively investigate outdoor human thermal comfort in urban areas. Two UCMSs were developed in Novi Sad (Serbia) and Szeged (Hungary) in 2014 as part of the EU-founded research (URBAN-PATH, http://urban-path.hu) (Unger, J. *et al.* 2014). The networks were planned and based on the local climate zone classification system scheme developed by Stewart, I.D. and Oke, T.R. (2012). LCZs are defined as "regions of uniform surface cover, structure, material, and human activity that span hundreds of metres to several kilometres in horizontal scale" (Stewart, I.D. and Oke,

[1] Climatology and Hydrology Research Centre, Faculty of Sciences, University of Novi Sad, Trg Dositeja Obradovića 3, 21000 Novi Sad, Serbia. E-mails: dragan.milosevic@dgt.uns.ac.rs, stevan.savic@dgt.uns.ac.rs

[2] Center for Spatial Information of Vojvodina Province, Faculty of Sciences, University of Novi Sad; Trg Dositeja Obradovića 3, 21000 Novi Sad, Serbia. E-mails: vladimir.markovic@dgt.uns.ac.rs; daniela.arsenovic@dgt.uns.ac.rs

[3] Department of Geography, Tourism and Hotel Management, Faculty of Sciences, University of Novi Sad, Trg Dositeja Obradovića 3, 21000 Novi Sad, Serbia.

T.R. 2012). LCZ mapping method by Lelovics, E. *et al.* (2014), local urban climate knowledge and field work were needed in the process of delineation of LCZs in Novi Sad and the selection of suitable sites for the meteorological sensors deployment. Seven built and two land cover LCZ types were delineated in Novi Sad and air temperature *(Ta)* and relative humidity *(RH)* sensors were deployed on 27 locations inside them (Unger, J. *et al.* 2014). URBAN-PATH Portal and Urban Path System tool (UP-SYS tool) were created in order to visualise, process and save measured data for urban climate studies and for analysing entire systems work (Šećerov, I. *et al.* 2015).

To further improve the LCZ system, Stewart, I.D. *et al.* (2014) encouraged researchers to observe the climatic conditions of different LCZs. Recently, evaluation of LCZ scheme using stationary and (or) mobile measurements was performed in Glasgow (United Kingdom) (Emmanuel, R. and Krüger, E. 2012), Hong Kong SAR (China) (Siu, L.W. and Hart, M.A. 2013), Mendoza (Argentina) (Puliafito, S. *et al.* 2013), Dublin (Ireland) (Alexander, P.J. and Mills, G. 2014), Berlin (Germany) (Fenner, D. *et al.* 2014), Oberhausen (Germany) (Muller, N. *et al.* 2014), Olomouc (Czech Republic) (Lehnert, M. *et al.* 2014), Barranquilla (Colombia) (Villadiego, K. and Velay-Dabat, M.A. 2014), Kochi (India) (Thomas, G. *et al.* 2014), Nagano (Japan), Vancouver (Canada) and Uppsala (Sweden) (Stewart, I.D. *et al.* 2014) as well as Nancy (France) (Leconte, F. *et al.* 2015), Novi Sad (Serbia) (Unger, J. *et al.* 2011; Savić, S. *et al.* 2013; Milošević, D.D. *et al.* 2015a,b; Savić, S. *et al.* 2015), Dar es Salaam (Tanzania) (Ndetto, E.L. and Matzarakis, A. 2015) and Szeged (Hungary) (Unger, J. *et al.* 2015; Lelovics, E. *et al.* 2016). Nevertheless, further evaluations of conceptual division of urban-rural landscape into LCZs with meteorological and climatologic data as well as numerical models are needed. Obtained results will highlight necessary changes to the LCZ classification system needed to more accurately classify urban thermal environments (Stewart, I.D. *et al.* 2014).

In this study, we analyse the outdoor human thermal comfort conditions in different LCZs of the city of Novi Sad (Serbia). Results and conclusions will provide insight into outdoor comfort conditions in different LCZs of the city and reveal whether the urban climate monitoring network based on LCZ scheme is suitable for the intra-urban thermal comfort research. Temporary analysis was performed using weather data from extreme temperature event (HW).

Materials and methods

Novi Sad is a mid-sized city in the northern part of the Republic of Serbia (Southeast Europe), located on a plain from 80 to 86 m a.s.l. (45°15′N, 19°50′E). The river Danube flows along the southern and the south-eastern edge of the city, and its width varies from 260 to 680 m. The relatively narrow Danube–Tisza–Danube Canal passes through the northern part of the city (*Figure 1*). To the South of Novi Sad urban area, the northern slopes of Fruška Gora Mountain are located (the highest peak is 538 m a.s.l.) which descend steeply towards the Danube (Unger, J. *et al.* 2011). Novi Sad is the second largest city in Serbia with a population of 340,000 (Bajšanski, I.V. *et al.* 2015) and built-up area of 112 km^2.

The area is in Köppen-Geiger climate region *Cfb* (temperate warm climate with a rather uniform annual distribution of precipitation) (Kottek, M. *et al.* 2006). The mean annual air temperature in Novi Sad is 11.2 °C with an annual range of 22.1 °C. The coldest month is January (-0.4 °C) and the warmest month is July (21.7 °C). The mean annual amount of precipitation is 598 mm (based on the data from 1949 to 2013) (Bajšanski, I.V. *et al.* 2015).

For the determination of outdoor human thermal comfort conditions in different LCZs during a HW period (from 5th to 8th July 2014), PET index (*Table 1*) was calculated in RayMan model (Matzarakis, A. *et al.* 2007). Selected days were characterized by prevailing anticyclonic conditions.

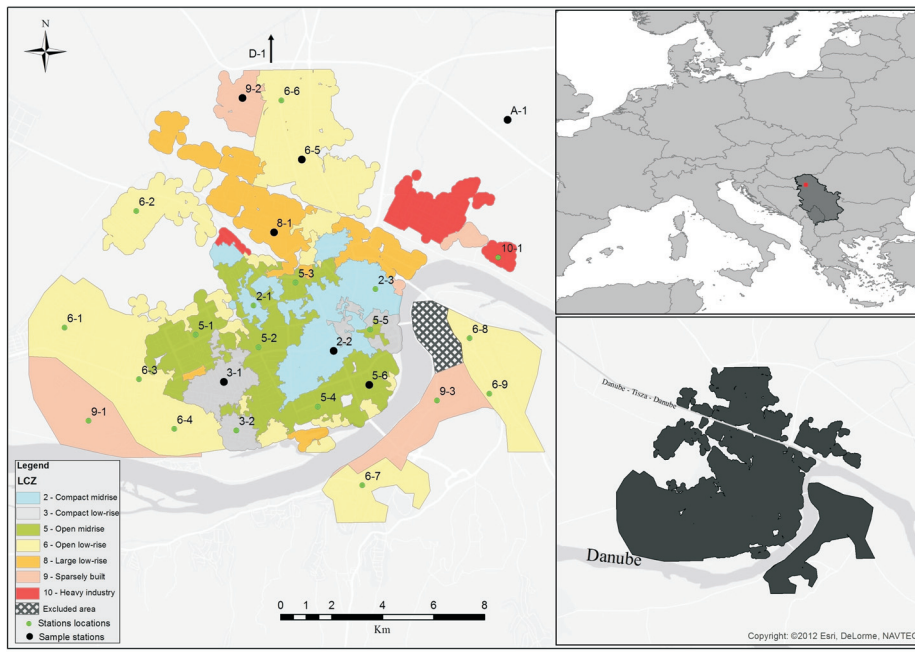

Fig. 1. Location of Novi Sad in Europe and Serbia (the red square upper right) and its built-up area (down right) as well as LCZs and stations sites (left; black dots = investigated sites). First number = LCZ class number, second number = station's identity number in the given LCZ class

*Table 1. PET index threshold values for thermal sensation and the physiological stress level of human beings**

PET, °C	Thermal sensation	Physiological stress level
under 4	Very cold	Extreme cold stress
4– 8	Cold	Strong cold stress
8–13	Cool	Moderate cool stress
13–18	Slightly cool	Slight cold stress
18–23	Comfortable	No thermal stress
23–29	Slightly warm	Slight heat stress
29–35	Warm	Moderate heat stress
35–41	Hot	Strong heat stress
over 41	Very hot	Extreme heat stress

*After Matzarakis, A. and Mayer, H. 1996.

The input data for the calculation of PET are hourly air temperature (*Ta*), relative humidity (*RH*), wind speed (*v*) and global radiation fluxes (*g*) for selected days. The *Ta* and *RH* are measured by the stations network, while the *v* for Novi Sad are from daily WRF model (Michalakes, J. *et al.* 2004) predictions initiated at 0 UTC for the Pannonian Basin using and NOAA/NCEP global forecast (GFS) (EMC 2003). The *v* was corrected using the roughness length calculated by the Roughness Mapping Tool (Gál, T. and Unger, J. 2009). RayMan model was used for the calculation of *g*. Time is given in Universal Time Coordinated (UTC). Local Standard Time in Serbia during summer is UTC + 2 h (Central European Summer Time). Representative station (*Figure 2*) for each LCZ was selected and their urban environment was modelled in RayMan model. The excep-

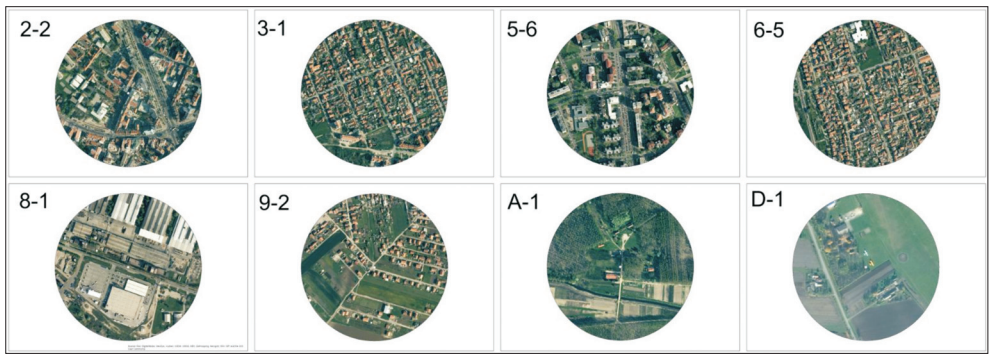

Fig. 2. Aerial photographs illustrating selected measurement sites (in the middle of the photo) with an environment of 500 m diameter in Novi Sad. First number = LCZ class number, second number = station's identity number in the given LCZ class: 2-2 (*compact midrise*), 3-1 (*compact low-rise*), 5-6 (*open midrise*), 6-5 (*open low-rise*), 8-1 (*large low-rise*), 9-2 (*sparsely built*), A-1 (*dense trees*), D-1 (*low plants*)

tion is station 10-1 (*heavy industry*) that did not work in the analysed period and could not be part of the analysis.

Several methods were applied in order to assess the statistical significance of average hourly PET differences between LCZs for whole HW as well as for daytime (from 4 UTC to 18 UTC) and night-time period (from 19 UTC to 3 UTC).

Firstly, hourly PET values in LCZ (PET x) were used to calculate average hourly PET values in individual LCZ for the whole HW period ($\overline{PET}\ x,i$).

Secondly, the average hourly PET difference between two LCZs x and y at time i ($\Delta\overline{PET}\ x-y,i$) was calculated according to ($\Delta\overline{PET}\ x-y,i = \overline{PET}\ x,i - \overline{PET}\ y,i$).

Thirdly, paired Student's t-tests were conducted to identify significant (p<0.05) differences in PET between individual LCZs.

Results

Thermal comfort conditions in different LCZs of the city and its surroundings are analyzed based on the average hourly PET during the HW period. PET magnitude is used to express thermal comfort differences between defined LCZ classes ($\Delta PET_{LCZ\ X\text{-}Y}$).

At daytime, LCZs 5, *D* and 3 show particularly high thermal loads (*Figure 3*). Conversely, areas with substantial shading effect (e.g. LCZs *A* and 2) have lower thermal load levels. The afternoon delayed reach of maximum PET value in LCZ 2 and decline and rise of PET in the LCZ *A* is due to the shading effects of buildings and trees in the vicinity of the stations. At night, the highest PET values are in the ′street canyon′ of the LCZ 2, whereas all other LCZs, especially the land cover LCZs *A* and *D* shows a deviation below the comfort range. In general, LCZ 5 had the highest average PET (28.0 °C) during HW, while LCZ *A* had the lowest PET (23.8 °C).

In order to quantify relative differences in diurnal thermal comfort conditions between urban and non-urban areas, we have compared average hourly PET in each selected LCZ with average hourly PET values in LCZ D (*low plants*) during HW ($\Delta PET_{LCZ\ X\text{-}D}$). *Figure 4* shows that all LCZs (except LCZ *A*) has higher PET values compared to LCZ *D* from 17:00 UTC to 5:00 UTC. Maximum PET difference of 7.1 °C is noticed between LCZs 2 and *D* at 0:00 UTC. These results agree with the literature which states that largest thermal contrasts occur during calm and clear nights. Contrary to this, LCZ D have higher PET values compared to majority of LCZs in the period 7:00–16:00 UTC with maximum difference of 8.5 °C compared to LCZ A at 9:00 UTC.

When comparing average hourly PET between LCZs ($\Delta PET_{LCZ\ X\text{-}Y}$) (intra-urban analy-

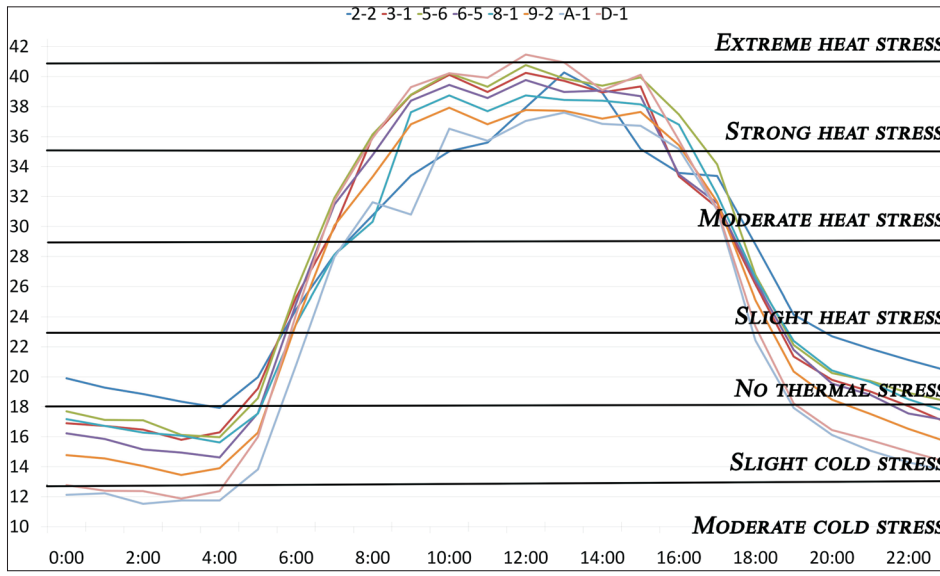

Fig. 3. Average hourly PET at measurements sites of the urban climate monitoring network in Novi Sad during HW (from 5th to 8th July 2014)

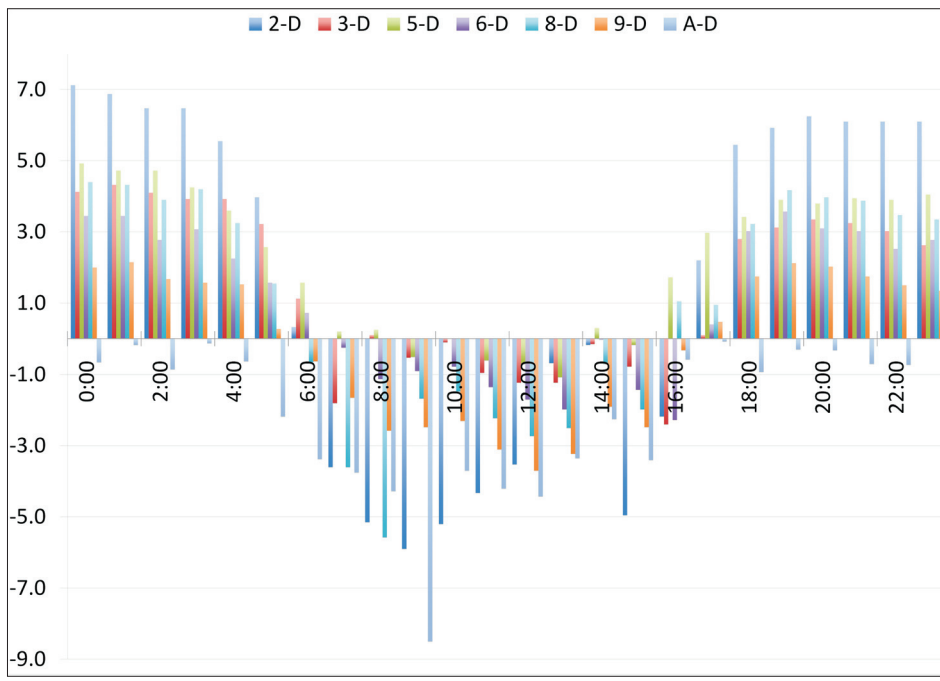

Fig. 4. Hourly PET magnitude ($\Delta PET_{LCZ\ X\text{-}D}$) in Novi Sad during HW (from 5th to 8th July 2014)

sis) during HW, obtained differences can suggest similarity or contrasts of their thermal environment. Statistically significant thermal comfort differences occur between all LCZs except LCZs 6 and 8 (0.1 °C), 2 and 3, as well as *D* and 9 (0.2 °C). This is presumably a consequence of similar values of surface structure (e.g. height and spacing of buildings and trees), cover (e.g. pervious or impervious) and fabric properties (e.g. albedo) between these LCZ pairs that lead to the creation of similar thermal comfort sensations inside them. Contrary to this, large differences in surface structure and cover properties essentially drive largest PET differences between built LCZs (5, 2 and 3) and natural LCZ *A* (4.2 °C, 3.7 °C and 3.5 °C, respectively). In general, highest thermal load is obtained in *midrise*, followed by *low-rise*, *sparsely built*, *low plants* and *dense trees* LCZs (*Table 2*).

At daytime, the LCZs do not show characteristic thermal comfort regimes with significant PET differences occurring between morphologically dissimilar LCZs (e.g. LCZs 2 and 9, 3 and *D*). The most intense physiological stress is calculated for LCZ 5 while the least intense is calculated for LCZ *A*. This can be explained by more solar radiation reaching the open midrise areas of the city leading to more heating during the day in contrast to the dense trees zone. During the night the highest PET values are in LCZ 2 while the lowest are in LCZ *A*. This could be the effect of trapping of long-wave radiation inside the ´street canyon´ of compact midrise zone. Thermal comfort differences between all LCZs are statistically significant during the night-time and more pronounced (up to 6.9 °C) than at daytime (up to 3.9 °C). This suggests that each LCZ has characteristic thermal comfort regime during the night-time. The largest PET differences are between urban LCZ 2 and non-urban LCZs *D* and *A* (6.9 °C and 6.4 °C, respectively) (*Table 3*).

Table 2. PET magnitude in Novi Sad during HW (from 5 to 8 July 2014)***

Station	2–1	3–2	5–6	6–5	8–1	9–2	A–1	D–1
2–1	–	-0.2	*0.5*	*-0.6*	*-0.7*	*-1.8*	*-3.7*	*-1.6*
3–2	0.2	–	*0.7*	*-0.4*	*-0.5*	*-1.6*	*-3.5*	*-1.4*
5–6	*-0.5*	*-0.7*	–	*-1.2*	*-1.2*	*-2.3*	*-4.2*	*-2.2*
6–5	*0.6*	*0.4*	*1.2*	–	-0.1	*-1.2*	*-3.1*	*-1.0*
8–1	*0.7*	*0.5*	*1.2*	0.1	–	*-1.2*	*-3.0*	*-0.9*
9–2	*1.8*	*1.6*	*2.3*	*1.2*	*1.1*	–	*-1.9*	0.2
A–1	*3.7*	*3.5*	*4.2*	*3.1*	*3.0*	*1.9*	–	*2.1*
D–1	*1.6*	*1.4*	*2.2*	*1.0*	*0.9*	-0.2	*-2.1*	–

*$\Delta PET_{LCZ\ X\text{-}Y}$. **Differences are presented as the LCZ type in column minus the LCZ type in row. Italics: statistically significant PET differences at the 5% level (paired t-test). Normal: statistically insignificant PET differences at the 5% level (paired t-test)

Table 3. PET magnitudes for day-time and night-time** in Novi Sad during HW from 5th to 8th July 2014.*

Station	2–1	3–2	5–6	6–5	8–1	9–2	A–1	D–1
2–1	–	*2.9*	*2.2*	*3.3*	*2.4*	*4.6*	*6.9*	*6.4*
3–2	*-1.4*	–	*-0.7*	*0.5*	*-0.4*	*1.7*	*4.1*	*3.5*
5–6	*-2.1*	*-0.8*	–	*1.2*	*0.3*	*2.5*	*4.8*	*4.3*
6–5	*-1.0*	*0.4*	*1.2*	–	*-0.9*	*1.3*	*3.6*	*3.1*
8–1	-0.3	*1.0*	*1.8*	*0.6*	–	*2.2*	*4.5*	*4.0*
9–2	0.1	*1.5*	*2.3*	*1.1*	*0.5*	–	*2.3*	*1.8*
A–1	*1.8*	*3.2*	*3.9*	*2.8*	*2.2*	*1.7*	–	*-0.5*
D–1	*-1.2*	0.1	*0.9*	-0.3	*-0.9*	*-1.4*	*-3.0*	–

*Bottom left area. Differences are presented as the LCZ type in column minus the LCZ type in row.
**Upper right area. Differences are presented as the LCZ type in row minus the LCZ type in column; Italics: statistically significant PET differences at the 5% level (paired t-test). Normal: statistically insignificant PET differences at the 5% level (paired t-test).

Discussion and conclusions

Outdoor human thermal comfort conditions were evaluated in different LCZs of the city of Novi Sad during a HW period. The data originated from the UCMS developed in Novi Sad. The highest average PET was noticed in built up LCZs 5 and 2, while the lowest were in areas with a substantial pervious land cover, namely the LCZs *A*, 9 and *D*. The results showed that statistically significant thermal comfort differences exist between the majorities of the LCZs. Only between LCZs 2 and 3, 6 and 8 as well as 9 and *D* this was not the case. Reasons for this could be the similar values of surface structure, cover and fabric properties (e.g. albedo) between these LCZ pairs.

During the daytime hours, the smallest thermal comfort differences occurred between LCZs with substantially different structural, cover, fabric and metabolism properties (i.e. between *compact midrise* and *sparsely built* LCZs) suggesting that LCZs do not have unique thermal environment at that time. Contrary to this, during the night all LCZs are thermally unique and exhibit statistically significant PET differences. Highest PET values were observed in midrise zones, followed by low-rise and sparsely built zones and lastly by low plants and dense trees zones. Furthermore, higher PET values were observed in compact zones when compared to open zones.

Research of human bio-climatologic comfort sensation in different LCZs is still scarce. This is no surprise as LCZ scheme is mainly introduced as a concept to enhance the understanding of air temperature differences within the urban area. Nevertheless this scheme can be used to observe the values of thermal comfort indices in different areas of cities. Previous studies regarding thermal comfort in Novi Sad showed PET differences up to 1.6 °C between subsequent LCZs and up to 5.1 °C for dissimilar LCZs on tropical day. On cold freezing day, PET differences were larger with up to 2.0 °C between close LCZs and up to 6.3 °C between dissimilar LCZs (Milošević, D.D. *et al.* 2015a). Results of our study are in accordance with findings of Kovács, A. and Németh, Á (2012) who found that LCZ 2 of Budapest has average PET values higher by 3 °C when compared to the suburbs (between LCZs 6 and *A*). The lower PET values during the daytime in residential area of the city correspond with the findings of Puliafito, S.E. *et al.* (2013) who point out that residential areas in Mendoza (Argentina) had from 2.0 °C to 4.0 °C lower PET values than the periphery of the city during the summer afternoon. In accordance with our results, higher thermal loads (i.e. PET values) were obtained for built LCZs 2 and 5 in Oberhausen (Germany) during the hot days (Ta_{max} > 30 °C) when compared to LCZs 9 and *A* (Muller, N. *et al.* 2014).

Numerous UHI studies used LCZ scheme to assess *Ta* differences in urban areas. Results from these studies showed that *Ta* during summer nights in LCZs with high impervious/building coverage in Berlin (Fenner, D. *et al.* 2014), Szeged (Lelovics, E. *et al.* 2016), Nancy (Leconte, F. *et al.* 2015) and Dublin (Alexander, P.J. and Mills, G. 2014) were higher up to 6.0 °C, 5.2 °C, 4.4 °C and 4.2 °C than *Ta* in LCZs with high pervious/vegetated coverage in these cities, respectively. This is in accordance with our results as nocturnal PET values in built LCZs of Novi Sad were up to 6.9 °C higher than in land cover LCZs which is not a surprise as *Ta* is part of the PET calculation.

The urban climate monitoring network in Novi Sad based on LCZ scheme showed to be suitable for the intra-urban thermal comfort research during the HW period. Comfortable and uncomfortable outdoor areas in the cities were detected and thermal comfort differences were quantified. Nevertheless, further long-term UHI and thermal comfort investigations from different cities are needed in order to evaluate and improve the proposed LCZ scheme. Measurements of meteorological elements from UCMSs based on LCZ scheme will help in achieving this goal. Furthermore, measured and calculated parameters of human thermal comfort from

UCMSs will provide urban planners and architects the opportunity to propose and design comfortable areas in the city in order to mitigate the negative effects of urban climate.

Acknowledgement: The study was supported by the Hungary-Serbia IPA Cross-border Co-operation EU Programme (HUSRB/1203/122/166 – URBAN-PATH) and the Serbian Ministry of Education, Science and Technological Development (project no. 43002).

REFERENCES

Alexander, P.J. and Mills, G. 2014. Local climate classification and Dublin's urban heat island. *Atmosphere* 5. 755–774.

Bajšanski, I.V., Milošević, D.D. and Savić, S.M. 2015. Evaluation and improvement of outdoor thermal comfort in urban areas on extreme temperature days: Applications of automatic algorithms. *Building and Environment* 94. 632–643.

Christensen, J., Hewitson, B., Busuioc, A., Chen, A., Gao, X. and Held, I. 2007. Regional climate projection. Technical report. In *Climate Change 2007: The Physical Science Basis. Contribution of Working Group I to the fourth assessment report of the Intergovernmental Panel on Climate Change*. Eds.: Solomon, S., Qin, D., Manning, M., Chen, Z., Marquis, M. and Averyt, K.B. Cambridge UK and New York, Cambridge University Press.

EMC 2003. *The GFS Atmospheric Model*. NCEP Office Note 442, 14 p.

Emmanuel, R. and Krüger, E. 2012. Urban heat island and its impact on climate change resilience in a shrinking city: The case of Glasgow, UK. *Building and Environment* 53. 137–149.

Fenner, D., Meier, F., Scherer, A. and Polze, A. 2014. Spatial and temporal air temperature variability in Berlin, Germany, during the years 2001–2010. *Urban Climate* 10. 308–331.

Gál, T. and Unger, J. 2009. Detection of ventilation paths using high-resolution roughness parameter mapping in a large urban area. *Building and Environment* 44. 198–206.

Kottek, M., Grieser, J., Beck, C., Rudolf, B. and Rubel, F. 2006. World map of the Köppen-Geiger climate classification updated. *Meteorologische Zeitschrift* 15. 259–263.

Kovács, A. and Németh, Á. 2012. Tendencies and differences in human thermal comfort in distinct urban areas in Budapest, Hungary. *Acta Climatologica et Chorologica* 46. 115–124.

Leconte, F., Bouyer, J., Claverie, R. and Petrissans, M. 2015. Using Local Climate Zone scheme for UHI assessment: Evaluation of the method using mobile measurements. *Building and Environment* 83. 39–49.

Lehnert, M., Geletič, J., Husák, J. and Vysoudil, M. 2014. Urban field classification by "local climate zones" in a medium-sized Central European city: the case of Olomouc (Czech Republic). *Theoretical and Applied Climatology* 122. 531–541.

Lelovics, E., Unger, J., Gál, T. and Gál, C.V. 2014. Design of an urban monitoring network based on Local Climate Zone mapping and temperature pattern modeling. *Climate Research* 60. 51–62.

Lelovics, E., Unger, J., Savić, S., Gál, T., Milošević, D., Gulyás, Á., Marković, V., Arsenović, D. and Gál, CV. 2016. Intra-urban temperature observations in two Central European cities: a summer study. *Időjárás* (in print)

Matzarakis, A. and Mayer, H. 1996. *Another kind of environmental stress: thermal stress*. In WHO Collaborating Centre for Air Quality Management and Air Pollution Control 18. 7–10.

Matzrakis, A., Rutz, F. and Mayer, H. 2007. Modelling radiation fluxes in simple and complex environments: application of the RayMan model. *International Journal of Biometeorology* 51. 323–334.

Michalakes, J., Dudhia, J, Gill, D., Henderson, T., Klemp, J., Skamarock, W. and Wang, W. 2004. The Weather Reseach and Forecast Model: Software architecture and performance. *Proceedings of the 11th ECMWF Workshop on the Use of High Performance Computing In Meteorology*, Reading, UK.

Milošević, D.D., Savić, S.M., Unger, J. and Gál, T. 2015a. Urban climate monitoring system suitability for intra-urban thermal comfort observations in Novi Sad (Serbia) – with 2014 examples. *9th International Conference on Urban Climate jointly with 12th Symposium on the Urban Environment*. Toulouse, France, 1–6.

Milošević, D.D. and Savić, S.M. 2015b. *Thermal comfort observations in the City of Novi Sad (Serbia) in 2014*. EUGEO 2015 – Convergences and Divergences of Geography in Europe, Budapest, p. 78.

Muller, N., Kuttler, W. and Barlag, A.-B. 2014. Counteracting urban climate change: adaptation measures and their effect on thermal comfort. *Theoretical and Applied Climatology* 115. 243–257.

Ndetto, L.E. and Matzarakis, A. 2015. Urban atmospheric environment and human biometeorological studies in Dar es Salaam, Tanzania. *Air Quality, Atmosphere and Health* 8. 175–191.

Puliafito, S., Bochaca, F., Allende, D. and Fernandez, R. 2013. Green areas and microscale thermal comfort in arid environments: A case study in Mendoza, Argentina. *Atmospheric and Climate Sciences* 3. 372–384.

Savić, S., Bajšanski, I. and Milošević, D.D. 2015. *Evaluation of outdoor thermal comfort in urban transformations of Novi Sad (Serbia).* EUGEO 2015

– Convergences and Divergences of Geography in Europe, Budapest, p. 79.

Savić, S., Milošević, D., Lazić, L., Marković, V., Arsenović, D. and Pavić, D. 2013. Classifying urban meteorological stations sites by "Local Climate Zones": Preliminary results for the City of Novi Sad (Serbia). *Geographica Pannonica* 17. (3): 60–68.

Šećerov, I., Savić, S., Milošević, D., Marković, V. and Bajšanski, I. 2015. Development of an automated urban climate monitoring system in Novi Sad (Serbia). *Geographica Pannonica* 19. (4): 174–183.

Siu, L.W. and Hart, M.A. 2013. Quantifying urban heat island intensity in Hong Kong SAR, China. *Environmental Monitoring and Assessment* 185. 4383–4398.

Stewart, I.D. and Oke, T.R. 2012. Local Climate Zones for urban temperature studies. *Bulletin of American Meteorological Society* 93. 1879–1900.

Stewart, I.D., Oke, T.R. and Krayenhoff, E.S. 2014. Evaluation of the "local climate zone" scheme using temperature observations and model simulations. *International Journal of Climatology* 34. 1062–1080.

Thomas, G., Sherin, A.P., Ansar, S. and Zachariah, E.J. 2014. Analysis of urban heat island in Kochi, India, using a modified local climate zone classification. *Procedia Environmental Sciences* 21. 3–13.

Unger, J., Savić, S. and Gál, T. 2011. Modelling of the annual mean urban heat island pattern for planning of representative urban climate station network. *Advances in Meteorology* 2011. ID 398613, 9 p.

Unger, J., Savic, S., Gál, T. and Milošević, D. 2014. *Urban climate and monitoring network system in Central European cities*. Novi Sad, 103 p.

Unger, J., Savić, S., Gál, T., Milošević, D., Marković, V., Gulyás, Á. and Arsenović, D. 2015. Urban climate monitoring networks based on LCZ concept. *9th International Conference on Urban Climate jointly with 12th Symposium on the Urban Environment,* Toulouse, France, 1–6.

Villadiego, K. and Velay-Dabat, M.A. 2014. Outdoor thermal comfort in a hot and humid climate of Colombia: A field study in Barranquilla. *Building and Environment* 75. 142–152.

AQUINCUM
Ancient landscape – ancient town

Edited by
Katalin H. Kérdő and Ferenc Schweitzer

Geographical Institute Research Centre for Astronomy and Earth Sciences MTA

Budapest, 2014. 188 p.

Geomorphological–paleoenvironmental studies supporting archeological excavations and investigations are to be considered a new trend within the broader sphere of studies on environment and geomorphology. By publishing the latest achievements of researches of this kind carried out on the territory of Aquincum and in its wider surroundings this book may equally reckon on the interest of professional circles and inquiring audience.

Therefore the publication of such a volume of somewhat unusual character is welcome. The project could be completed as a result of the close cooperation of two important branches of studies, notably geography and archeology. They both have long lasting traditions in our country and on this occasion were represented by two prominent institutions, the Geographical Institute of the Hungarian Academy of Sciences, and the Aquincum Museum of the Budapest History Museum. Their contribution has made possible the publication of this book.

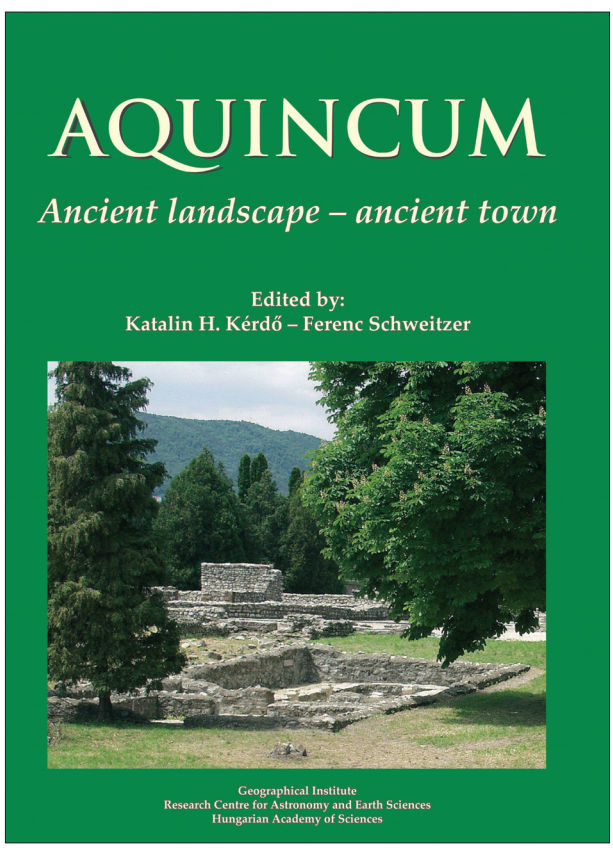

The studies were aimed to clear up the role of those natural factors which exerted a profound influence on the development of the settlement structure during the Roman Period. Romans had a special ability to realize advantages provided by geomorphological characteristics and they had made a good use of natural waters, flood-plain surface features and parent rocks for their creativity.

The volume is also deemed as a pioneering work with regard to the richly illustrated presentation of geological, geographical and other natural features exposed in several places in the course of archeological excavations. A short summary shows the most important objects of the Roman Period related to natural endowments and traces of activities of the time leading to environmental transformation.

Based on geomorphological evidence a new answer is proposed to a previously raised problem whether the Hajógyári Island existed as an islet already in the time of the Romans. Another intriguing issue tackled is the purpose of the system of trenches found in several places along the Danube River.

Price: EUR 20.00
Order: Geographical Institute of RCAES MTA. H-1112 Budapest, Budaörsi u. 44.
E-mail: magyar.arpad@csfk.mta.hu

DOI: 10.15201/hungeobull.65.2.5 Hungarian Geographical Bulletin 65 2016 (2) 139–153.

Differences between the evaluation of thermal environment in shaded and sunny position

Noémi KÁNTOR[1]

Abstract

Great attention has been paid in the last one and a half decade to the subjective evaluation of atmospheric conditions in different outdoor and semi-outdoor urban environments. Several field surveys were conducted all around the world in order to specify those physical and personal factors that influence the perception of thermal environment. Many studies reported about seasonal differences in the subjective assessment concerning thermal sensitivity as well as the so-called neutral temperature. The present investigation aims to reveal these seasonal differences in Hungary and to scrutinise the effect of solar exposure (staying in shaded position or in the sun) on these patterns. The analyses are based on a long-term outdoor thermal comfort project with 78 measurements days conducted on six recreational places in Szeged, Hungary. In the frame of the project thousands of people were asked about their actual thermal sensation and about their preference for any change regarding the thermal environment. Parallel to the questionnaire survey, detailed human bio-meteorological measurements were carried out in the vicinity of the questioned individuals. A well-established human bio-meteorological index was calculated from the measured atmospheric parameters: the Physiologically Equivalent Temperature (*PET*). Regression analysis was performed between the subjective and objective measures in order to specify neutral and preferred temperatures (*nPET, pPET*). Furthermore, in the case *pPET* values a new assignment procedure was also implemented building on probit model technique. The two analytical approaches resulted in very similar *pPET* values in every case when the sample size was sufficiently large. The study revealed much higher *pPET* than *nPET* values in every season; moreover, significant differences depending on the sun exposure of the subjects.

Keywords: subjective assessment, Physiologically Equivalent Temperature, neutral and preferred temperature, solar exposure

Introduction

The excessive level of urbanization (UNFPA 2011) and the projected challenges due to climate change (IPCC 2014) necessitate dealing with urban climate issues all around the world. Correspondingly, the number of studies with focus on the thermal conditions within cities is rapidly growing (Chen, L. and Ng, L. 2012; Rupp, R.F. *et al.* 2015). Several from the earlier investigations applied well-established human bio-meteorological indices, for example the Physiologically Equivalent Temperature – *PET* (Höppe, P. 1999), in order to express the physiological and comfort aspects of small-scale meteorological conditions in outdoor urban spaces. A great portion of these examinations was built on micrometeorological measurements (e.g. Mayer, H. *et al.* 2008; Lin, T.-P. *et al.* 2010; Hwang, R.-L. *et al.* 2011; Gómez, F. *et al.* 2013), while others applied numerical models in order to simulate the consequences of different landscape design strategies on thermal comfort and human health (e.g. Fröhlich, D. and Matzarakis, A. 2013; Müller, N. *et al.* 2014). Most of the existing analyzes were based on the original threshold values of the applied index. In the case of the aforementioned *PET* index the category benchmarks (*Figure 1*) are based on the physiological reactions of a 'typical' Central European man (Matzarakis, A. and Mayer,

[1] Department of Climatology and Landscape Ecology, University of Szeged. H-6722 Szeged, Egyetem u. 2. E-mail: sztyepp@gmail.com

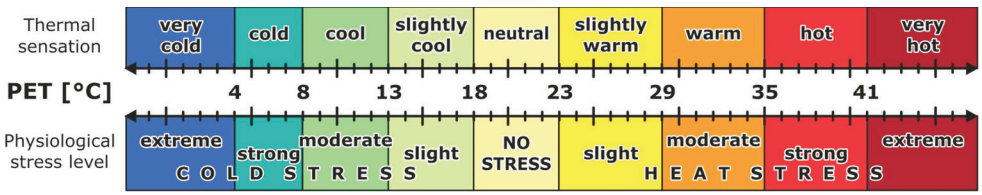

Fig. 1. The original threshold values of the *PET* index reflecting the thermal sensation categories and the level of physiological stress

H. 1996; Matzarakis, A. *et al.* 1999). However, adopting the preset threshold values regardless of the geographical location raises the question of the result's relevance regarding the thermal perception of local inhabitants.

Indeed, numerous studies found considerable differences between the actual thermal perception of people and the predicted evaluation based on the well-known objective indices (e.g. Lin, T.-P. and Matzarakis, A. 2008; Kántor, N. *et al.* 2012a; Yin, J.F. *et al.* 2012; Krüger, E.L. *et al.* 2013; Lai, D. *et al.* 2014; Tung, C.-H. *et al.* 2014). Several papers reported that those thermal conditions at which people feel generally neutral depend on the geographical location and even on the time of the year (e.g. Nikolopoulou, M. and Lykoudis, S. 2006; Hwang, R.-L. and Lin, T.-P. 2007; Lin, T.-P. 2009; Lin, T.-P. *et al.* 2011; Kántor, N. *et al.* 2012b; Lindner-Cendrowska, K. 2013; Yahia, M.W. and Johansson, E. 2013; Yang, W. *et al.* 2013a,b; Pearlmutter, D. *et al.* 2014; Chen, L. *et al.* 2015; Zeng, Y. and Dong, L. 2015). These results prove that living under various background climates lead to different degree of thermal adaptation in people, and even in the case of the same population, there are seasonal differences in the subjective evaluation.

Hungarian studies contributed also to this extensive research area and revealed obvious seasonal differences in the subjective thermal perception and preference patterns of local people (Kántor, N. *et al.* 2012a; Kovács, A. *et al.* 2015). Personal differences, time of the day (Pearlmutter, D. *et al.* 2014) and outdoor or semi-outdoor nature of the physical environment (Hwang, R.-L. and Lin, T.-P. 2007) were also investigated as affecting factors. However, to date, no studies have examined the influence of solar exposure on the subjective assessment of thermal environment. Therefore the present study aims to reveal these differences using the data of a long-term Hungarian outdoor thermal comfort (OTC) project. The main targets of this paper are set as follows:

1. Determining exposure-dependent differences in the subjective thermal sensation and thermal preference patterns in different seasons.

2. Specifying the so-called neutral and preferred temperature values of Hungarians according to season and solar exposure.

Methods

The city of Szeged

Building on the experiences of earlier investigations a long-term OTC project was conducted in the city of Szeged (Hungary) (46°15′N, 20°09′E). Szeged is the regional centre of the Southern Hungarian Great Plain with an urbanized area of about 50 km^2. The city offers ideal study areas for urban climate and human bio-meteorological investigations (e.g. Unger, J. 1996; Gulyás, Á. *et al.* 2006, 2009) because it is spread on a flat area without considerable topographical differences (78–85 m a.s.l.) which allows small-scale meteorological results to be generalized. Land-use types vary from the densely built-up inner city to the detached housing suburban areas, allowing the development of several local climate zone types (Unger, J. *et al.* 2014).

Szeged has warm temperate climate with uniform annual distribution of precipitation. The yearly amount of precipitation is low (489 mm), while the sunshine duration is high (1978 hours). The annual temperature is 10.6 °C. July and August are the hottest months and January is the coldest time of the year. The daily maximum temperature is generally above 10 °C from March to October, therefore these eight months are more suitable for outdoor activities. On the contrary, the period from November to February is cold when the monthly amount of sunshine remains below 100 hours (HMS 2015).

Being already one of the warmest cities in Hungary, the urban climate of Szeged is expected to be affected more intensively by the predicted warming tendencies in the Carpathian Basin (Pongrácz, R. *et al.* 2013). Moreover, Szeged is the third most populated city in the country with more than 170,000 permanent residents. All of these attributes make it very interesting from the viewpoint of OTC investigations.

Outdoor thermal comfort surveys in Szeged

Generally, OTC surveys consist of on-site human bio-meteorological measurements as well as transverse questionnaire surveys when great numbers of people are inquired about their subjective assessments regarding the actual thermal environment (Chen, L. and Ng, E. 2012; Rupp, R.F. *et al.* 2015). The Hungarian OTC measurements were carried out in 2011, 2012 and 2015. The investigations took place on six recreational areas, including popular urban squares, parks, playgrounds, and pedestrian zones (*Figure 2*). Two of the investigated squares (Szent István square and Dugonics square) received an Award of excellence for complete reconstruction from the Hungarian Society for Urban Planning. All survey sites are in the urbanized region of Szeged, allowing large number of visitors attending on them. The study areas can be characterized with a variety of landscape-design solutions, materials, orientations, vegetation cover, etc. For that reason, a wide range of small-scale human bio-meteorological conditions may be expected on them.

With respect to outdoor activity, summer and the two transient seasons are of particular importance in Hungary. Accordingly, the OTC investigations covered the period from the end of March to the end of October, resulting, altogether, in 78 measurement days (*Table 1*). The data collection lasted from 10 a.m. to 6 p.m. except for those days when significant precipitation events interrupted the measurements.

Micrometeorological measurements

Two special human bio-meteorological stations were used to collect all important atmospheric variables that influence human thermal sensation. The stations were placed simultaneously at two significantly different sites of the same study area; typically in sunny and shaded (shaded by tree or building) position. Depending on the specific design of the study areas, the stations were placed sometimes on grassy surface, while other times on different types of artificial ground cover like asphalt pavement, red-coloured paving stones and light-coloured gravel (*Figure 3*).

The stations recorded one-minute averages of all meteorological variables. Air temperature (T_a), relative humidity (*RH*) and wind speed (v) were measured by a WXT520 Vaisala weather transmitter in the case of both stations (*Figure 3*). Rotatable net radiometers were used to monitor the 3D radiant environment, i.e. to record short-wave and long-wave radiation flux densities from six perpendicular directions (K_i and L_i [W/m^2], i: up, down, East, West, South, North). One of the stations was equipped with CNR1, and the other with CNR4 type Kipp & Zonen net radiometer. By means of telescopic tripods the sensors were placed at a height of 1.1–1.2 m above ground level which is suitable for OTC investigations (Mayer, H. *et al.* 2008).

Normally, the arm of the net radiometer points to the South. In this position the two pyranometers and two pyrgeometers faces

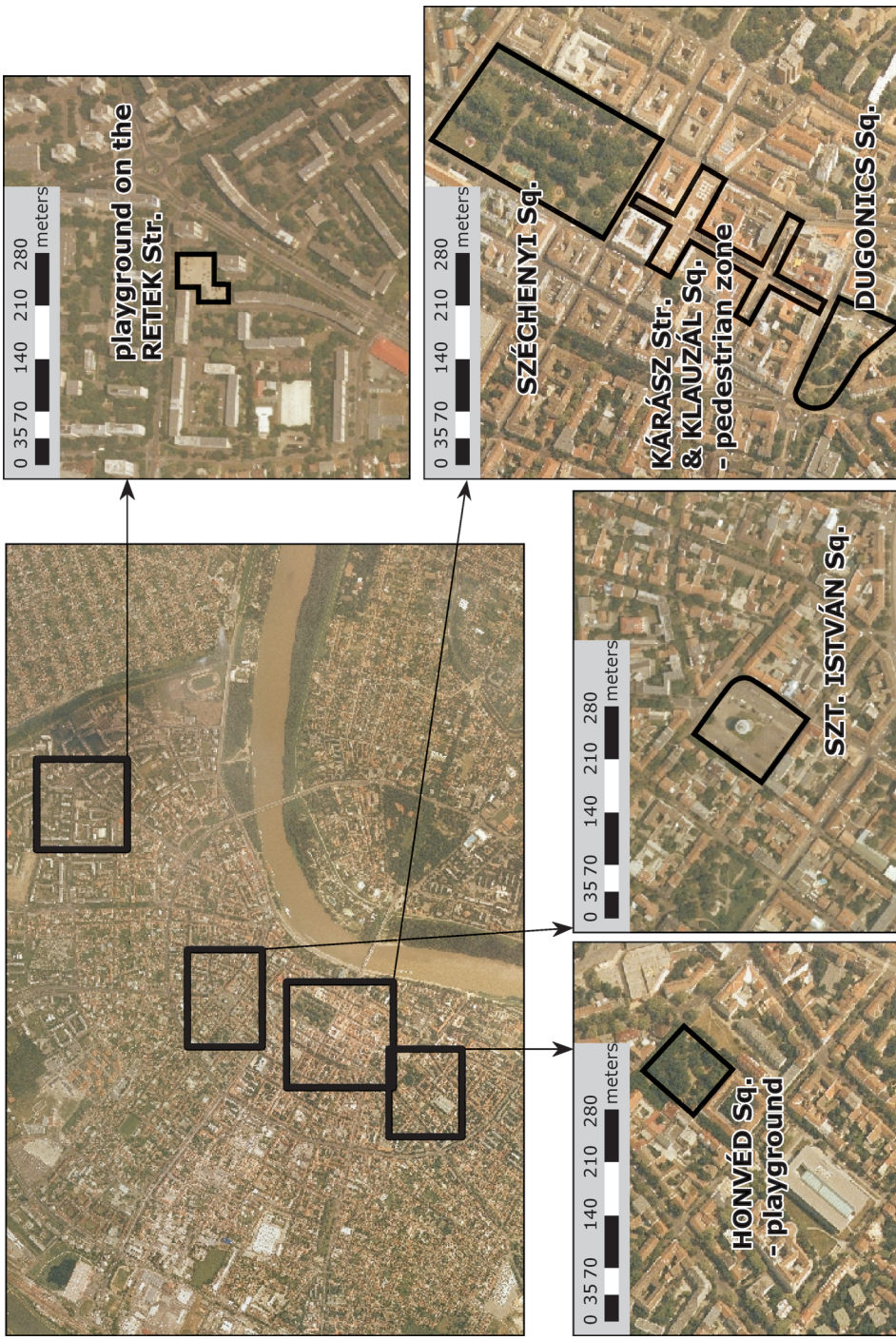

Fig. 2. Aerial photos about Szeged indicating the location of the study areas

Table 1. Seasonal distribution of OTC measurement days in Szeged

Spring (26 days)			Summer (28 days)			Autumn (24 days)	
March	April	May	June	July	August	September	October
29.03.2011	12.04.2011	03.05.2011	22.06.2011	04.07.2011	03.08.2011	12.09.2011	03.10.2011
30.03.2011	13.04.2011	04.05.2011	07.06.2012	08.07.2011	04.08.2011	13.09.2011	04.10.2011
26.03.2012	19.04.2011	10.05.2011	08.06.2012	12.07.2011	22.08.2011	19.09.2011	10.10.2011
27.03.2012	20.04.2011	11.05.2011	21.06.2012	02.07.2012	23.08.2011	26.09.2011	17.10.2011
–	26.04.2011	08.05.2012	25.06.2012	05.07.2012	02.08.2012	27.09.2011	18.10.2011
–	27.04.2011	15.05.2012	08.06.2015	06.07.2012	27.08.2012	17.09.2012	25.10.2011
–	02.04.2012	16.05.2012	15.06.2015	09.07.2012	28.08.2012	18.09.2012	01.10.2012
–	03.04.2012	08.05.2015	17.06.2015	10.07.2012	–	19.09.2012	03.10.2012
–	16.04.2012	13.05.2015	18.06.2015	19.07.2012	–	21.09.2012	05.10.2012
–	23.04.2012	19.05.2015	–	20.07.2012	–	24.09.2012	08.10.2012
–	24.04.2012	20.05.2015	–	23.07.2012	–	26.09.2012	10.10.2012
–	–	–	–	24.07.2012	–	–	17.10.2012
–	–	–	–	–	–	–	19.10.2012

Fig. 3. Human bio-meteorological measurements and questionnaire surveys on popular recreational areas of Szeged. (Accuracy of measured parameters are also indicated).

upward and downward, allowing the measurement of K_i and L_i separately from the upper and lower hemisphere (K_u, K_d, L_u, L_d). After 3-minute measurement in this position, the net radio-meters were rotated manually into the second position when the sensors faced to East and West (K_e, K_w, L_e, L_w). Again, after 3-minute measurement the arms were turned with 90° to measure from South and North (K_s, K_n, L_s, L_n). Considering the 10 a.m. – 6 p.m. measurement interval, this procedure required 160 rotations per day in the case of both stations. Taking into account the response time of the sensors as well as the time delay due to the manual rotation, all K_i and L_i were deleted that were recorded first time after the rotations.

Index calculation

Mean radiant temperature (T_{mrt} [°C]) is a parameter with primary importance in the field of human bio-meteorology and OTC surveys. It combines all long-wave and short-wave radiant flux densities into a single value with °C-dimension. T_{mrt} is defined as the uniform temperature of an imaginary black body-radiating surrounding, which results in the same radiant heat exchange for the human body inside this hypothetical environment as the complex 3D-radiant environment in the reality (Höppe, P. 1992; Kántor, N. and Unger, J. 2011). T_{mrt} is usually calculated for a standardized standing person. In the case of this study, T_{mrt} was determined based on six K_i and six L_i flux densities, which were obtained from three consecutive stands of the net radiometer:

$$T_{mrt} = \left(\frac{\sum_{i=1}^{6} W_i \cdot (a_k \cdot K_i + a_l \cdot L_i)}{a_l \cdot \sigma} \right)^{\frac{1}{4}} - 273.15$$

where a_k and a_l are absorption coefficients of the clothed human body in the short- and long-wave radiation domain (assumed to be 0.7 and 0.97, respectively), σ is the Stefan–Boltzmann constant ($5.67 \cdot 10^{-8}$ W/m^{2}K^4) and W_i is a direction-dependent weighting factor. Assuming standing reference subject, W_i is 0.06 for vertical and 0.22 for horizontal directions (Höppe, P. 1992).

PET index was selected for the purpose of this study to describe the thermal environment along with the possible thermal sensation and degree of physiological stress (*Figure 1*). *PET* is regarded to be one of the most comprehensive human bio-meteorological indices and it has been widely used for different OTC studies all around the world (e.g. Gulyás, Á. *et al.* 2006; Lin, T.-P. 2009; Kántor, N. *et al.* 2012a; Yahia, M.W. Johansson, E. 2013; Pearlmutter, D. *et al.* 2014; Kovács, A. *et al.* 2015; Zeng, Y. and Dong, L. 2015). PET calculations were performed with the RayMan software (Matzarakis, A. *et al.* 2010) by using the formerly obtained T_{mrt} values and the directly measured T_a, *RH*, *v* values. The evaluation by *PET* (*Figure 1*) always refers to a standardized subject (a 'typical' 35 years old Central European man performing light activity and wearing light business suit) representing a large group of people (Höppe, P. 1999).

Recording subjective assessment of thermal environment

The assessment of thermal conditions is highly subjective, meaning that different individuals may evaluate the same thermal environment differently (Mayer, H. 2008). In order to reveal these patterns, structured interviews were carried out with thousands of people spending their time in the study areas during the human-meteorological measurements. People who walked, stood or sat near to the stations were invited to fill an OTC questionnaire which could be finished within five minutes (*Figure 3*). Similarly to many international examples (e.g. Nikolopoulou, M. and Lykoudis, S. 2006; Hwang, R.-L. and Lin, T.-P. 2007; Lin, T.-P. 2009; Krüger, E.L. *et al.* 2013; Yang, W. *et al.* 2013a,b; Pearlmutter, D. *et al.* 2014; Chen, L. *et al.* 2015; Zeng, Y. and Dong, L. 2015), the questionnaire consisted of more question blocks regarding personal factors, area usage, behavioral reactions, evaluation of the area and subjective assessment of the thermal environment (Kántor, N. *et al.* 2012a).

This paper focuses on the subjective thermal sensation and thermal preference. Thermal Sensation Votes (*TSV*) were collected by means of a semantic differential scale with 9 main ordered categories: very cold (-4), cold (-3), cool (-2), slightly cool (-1), neutral (0), slightly warm (1), warm (2), hot (3), very hot (4). Selection of intermediate options was also possible. Thermal Preference Votes were recorded by answering the question 'Would you like any changes in the actual thermal conditions to feel (more) comfortable?' In this case, people could choose from three options: want cooler (-1), want no change (0), want warmer (+1).

From the collected personal information this paper focuses on the solar exposure of subjects – whether they stayed in the sun, or in the shade. Sometimes the ascertainment of the position was not possible because clouds reduced the intensity of global radiation, thus made impossible to distinguish shaded and sunny areas. These questionnaires were excluded from the analyses. Additionally, many samples were removed due to missing meteorological data (failure in the recordings of any micrometeorological parameters which hindered the calculation of *PET* index).

Analysis methods

Regression analysis was performed for comparing subjective thermal sensation (and thermal preference) patterns and specifying neutral (and preferred) temperatures according to the investigated seasons and solar exposure. Besides, probit model was adopted to analyse the thermal preferences of Hungarians among different circumstances. These main analyses were supplemented with simple descriptive statistics. The analyses were performed within the PASW Statistics software, and some of the artworks were created within MS Excel.

Results and discussion

Thermal sensation according to seasons and solar exposure

6,764 questionnaires were obtained during the field surveys, but only 4,700 subjects were selected for the purpose of this study; only those who had valid *PET* index and solar exposure. All interviewees were Hungarian citizens, generally they reported about good health conditions and 2/3 of them were female. The individuals' age varied between 5 to 95 years, and most of them belonged to the young age group (14 to 30 years).

People selected generally from the main thermal sensation votes (*Figure 4*). Nevertheless, more than 20% of the questioned individuals selected intermediates (votes of 1.5 and 2.5 occurred most frequently). The most frequent vote was *slightly warm* (1) in both transient seasons. In summer however, in accordance with the warmer thermal

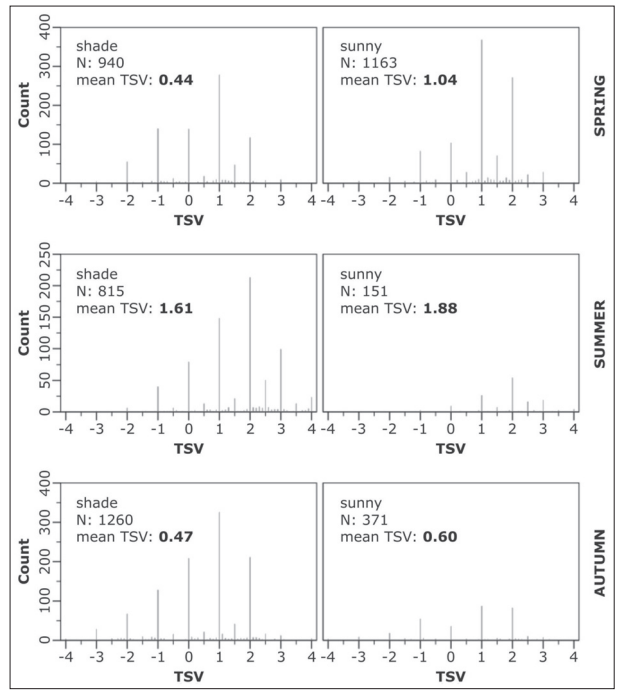

Fig. 4. Distribution of *TSV* according to seasons and subjects' solar exposure

conditions, people reported most frequently *warm* (2) thermal sensation. In each season, mean *TSV* values were lower if subjects stayed in the 'shade'. The greatest difference between the two exposure groups was found in spring (*Figure 4*).

Neutral temperature and neutral PET zone

Neutral temperature (*nPET*) refers to those thermal conditions at which people feel neither cool, nor warm, i.e. which are perceived as neutral. Several studies determined *nPET* by regression analysis between *TSV* and *PET* (e.g. Lin, T.-P. 2009; Kántor, N. *et al.* 2012a,b; Yang, W. *et al.* 2012b; Krüger, E.L. *et al.* 2013; Yahia, M.W. and Johansson, E. 2013; Kovács, A. *et al.* 2015). Since thermal sensation varies greatly among subjects even in the same thermal conditions (i.e. at the same *PET* value), mean thermal sensation votes (*MTSV*) were calculated according to 1 °C wide *PET* intervals. Considerably different thermal perception patterns were revealed among the investigated groups by plotting mean *TSV* values against *PET* index, and weighting them with the case numbers per *PET* bin (*Figure 5*).

Quadratic regression fit the *TSV–PET* data pairs well with considerable statistical significance (*Table 2*). According to the determination coefficients (R^2) at least 92% of the variability in Hungarians' subjective thermal sensation can be explained by the *PET* index in every season if the subjects stay in shaded position. The worst R^2 value was found in the summertime 'sunny' group; probably due to the small sample size ($N = 151$).

Neutral temperature (*nPET*) can be determined by solving the regression equation for $TSV = 0$, or reading its value from the regression chart. The fitted quadratic functions intersect the $TSV = 0$ line at different *PET* values, indicating sometimes considerably different *nPET* (*Figure 5*). Substituting -0.5 and 0.5 into the quadratic equations assign the lower and upper PET thresholds of the neutral category. Worth noting that for the 'sunny' group in summer the values of *nPET* and the lower boundary of neutrality could be determined only by extrapolation, i.e. outside from the covered *PET* range (*Figure 5*).

Preferred temperature and preferred PET zone

Two analysis techniques were adopted aiming to allocate the preferred thermal conditions in different seasons and different exposure groups. First, the above presented regression procedure was repeated for thermal preference votes (Kovács, A. *et al.* 2015; *Table 3*). Compared to the case of *TSV*, the obtained R^2 values were lower in this case, probably due to people had only three preference options to choose. However, the significance level was 0.000 in every group and the quadratic functions fitted the *TPV–PET* data pairs fairly well. Preferred temperature (*pPET*), as well as the boundaries of the preferred *PET* zone were calculated by substituting 0, 0.125 and -0.125 into the quadratic equations. The obtained results will be demonstrated later.

The other way of *pPET* determination is based on probit model (Ballantyne, E.R. *et al.* 1977). Generally, probit analysis is used to investigate many kinds of dichotomous response variables in a variety of research fields. In this study, two binomial response variables were investigated as a function of *PET*: the relative frequency of $TPV>0$ (want warmer) and $TPV<0$ (want cooler) votes per *PET* bin. 1 °C wide *PET* intervals were utilized for both models. The occurrence probability of the mentioned preference votes depends on *PE*T according to a sigmoid function (a mathematical function having an 'S' shape), and with the increment of *PET* the probability of $TPV>0$ votes decreases, while the probability of $TPV<0$ votes increases (*Figure 6*). Pearson goodness of fit test (building on χ^2 statistics) was utilized to check the obtained probit models (*Table 4*). The significance level was generally below 0.150, indicating that the fit was sufficient in most of the cases.

Researchers from East Asia assumed that the intersection point of the fitted probit models $TPV<0$ and $TPV>0$ indicates the preferred temperature (Hwang, R.-L. and Lin, T.-P. 2007;

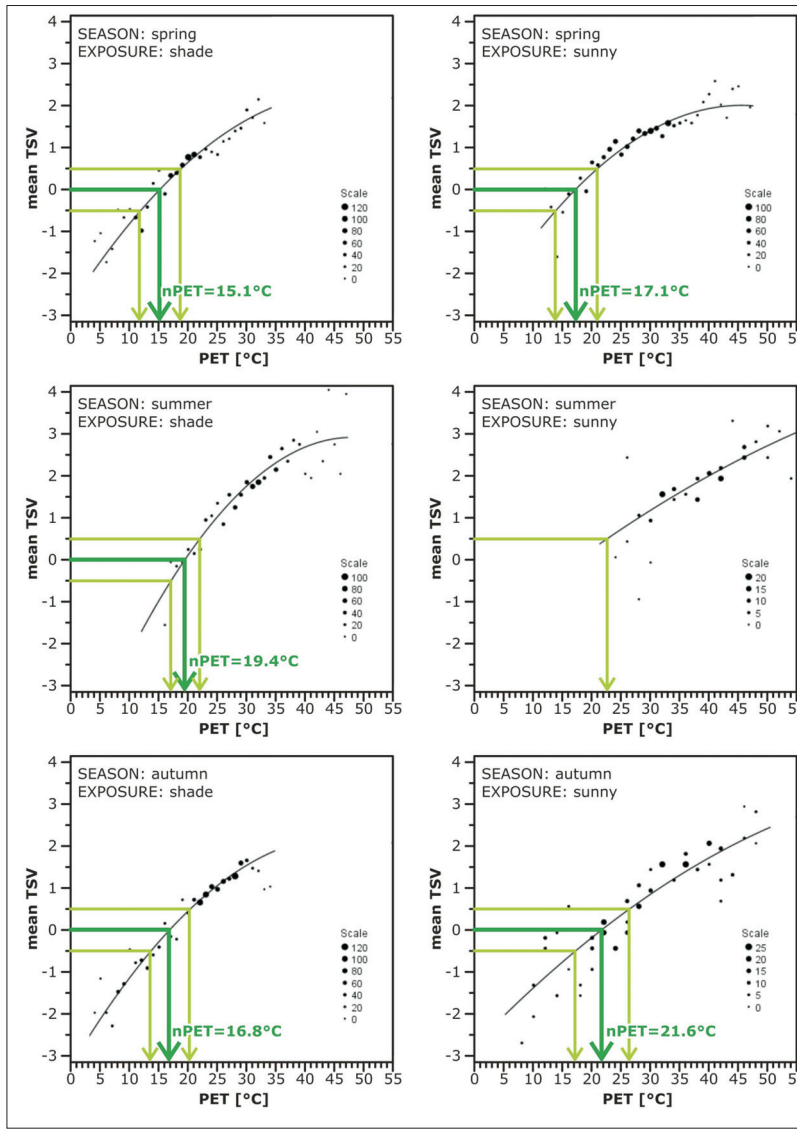

Fig. 5. Determination of neutral temperature (*nPET*) and neutral *PET* zone according to seasons and exposure groups

Table 2. Quadratic regression between 'weighted mean TSV' and PET

Conditions		N	R^2	Sig.	Equation
Spring	shade	940	0.919	0.000	$-2.28 \cdot 10^{-3} \cdot PET^2 + 0.215 \cdot PET - 2.715$
	sunny	1,163	0.899	0.000	$-2.50 \cdot 10^{-3} \cdot PET^2 + 0.227 \cdot PET - 3.152$
Summer	shade	815	0.928	0.000	$-3.56 \cdot 10^{-3} \cdot PET^2 + 0.342 \cdot PET - 5.294$
	sunny	151	0.645	0.000	$-0.53 \cdot 10^{-3} \cdot PET^2 + 0.119 \cdot PET - 1.921$
Autumn	shade	1,260	0.967	0.000	$-2.50 \cdot 10^{-3} \cdot PET^2 + 0.234 \cdot PET - 3.218$
	sunny	371	0.811	0.000	$-0.83 \cdot 10^{-3} \cdot PET^2 + 0.144 \cdot PET - 2.735$

Table 3. Quadratic regression between 'weighted mean TPV' and PET

Conditions		N	R^2	Sig.	Equation
Spring	shade	940	0.935	0.000	$-1.77 \cdot 10^{-3} \cdot PET^2 + 0.015 \cdot PET + 0.893$
	sunny	1,163	0.827	0.000	$-0.52 \cdot 10^{-3} \cdot PET^2 - 0.010 \cdot PET + 1.033$
Summer	shade	815	0.912	0.000	$2.90 \cdot 10^{-3} \cdot PET^2 - 0.235 \cdot PET + 3.918$
	sunny	151	0.593	0.000	$-0.87 \cdot 10^{-3} \cdot PET^2 + 0.019 \cdot PET + 0.288$
Autumn	shade	1,260	0.925	0.000	$-0.04 \cdot 10^{-3} \cdot PET^2 - 0.052 \cdot PET + 1.159$
	sunny	371	0.755	0.000	$-0.51 \cdot 10^{-3} \cdot PET^2 - 0.004 \cdot PET + 0.645$

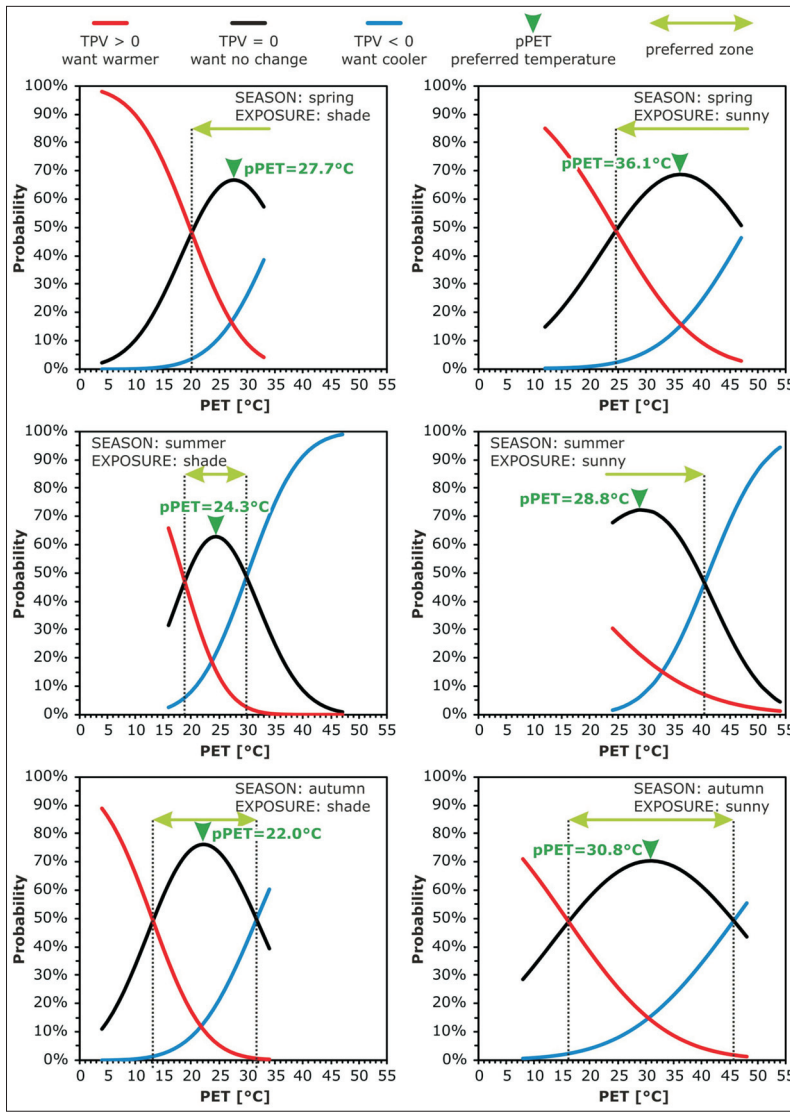

Fig. 6. Determination of preferred temperature (*pPET*) and thermal preference zone based on probit technique

Table 4. Goodness of fit of the probit models

Conditions		Number of PET bins	model TPV<0		model TPV>0	
			χ^2	Sig.	χ^2	Sig.
Spring	shade	30	51.618	0.004	31.534	0.294
	sunny	35	43.645	0.102	48.044	0.044
Summer	shade	32	89.711	0.000	13,894.862	0.000
	sunny	29	30.301	0.301	34.233	0.159
Autumn	shade	31	57.067	0.001	350.176	0.000
	sunny	41	53.028	0.066	40.031	0.424

Lin, T.-P. 2009; Lin, T.-P. *et al.* 2011; Yang, W. *et al.* 2013a,b). However, *TPV*<0 and *TPV*>0 curves intersect each other always below 50% level of probability, and considering a vertical axis, the two transition curves are usually not symmetrical to each other (*Figure 6*). That is, the rate of decline in the probability of 'want warmer' votes does not equal generally to the rate of incline in the probability of 'want cooler' votes. Therefore the intersection point does not necessarily coincide with the maximum probability of 'want no change' votes. Consequently, it seemed reasonable to depict the probability of *TPV* = 0 votes (calculated by substracting the probabilities of *TPV*<0 and *TPV*>0 from 100%) against the *PET* index and assign *pPET* where this curve reaches its maximum. Besides, preferred *PET* zone could be defined on those *PET* range where the occurrence probability of *TPV* = 0 vote exceeds the probability of the other votes (*Figure 6*).

Summary of the results

Figure 7 offers a graphical summary about the *pPET* values obtained through the different analysis approaches. The outcomes are very close to each other in almost every case. Moreover, the match is perfect in the cases of the sunny-spring, and the shade-autumn groups. The greatest difference (3.5 °C) was found in the sunny-summer group. Note that the probit-fit was less significant (sig = 0.301 for *TPV*<0 and 0.159 for *TPV*>0) in this group, moreover, this group had the lowest R^2 (0.593) value in quadratic regression.

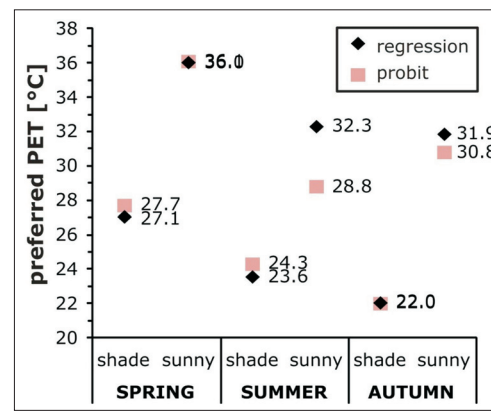

Fig. 7. Comparison of *pPET* values obtained through different analysis techniques

Figure 8 offers a graphical overview about the neutral and preferred thermal conditions (based on the results obtained through the regression technique). One can observe first of all the striking difference between the *nPET* and *pPET* values. Hungarians' *nPET* values ranged from 15.1 °C (spring-shade) to 21.6 °C (autumn-sunny), thereby falling into the original *PET*-zones of 'slight cold stress' and 'no thermal stress'. On the contrary, *pPET* values scattered from the 'no thermal stress' to 'strong heat stress' categories. The lowest *pPET* (22 °C) occurred in the autumn-shade group and the highest (36 °C) in the spring-sunny group.

The second most important feature is the remarkable difference between the sunny and shaded groups (*Figure 8*). Indeed, sunny *nPET* and *pPET* values were always higher than the corresponding shaded values. In terms of *nPET* the difference was only 2 °C in spring,

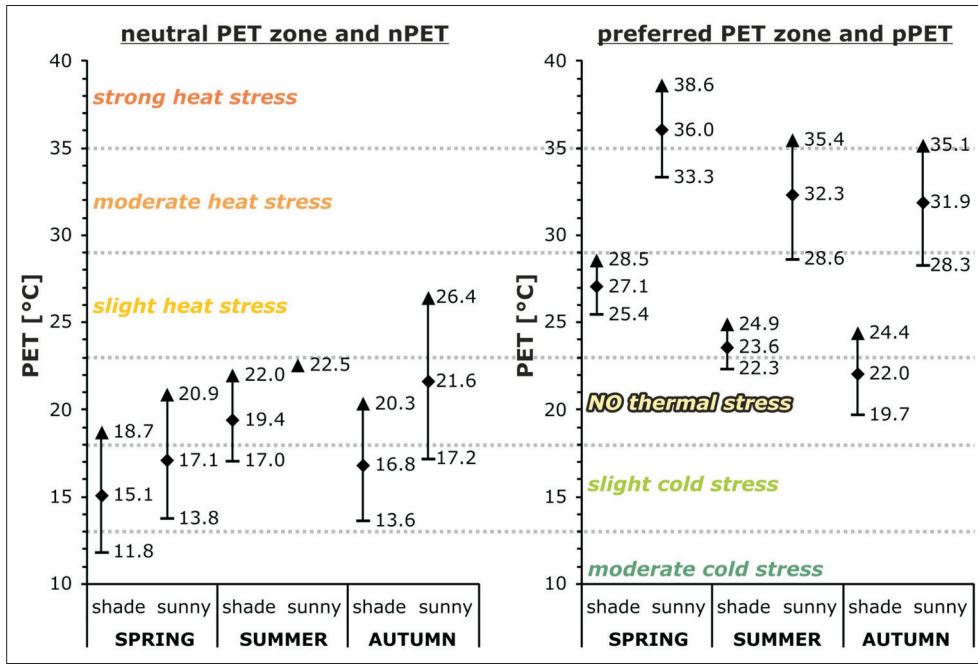

Fig. 8. Thermal conditions assessed as 'neutral' and 'preferred' by Hungarians according to their solar exposure in different seasons (all results are based on regression technique; level of thermal stress is indicated according to the original *PET* scale)

while it was almost 5 °C in autumn. The differences in *pPET* values were even greater: they were close to 10 degrees in every season.

Finally, different seasonal order can be observed in *nPET* and *pPET* values. (Merely the shaded exposure group is discussed here, because the sunny results are more uncertain due to the lower sample size.) The *nPET* values follow the increasing order of spring, autumn and summer (*Figure 8*), which corresponds both to the general seasonal background temperature differences, both to the differences in the recorded actual thermal conditions. This seasonal pattern proves that Hungarian people adapt themselves to the seasonally different climate conditions. In summer they perceive neutral between 17 °C and 22 °C (with a neutral temperature of 19.4 °C), while in the cooler transient seasons they feel neutral at lower *PET* values which can be assessed even as slight cool stress. Regarding the preferred thermal conditions, the seasonal order is different: *pPET* is around 22 °C in autumn and summer, while it is above 27 °C in spring. (The sunny-springtime value is even higher: it is 36 °C.)

The highest *pPET* in springtime, as well as the greatest difference between the *nPET* and *pPET* values in spring may be explained as follows. After the cold and dark winter period Hungarian people are looking for any environmental opportunities to feel warm. Although they are adapted to cooler temperatures during winter, they wish for warmer thermal sensation, even if this behaviour connotes certain degree of heat stress. The longing for warmer thermal conditions make most people to expose them to the intense direct sunlight in springtime (see the great portion of subjects in the spring-sunny group; *Figure 4*), which may have serious consequences regarding their sensitive skin and sensitive thermoregulation system at the end of the long winter-period.

Relevance of the research findings

Although *PET* and many other well-established indices are sufficiently and frequently used in the field of human-biometeorology for the objective assessment of the thermal environment, the outcomes of this study prove the importance of questionnaire-supported OTC investigations. Having knowledge about the subjective thermal assessment of local people allows explaining such 'illogical' outdoor behaviours which are reported by Kántor, N. and Unger, J. (2010). By comparing the number of visitors and their outdoor behaviours in a small urban park in the transient seasons they revealed that in spite of the strong heat stress, most people tend to sit or lie in sunny places in springtime. At the same level of thermal stress in autumn, people rather choose shady places to spend their time outdoors (Kántor, N. and Unger, J. 2010).

This investigation demonstrated clear seasonal differences in neutral temperature and preferred temperature, similarly to previous studies (e.g. Spagnolo, J. and de Dear, R. 2003; Nikolopoulou, M. and Lykoudis, S. 2006; Lin, T.-P. 2009). Additionally, this paper evinced that subjective thermal sensation may greatly differ from the original PET categorization system which was established for Central European people (Matzarakis, A. and Mayer, H. 1996). Indeed, except the shady-summer group, the neutral zone of Hungarian people (*Figure 8*) was considerably wider than the original 5 °C-wide zone (18–23 °C; *Figure 1*) indicating greater tolerance against the changes of outdoor thermal environment. The width of the neutral zone exceeded 7 °C in the transient seasons, being more than 9 °C wide in the sunny-autumn group. This finding may be explained by the multifarious and changeable weather conditions in the transient seasons, which make people less sensitive against the variations of outdoor thermal conditions.

As most important achievement, this paper revealed that solar exposure has significant influence on the subjective evaluation of thermal conditions. This finding may have international significance. As mentioned above, several studies reported about seasonal differences in neutral temperature without scrutinizing the role of exposure on the obtained results. However, people choose different positions in different seasons: seeking to expose them to direct sunlight after the cold and dark winter months, and stay in the shade during summer and the warm months of autumn. The different seasonal exposure-patterns mean that the neutral temperature reflects more the assessment of sun-exposed subjects in spring, and the assessment of people in the shade in summer and autumn. Thorough analysis of the seasonal neutral (and preferred) temperature values according to exposure-groups sheds more light on the real assessment patterns of local people, which explains better the seasonal differences in their outdoor behaviour.

***Acknowledgement*:** The author would like to acknowledge Lilla Egerházi, Ágnes Takács and Attila Kovács for their valuable help in the course of field measurements or later in the period of data processing.

REFERENCES

Ballantyne, E.R., Hill, R.K. and Spencer, J.W. 1977. Probit analysis of thermal sensation assessments. *International Journal of Biometeorology* 21. 29–43.

Chen, L. and Ng, E. 2012. Outdoor thermal comfort and outdoor activities: a review of research in the past decade. *Cities* 29. 118–125.

Chen, L., Wen, Y., Zhang, L. and Xiang, W.N. 2015. Studies of thermal comfort and space use in an urban park square in cool and cold seasons in Shanghai. *Building and Environment* 94. 644–653.

Fröhlich, D. and Matzarakis, A. 2013. Modelling of changes in thermal bioclimate: examples based on urban spaces in Freiburg, Germany. *Theoretical and Applied Climatology* 111. 547–558.

Gómez, F., Pérez Cueva, A., Valcuende, M. and Matzarakis, A. 2013. Research on ecological design to enhance comfort in open spaces of a city (Valencia, Spain). Utility of the physiological equivalent temperature (PET). *Ecological Engineering* 57. 27–39.

Gulyás, Á., Matzarakis, A. and Unger, J. 2009. Differences in the thermal bioclimatic conditions on the urban and rural areas in a southern Hungarian city (Szeged). *Berichte des Meteorologischen Institutes der Universität Freiburg* 18. 229–234.

Gulyás, Á., Unger, J. and Matzarakis, A. 2006. Assessment of the microclimatic and human comfort conditions in a complex urban environment: modelling and measurements. *Building and Environment* 41. 1713–1722.

HMS 2015. Climate characteristics of Szeged. http://www.met.hu/eghajlat/magyarorszag_ eghajlata/varosok_jellemzoi/Szeged/

Höppe, P. 1992. Ein neues Verfahren zur Bestimmung der mittleren Strahlungstemperatur im Freien. *Wetter und Leben* 44. 147–151.

Höppe, P. 1999. The physiological equivalent temperature – a universal index for the biometeorological assessment of the thermal environment. *International Journal of Biometeorology* 43. 71–75.

Hwang, R-L. and Lin, T-P. 2007. Thermal comfort requirements for occupants of semi-outdoor and outdoor environments in hot-humid regions. *Architectural Science Review* 50. 357–364.

Hwang, R-L., Lin, T-P. and Matzarakis, A. 2011. Seasonal effects of urban street shading on long-term outdoor thermal comfort. *Building and Environment* 46. 863–870.

IPCC 2014. *Climate Change 2014: Synthesis Report, 2014. Contribution of Working Groups I, II and III to the Fifth Assessment Report of the Intergovernmental Panel on Climate Change* (Core Writing Team, eds. Pachauri, R.K. and Meyer, L.A.), Geneva, IPCC.

Kántor, N. and Unger, J. 2010. Benefits and opportunities of adopting GIS in thermal comfort studies in resting places: An urban park as an example. *Landscape and Urban Planning* 98. 36–46.

Kántor, N. and Unger, J. 2011. The most problematic variable in the course of human biometeorological comfort assessment – the mean radiant temperature. *Central European Journal of Geosciences* 3. 90–100.

Kántor, N., Égerházi, L.A. and Unger, J. 2012a. Subjective estimation of thermal environment in recreational urban spaces. Part 1: investigations in Szeged, Hungary. *International Journal of Biometeorology* 56. 1075–1088.

Kántor, N., Unger, J. and Gulyás, Á. 2012b. Subjective estimations of thermal environment in recreational urban spaces – Part 2: international comparison. *International Journal of Biometeorology* 56. 1089–1101.

Kovács, A., Unger, J., Gál, C.V. and Kántor, N. 2015. Adjustment of the thermal component of two tourism climatological assessment tools using thermal perception and preference surveys from Hungary. *Theoretical and Applied Climatology*. Doi: 10.1007/s00704-015-1488-9.

Krüger, E.L., Drach, P., Emmanuel, R. and Corbella, O. 2013. Assessment of daytime outdoor comfort levels in and outside the urban area of Glasgow, UK. *International Journal of Biometeorology* 57. 521–533.

Lai, D., Guo, D., Hou, Y., Lin, C. and Chen, Q. 2014. Studies of outdoor thermal comfort in northern China. *Building and Environment* 77. 110–118.

Lin, T.-P. 2009. Thermal perception, adaptation and attendance in a public square in hot and humid regions. *Building and Environment* 44. 2017–2026.

Lin, T.-P. and Matzarakis, A. 2008. Tourism climate and thermal comfort in Sun Moon Lake, Taiwan. *International Journal of Biometeorology* 52. 281–290.

Lin, T.-P., de Dear, R. and Hwang. R.-L. 2011. Effect of thermal adaptation on seasonal outdoor thermal comfort. *International Journal of Climatology* 31. 302–312.

Lin, T.-P., Matzarakis, A. and Hwang, R.-L. 2010. Shading effect on long-term outdoor thermal comfort. *Building and Environment* 45. 213–221.

Lindner-Cendrowska, K. 2013. Assessment of bioclimatic conditions in cities for tourism and recreational purposes (a Warsaw case study). *Geographia Polonica* 86. 55–66.

Matzarakis, A. and Mayer, H. 1996. Another kind of environmental stress: thermal stress. *WHO Newsletter* 18. 7–10.

Matzarakis, A., Mayer, H. and Iziomon, M.G. 1999. Application of a universal thermal index: physiological equivalent temperature. *International Journal of Biometeorology* 43. 76–84.

Matzarakis, A., Rutz, F. and Mayer, H. 2010. Modelling radiation fluxes in simple and complex environments: basics of the RayMan model. *International Journal of Biometeorology* 54. 131–139.

Mayer, H., Holst, J., Dostal, P., Imbery, F. and Schindler, D. 2008. Human thermal comfort in summer within an urban street canyon in Central Europe. *Meteorologische Zeitschrift* 17. 241–250.

Müller, N., Kuttler, W. and Barlag, A.B. 2014. Counteracting urban climate change: adaptation measures and their effect on thermal comfort. *Theoretical and Applied Climatology* 115. 243–257.

Nikolopoulou, M. and Lykoudis, S. 2006. Thermal comfort in outdoor urban spaces: Analysis across different European countries. *Building and Environment* 41. 1455–1470.

Pearlmutter, D., Jiao, D. and Garb, Y. 2014. The relationship between bioclimatic thermal stress and subjective thermal sensation in pedestrian spaces. *International Journal of Biometeorology* 58. 2111–2127.

Pongrácz, R., Bartholy, J. and Bartha, E.B. 2013. Analysis of projected changes in the occurrence of heat waves in Hungary. *Advances in Geosciences* 35. 115–122.

Rupp, R.F., Vásquez, N.G. and Lamberts, R. 2015. A review of human thermal comfort in the built environment. *Energy and Buildings* 105. 178–205.

Spagnolo, J. and de Dear, R. 2003. A field study of thermal comfort in outdoor and semi-outdoor environments in subtropical Sydney Australia. *Building and Environment* 38. 721–738.

Tung, C.-H., Chen, C.-P., Tsai, K.-T., Kántor, N., Hwang, R.-L., Matzarakis, A. and Lin, T.-P. 2014. Outdoor thermal comfort characteristics in the hot and humid region from a gender perspective. *International Journal of Biometeorology* 58. 1927–1939.

UNFPA 2011. *The state of world population 2011. Report of the United Nations Population Fund.* New York, UNFPA.

Unger, J. 1996. Heat island intensity with different meteorological conditions in a medium-sized town: Szeged, Hungary. *Theoretical and Applied Climatology* 54. 147–151.

Unger, J., Lelovics, E. and Gál, T. 2014. Local Climate Zone mapping using GIS methods in Szeged. *Hungarian Geographical Bulletin* 63. 29–41.

Yahia, M.W. and Johansson, E. 2013. Evaluating the behaviour of different thermal indices by investigating various outdoor urban environments in the hot dry city of Damascus, Syria. *International Journal of Biometeorology* 57. 615–630.

Yang, W., Wong, N.H. and Jusuf, S.K. 2013a. Thermal comfort in outdoor urban spaces in Singapore. *Building and Environment* 5. 426–435.

Yang, W., Wong, N.H. and Zhang, G. 2013b. A comparative analysis of human thermal conditions in outdoor urban spaces in the summer season in Singapore and Changsha, China. *International Journal of Biometeorology* 57. 895–907.

Yin, J.F., Zheng, Y.F., Wu, R.J., Tan, J.G., Ye, D.X. and Wang, W. 2012. An analysis of influential factors on outdoor thermal comfort in summer. *International Journal of Biometeorology* 56. 941–948.

Zeng, Y. and Dong, L. 2015. Thermal human biometeorological conditions and subjective thermal sensation in pedestrian streets in Chengdu, China. *International Journal of Biometeorology* 59. 99–108.

Ukraine in Maps

Edited by: **Kocsis, K., Rudenko, L. and Schweitzer, F.**

Institute of Geography National Academy of Sciences of Ukraine
Geographical Research Institute Hungarian Academy of Sciences.
Kyiv–Budapest, 2008, 148 p.

Since the disintegration of the USSR, the Western world has shown an ever-growing interest in Ukraine, its people and its economy. As the second-largest country in Europe, Ukraine has a strategic geographical position at the crossroads between Europe and Asia. It is a key country for the transit of energy resources from Russia and Central Asia to the European Union, which is one reason why Ukraine has become a priority partner in the neighbourhood policy of the EU. Ukraine has pursued a path towards the democratic consolidation of statehood, which encompasses vigorous economic changes, the development of institutions and integration into European and global political and economic structures. In a complex and controversial world, Ukraine is building collaboration with other countries upon the principles of mutual understanding and trust, and is establishing initiatives aimed at the creation of a system that bestows international security.

This recognition has prompted the Institute of Geography of the National Academy of Sciences of Ukraine (Kyiv) and the Geographical Research Institute of the Hungarian Academy of Sciences (Budapest) to initiate cooperation, and the volume entitled "Ukraine in Maps" is the outcome of their joint effort. The intention of this publication is to make available the results of research conducted by Ukrainian and Hungarian geographers, to the English-speaking public. This atlas follows in the footsteps of previous publications from the Geographical Research Institute of the Hungarian Academy of Sciences. Similar to the work entitled South Eastern Europe in Maps (2005, 2007), it includes 64 maps, dozens of figures and tables accompanied by an explanatory text, written in a popular, scientific manner. The book is an attempt to outline the geographical setting and geopolitical context of Ukraine, as well as its history, natural environment, population, settlements and economy. The authors greatly hope that this joint venture will bring Ukraine closer to the reader and make this neighbouring country to the European Union more familiar, and consequently, more appealing.

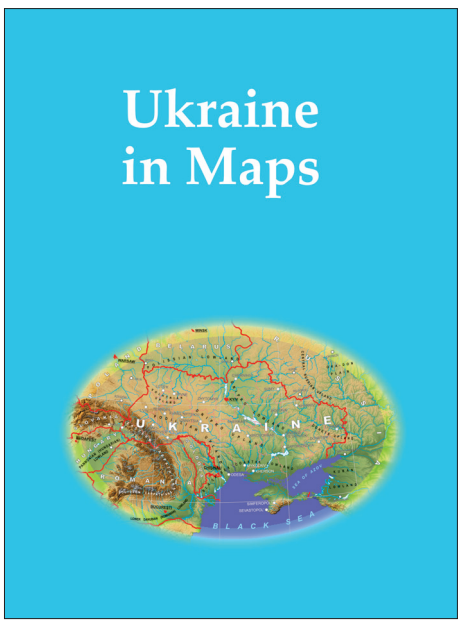

Price: EUR 35.00
Order: Geographical Institute RCAES MTA Library
H-1112 Budapest, Budaörsi út 45.
E-mail: magyar.arpad@csfk.mta.hu

DOI: 10.15201/hungeobull.65.2.6 Hungarian Geographical Bulletin 65 2016 (2) 155–167.

Study on the transmissivity characteristics of urban trees in Szeged, Hungary

Ágnes TAKÁCS, Attila KOVÁCS, Márton KISS, Ágnes GULYÁS and Noémi KÁNTOR[1]

Abstract

This study aims to determine the solar permeability characteristics of some common urban tree species in Hungary and to analyse their shading efficiency in mostly clear sky conditions. The results are based on a measurement-series implemented during the whole vegetation period in 2015. This paper compares different tree species regarding their transmissivity, and looks for differences between different sized tree individuals belonging to the same species. The following order was found among the investigated species regarding their shading-capacity: *T. cordata*, *A. hippocastanum* and *S. japonica*. Additionally, higher transmitted radiation and consequently higher transmisivity values were detected in the case of the smaller investigated *A. hippocastanum*.

Keywords: solar permeability, transmissivity, tree species, Hungary

Introduction

The global climate change has a considerable impact on the urban population, which makes up more than half of the Earth's population and it is predicted to be two-thirds of the ten billion people by 2050 (UN 2014). Projections of the regional climate models indicate that frequency of the heat waves is likely to be higher in the Carpathian Basin in the forthcoming decades. Indeed, by the last decades of this century a significant increase in the length of heat wave periods can be expected (Pongrácz, R. *et al.* 2013).

In urban areas significant excess heat is generated by modified surface coverage, complex morphology and anthropogenic heat emission. Compared to the neighbouring rural areas increased air temperature and modified radiation circumstances can be observed in cities; both at micro- and local level (Lelovics, E. *et al.* 2014; Thorsson, S. *et al.* 2014). Several investigations demonstrated the impact of these modifications on human thermal comfort and usage of public places (e.g. Kántor, N. and Unger, J. 2010; Égerházi, L.A. *et al.* 2013). Thermal comfort conditions can be improved by carefully selected construction materials (Yang, X. *et al.* 2013; Erell, E. *et al.* 2014), shading by appropriate building height (Bajsanski, I.V. *et al.* 2015), ensured ventilation (Gál, T. and Unger, J. 2009; Ng, E. 2009), established water surfaces (Sun, R. and Chen, L. 2012) as well as by planting effective vegetation (Dimoudi, A. and Nikolopoulou, M. 2003; Bowler, D.E. *et al.* 2010).

Urban forests provide a wide range of ecosystem services (from the environmental through the economic to the social benefits) to the city residents (Haase, D. *et al.* 2014; Mullaney, J. *et al.* 2015). One of the most important services from the viewpoint of the altering climatic background is their climate modification effect. Under Central European climate conditions extreme heat stress at the street level is usually the effect of high solar radiation and the resulting high radiation

[1] Department of Climatology and Landscape Ecology, University of Szeged. H-6722 Szeged, Egyetem u. 2. Corresponding author: takacsagi@geo.u-szeged.hu

budget of pedestrians (e.g. Kántor, N. and Unger, J. 2011; Lee, H. *et al.* 2014). On the one hand, urban tree stands have many positive impacts on the climatic characteristics and air quality in cities at local scale, for example by the sequestration of carbon dioxide and the removal of various air pollutants, and by reducing storm-water runoff (Jim, C.Y. and Chen, W.Y. 2008; Kirnbauer, M.C. *et al.* 2013; Nowak, D.J. *et al.* 2013).

On the other hand, vegetation decreases the level of heat stress at micro-scale directly through evapotranspiration and shading (reduction of direct solar radiation). Canopy-shading reduces slightly the near-surface air temperature under the trees (Abreu-Harbich, L.V. *et al.* 2015; Coutts, A.M. *et al.* 2016). Compared to air temperature the reduction of the radiation energy income is more important, which entails significant decrease of physiological thermal stress (Gulyás, Á. *et al.* 2006; Kántor, N. *et al.* 2016). Shading potential of trees depends on species-related characteristics (e.g. crown density, leaf area parameters), age and health status of the tree stands. Large differences can be shown in shading efficiency during the vegetation period, depending on the seasonal foliation-defoliation processes (Takács, Á. *et al.* 2016a). Even more important differences may exist among various species (Konarska, J. *et al.* 2014; Takács, Á. *et al.* 2015a). There is still a lack of information about the species-specific shading capacity of trees. However, broadening the knowledge about these features would help in designing more effective urban green areas.

In line with this general goal, the aim of our study is to determine the solar permeability characteristics of some of the most common urban tree species in Hungary during the whole vegetation period.

We set the specific targets of this study as follows:

– comparison of different tree species regarding their transmissivity, and
– looking for differences between different sized tree individuals belonging to the same species.

These results can be directly integrated into microclimate modelling and small-scale outdoor thermal stress projection. Thus, our investigations provide indirect help for urban designers and landscape architects in the planning of climate-conscious green infrastructure.

Methods and data

The city of Szeged

In order to achieve the above mentioned objectives, a long-term radiation measurement-series was implemented in Szeged. The city is situated in the south-eastern part of Hungary (46°N, 20°E), and can be characterized with a population of about 162,000 and an urbanized area of about 50 km^2. Szeged is spread on a flat area without considerable topographical differences (78–85 m a.s.l.), which allows small-scale meteorological results to be generalised (Andrade, H. and Vieira, R. 2007).

The region has a warm temperate climate with uniform annual distribution of precipitation. According to the multi-year (1971–2000) measurement series of the Hungarian Meteorological Service in Szeged the mean annual temperature is 10.6 °C. The daily mean temperature is normally above 10 °C from April to October; these months correspond to the woody vegetation period, and usually this period of the year is regarded to be the most suitable for outdoor activities. The annual amount of precipitation is 489 mm, while sunshine duration approaches 2000 hours per year (HMS 2015).

Preparations for the radiation measurements

In Szeged, the first measurement-series on the short-wave radiation-modification effect of urban trees was conducted in 2014. These field surveys lasted from June to November and involved 13 measurement days. Based on the experiences of this 'pilot campaign' (e.g. Takács, Á. *et al.* 2015a,b, 2016a), a second meas-

urement-series was implemented in 2015 with more measurement days. In the course of the second measurement campaign, we conducted simultaneous measurements with two human bio-meteorological stations. One of them was placed under carefully selected urban trees, and the other was placed to an open point of the same study area. The first station stood in the shade while the second instrument was fully exposed to direct solar radiation during the measurement period.

Before the micrometeorological measurement campaign, thorough field surveys were conducted in Szeged aiming to select the appropriate study locations and trees. We sought to represent those species that are frequently planted in Hungarian towns as street or park trees. The main criteria were to find healthy, adult, single shade tree specimens without the disturbing effect of other landscape elements (Shahidan, M.F. *et al.* 2010; Konarska, J. *et al.* 2014; Abreu-Harbich, L.V. *et al.* 2015), in order to ensure that other trees or buildings do not influence the recorded parameters. We selected trees that stood in a park or a square with considerable amount of open sunny locations in order to facilitate the nearby 'sunlit' measurements.

Finally, five specimens that met the above criteria were selected for the purpose of our investigations:
- one *Tilia cordata* (small-leaved linden),
- one *Sophora japonica* (pagoda tree),
- one *Celtis occidentalis* (common hackberry), and
- two *Aesculus hippocastanums* (horse chestnut).

The study areas comprised four recreational places in Szeged (Mátyás square, Búvár lake, Rákóczi square and Kodály square) (*Figure 1*).

It should be highlighted that the two *A. hippocastanums* have different dimensional characteristics. One of them has larger full height and canopy diameter while slightly lower trunk height. (This specimen is called hereinafter as 'larger' and abbreviated as *'l'*, while the other specimen is denominated as 'smaller' or *'s'*.) Regarding full height, trunk height and canopy diameter, the *T. cordata* has comparable dimensions with the two *A. hippocastanums*. However, the selected *S. japonica* and *C. occidentalis* have smaller full height but larger canopy diameter than the other species (*Table 1*).

Details of the radiation measurements in 2015

The data collection was carried out with two special human bio-meteorological stations, both of them equipped with sensors measuring the same meteorological variables in one-minute resolution. Each day, the instruments were installed 10–20 min. prior to the dedicated measurement period in order to allow sensors to stabilize. The stations allow us to record all meteorological parameters that influence the human energy budget (Takács, Á. *et al.* 2016b). However, since this study is focusing on the shading capacity of trees, we analyze the changes of one parameter only. This parameter is the global radiation (*G*), which involves the short-wave radiation flux densities from the upper hemisphere and includes both direct and diffuse parts of the solar radiation:

G_{trans} [W/m^2] is the transmitted solar radiation measured under the selected urban trees, at a distance of two meters on the northern side of the tree trunk,

G_{act} [W/m^2] is the actual value of global radiation measured at the nearby open site.

Transmissivity – a dimensionless value ranging from 0 to 1 – was calculated as the ratio of the measured *G* values:

$$Transmissivity = \frac{G_{trans}}{G_{act}}$$

G data were recorded by Kipp & Zonen radiometers, i.e. by the upper pyranometers of a CNR 1-type net radiometer in the case of the shaded station and of a CNR 4-type in the case of the sunlit instrument. Using telescopic legs, the sensors were placed at 1.1 m height above ground level. This height corresponds to the centre of gravity of a standing

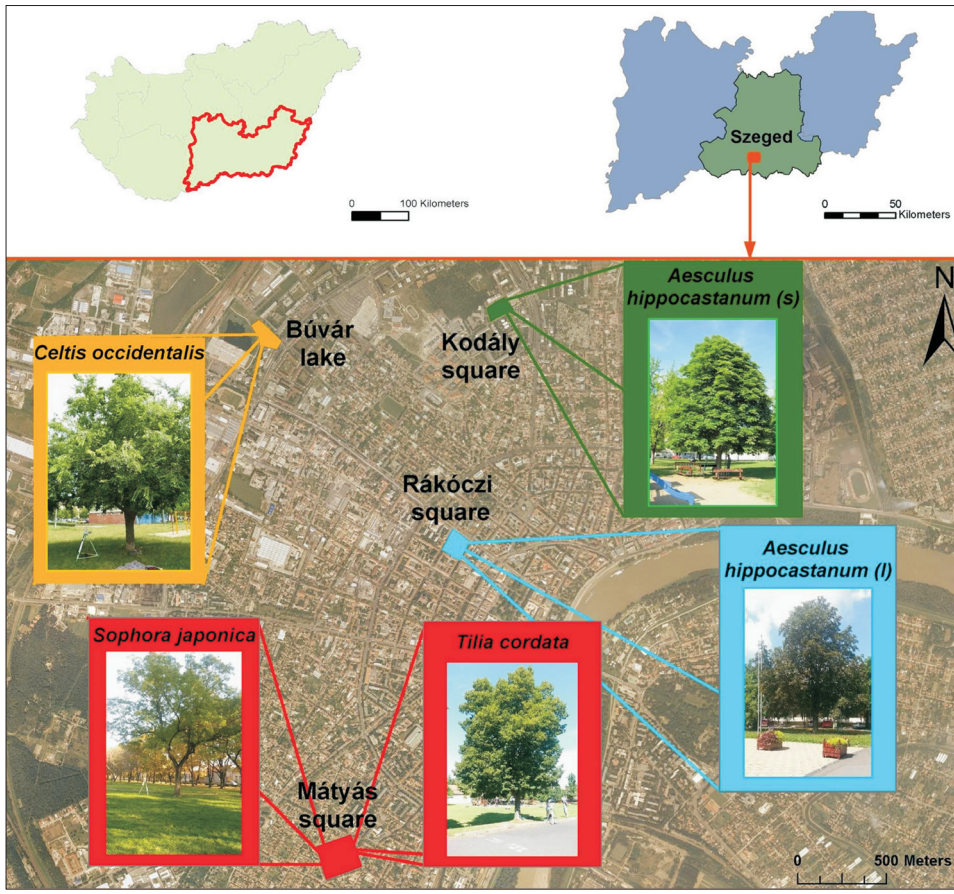

Fig. 1. Investigated trees and their location in the city of Szeged, Hungary

Table 1. Main dimensional attributes of the investigated urban trees

Species	*Aesculus hippocastanum (l)*	*Aesculus hippocastanum (s)*	*Tilia cordata*	*Sophora japonica*	*Celtis occidentalis*
Full height, m	15.0	13.5	15.5	12.0	9.0
Trunk height, m	2.0	2.5	2.5	3.0	1.8
Canopy diameter, m	10.0	9.0	9.0	12.0	14.0
Trunk diameter, cm	78.0	57.0	70.5	75.0	70.0

European man, the most frequently applied standard subject in outdoor thermal comfort investigations (Mayer, H. *et al.* 2008; Lee, H. *et al.* 2013, 2014). Following the instructions of the manual of the net radiometers, we took special care about the horizontal levelling and their orientation to South.

The comparability of the two pyranometers was tested on a cloudy and a totally clear summer day. In the frame of the test, both equipments were placed to the sun. The average differences between the measured global radiation values were only 10.14 and 3.8 W/m^2 on the two days, respectively. All data considered, the differences ranged from −35 to 50 W/m^2 and did not exceed 25 W/m^2 in absolute value in more than 80% of the cases.

The radiation measurements lasted from April to October in 2015 and consisted of 36 measurement days, i.e. the campaign covered the whole vegetation period (*Table 2*).

Data analysis

This study focuses on the differences regarding the shading-capacity of the investigated trees. For studying the inter-species differences we selected the *T. cordata*, the *S. japonica* and the smaller *A. hippocastanum*. Then we compared the two *A. hippocastanums* in order to examine the impact of mere dimensional inequalities. For these two analyses 20 days were selected from the total 36 measurement days (*Table 2*) based on the following aspects.

Inter-species differences were examined only in the hottest period of the year (summer). This comparison was based on the data of days when similar global radiation background was found. (Days close to each other were selected to improve the accuracy of comparison.) One of the main criteria was to select such day-combinations that can be characterized with the least disturbing effect of clouds.

In the case of the larger and smaller *A. hippocastanum*, the comparison period covered almost the whole measurement period (*Table 2*). Only three days were excluded: the sole day in April, as well as two days in late autumn due to the disturbing effect of other trees and buildings caused by the low sun elevation. The two *A. hippocastanum* specimens were monitored on consecutive days in almost every case in order to ensure as similar conditions regarding the potential global radiation background as possible. Data analyses were performed within the statistical software SPSS.

Results

Inter-species differences

One of the specific goal of the study was to explore differences in the solar permeability of different shade tree species during the hottest period of the year. The selected trees include the smaller *A. hippocastanum*, the *T. cordata* and the S. *japonica*; each of them represented with four measurement days in summer (*Table 2*). The smaller individual was selected from the two *A. hippocastanums* for the purpose of this comparison since it was monitored more frequently under favorable sky conditions.

Figure 2 illustrates the daily curves of G_{act}, G_{trans} and transmissivity, while *Table 3* shows

*Table 2. Measurement days in 2015 under the selected tree specimens**

Aesculus hippocastanum (l)	*Aesculus hippocastanum (s)*	*Tilia cordata*	*Sophora japonica*	*Celtis occidentalis*
–	23-Apr-2015	16-Apr-2015	–	–
12-May-2015	18-May-2015	11-May-2015	07-May-2015	06-May-2015
01-Jun-2015	02-Jun-2015	30-May-2015	29-May-2015	28-May-2015 03-Jun-2015
02-Jul-2015	01-Jul-2015	03-Jul-2015	06-Jul-2015	05-Jul-2015
21-Jul-2015	22-Jul-2015	01-Aug-2015	06-Aug-2015	23-Jul-2015
27-Aug-2015	28-Aug-2015	31-Aug-2015	01-Sep-2015	29-Aug-2015
01-Oct-2015	02-Oct-2015	–	–	03-Oct-2015
28-Oct-2015	29-Oct-2015	26-Oct-2015	27-Oct-2015	30-Oct-2015

*Coloured days were selected for the analyses.

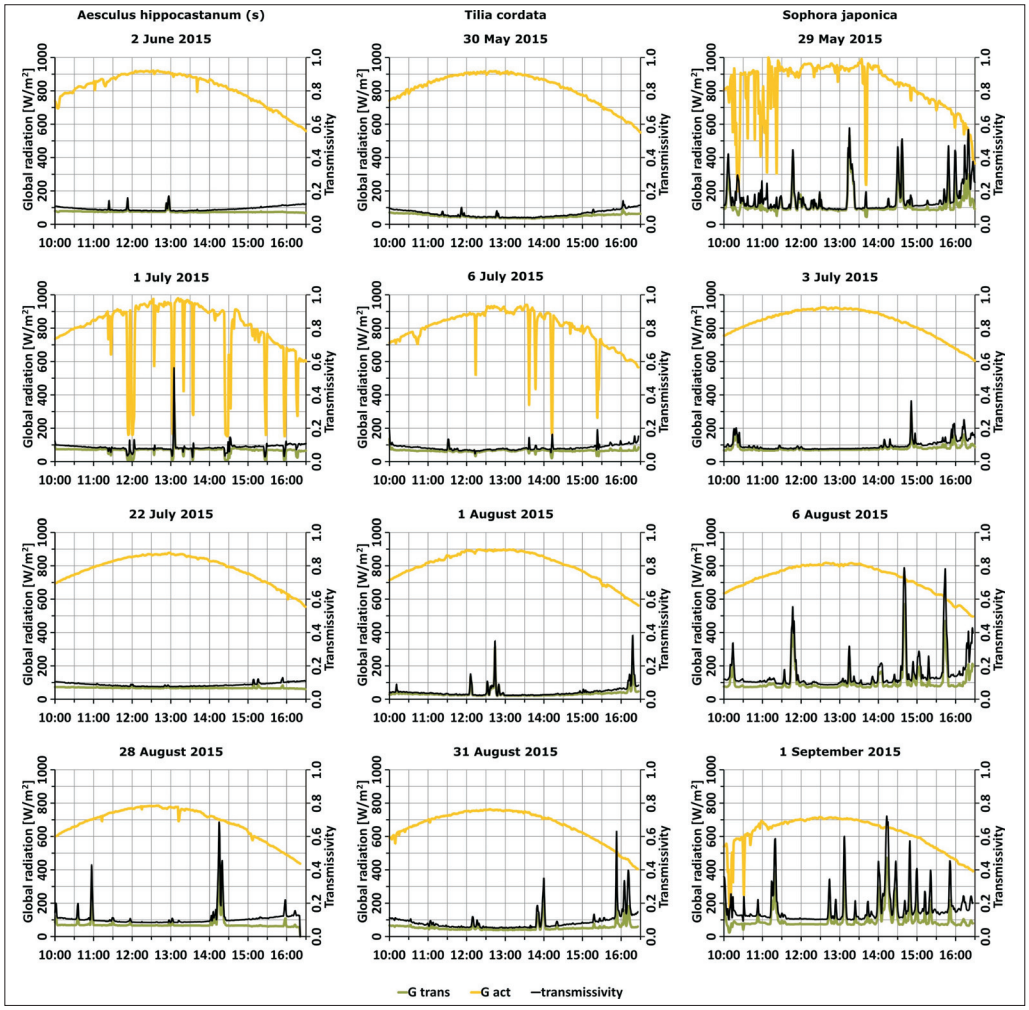

Fig. 2. Differences in solar permeability through the foliage of three different species: the smaller *Aesculus hippocastanum (s)*, *Tilia cordata* and *Sophora japonica*. Time is in CET; G_{trans} = transmitted radiation; G_{act} = actual value of global radiation

the corresponding descriptive statistics of daily transmissivity values. It is important to note that the statistic tables are based on the data of 'sunny minutes' only, aiming to get rid of the disturbing effect of clouds, which caused sometimes sharp 'apparent transmissivity increases': see for example the cases of July 1 (around 12 a.m. and 1 p.m.) as well as July 6 (around 1.40, 2.10 and 3.20 p.m.) when sharp decreases of G_{act} coinciding with moderate decreases of G_{trans} caused smaller or greater jumps in the transmissivity curve. Clear sky conditions, however, can be characterized with smooth, bell-shaped G_{act} curves, and in these circumstances the sharp increases in G_{trans} result in real jumps of transmissivity.

A slight temporal tendency can be observed within the summer period for all species, i.e. the lowest transmissivities were calculated for early or late July, while the highest ones were obtained at the end of

*Table 3. Basic descriptive statistics regarding the transmissivity values of the smaller Aesculus hippocastanum (A. h. (s)), Sophora japonica (S. j.) and Tilia cordata (T. c.) on their investigation days**

Tree	Date	N	Stand. Dev.	Min.	Median	Mean	Max.
S. j.	29-May-2015	345	0.097	0.086	0.113	0.154	0.578
T. c.	30-May-2015	389	0.021	0.038	0.057	0.063	0.141
A. h. (s)	02-Jun-2015	389	0.013	0.079	0.090	0.094	0.169
A. h. (s)	01-Jul-2015	350	0.014	0.057	0.085	0.087	0.269
S. j.	03-Jul-2015	388	0.034	0.074	0.086	0.099	0.364
T. c.	06-Jul-2015	373	0.016	0.047	0.079	0.083	0.191
A. h. (s)	22-Jul-2015	390	0.011	0.075	0.084	0.088	0.128
T. c.	01-Aug-2015	388	0.036	0.022	0.035	0.044	0.386
S. j.	06-Aug-2015	388	0.107	0.086	0.113	0.149	0.785
A. h. (s)	28-Aug-2015	381	0.059	0.083	0.099	0.111	0.686
T. c.	31-Aug-2015	387	0.056	0.051	0.073	0.088	0.634
S. j.	01-Sep-2015	376	0.104	0.101	0.133	0.172	0.722

*The statistics are based on the data of sunny minutes (N) only.

August (*Figure 2*, *Table 3*). *S. japonica* had the highest transmissivity in all measurement periods, generally exceeding 0.1, except for early July. According to the obtained transmissivity values, *T. cordata* can be considered to be the most effective shade tree species in the investigation period. In early August, its transmissivity values scattered around 0.04 and for most of the day its G_{trans} values were below 50 W/m^2 (*Figure 2*). Even at the end of August when the compared trees showed the highest solar permeability within summer we measured still fairly low transmissivities, being lower than 0.1 (median: 0.073, mean: 0.088) (*Figure 2*, *Table 3*). Thus, we can set a shading-capacity sequence among the investigated species as follows: *T. cordata*, *A. hippocastanum* and *S. japonica*.

Standard deviation of transmissivity of *S. japonica* approached or exceeded 0.1 in three-quarters of the cases (0.097, 0.107 and 0.104 in May, August and September, respectively), while *A. hippocastanum*'s transmissivity values had the lowest standard deviation (they were between 0.011–0.014 in three days) (*Table 3*).

There is an additional feature regarding the transmissivity of lonely shade trees that can be noticed on the charts of *Figure 2*, especially, in the cases of *T. cordata*: see that the transmissivity values tend to be the lowest when the global radiation reaches its daily maximum. On the other hand, during the earliest and latest hours of the measurement period, when the bell-shaped G_{act} curve reaches its lowest values, the transmissivity shows a slight but monotonic increase. That is, the rate of decline in global radiation is not followed by the decrase in transmitted radiation. In fact, G_{trans} keeps its level or may be even greater at lower sun elevations because more diffuse radiation may reach the 'shaded pyranometer' from lateral directions at these situations.

Dimensional differences

Now we are looking for the effectiveness of solar radiation reduction in the light of pure size differences. For this purpose we consider the two *A. hippocastanum* specimens with different dimensional attributes. The daily courses of actual global radiation, transmitted radiation as well as the transmissivity values are depicted on *Figure 3*. Besides, *Table 4* contains the main descripitive statistics regarding the daily transmissivity values. It should be highlighted again that only those minutes were considered for these statistics that were free from the effects of clouds (see the different case numbers – *N* – in the table).

The daily curves of actual global radiation reflect the normal seasonal differences occurring in our region: G_{act} approached 1,000 W/m^2 in early July while it remained below 700 W/m^2 during the autumn days (*Figure 3*).

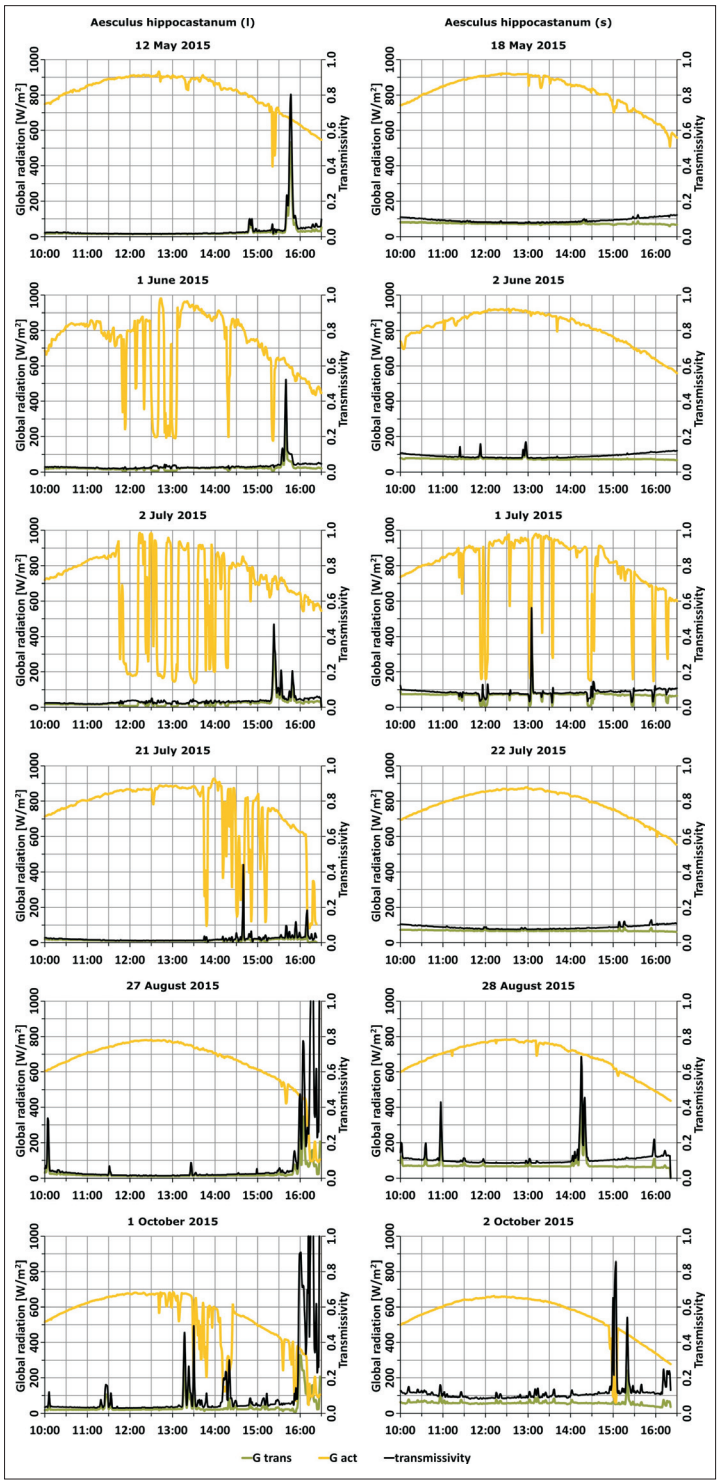

Fig. 3. Differences in solar permeability of the larger (*l*) and smaller *(s) Aesculus hippocastanum* from spring to autumn. Time is in CET; G_{trans} = transmitted radiation; G_{act} = actual value of global radiation

Different dimensional characteristics of the investigated specimens affected obviously the solar permeability of the tree crown in the case of each day-pair. Namely, higher transmitted radiation and consequently higher transmisivity values were detected in the case of the smaller *A. hippocastanum* (*Figure 3*). The descriptive statistics in *Table 4* confirm this statement: all median and mean transmissivity values were higher under the smaller individual.

The solar permeability showed a decreasing order along the spring and summer months in the case of both trees. In the case of the larger specimen the transmissivity values fell in the range of 0.02–0.04 in spring and they were below 0.02 in mid-summer, while they declined from 0.09 to 0.085 concerning the smaller tree. After that, the transmissivity values started to increase and they peaked in October when the values of the smaller individual often exceeded 0.1 (*Figure 3, Table 4*). This phenomenon can be explained obviously by the seasonal foliation status of the trees.

*Table 4. Basic descriptive statistics regarding the transmissivity of the larger (l) and smaller (s) Aesculus hippocastanum (A. h.) trees**

Tree	Date	N	Stan. Dev.	Min.	Median	Mean	Max.
A. h. (l)	12-May-2015	371	0.075	0.014	0.020	0.037	0.801
A. h. (s)	18-May-2015	360	0.012	0.077	0.087	0.091	0.122
A. h. (l)	01-Jun-2015	316	0.042	0.018	0.028	0.037	0.523
A. h. (s)	02-Jun-2015	389	0.013	0.079	0.090	0.094	0.169
A. h. (s)	01-Jul-2015	350	0.014	0.057	0.085	0.087	0.269
A. h. (l)	02-Jul-2015	301	0.045	0.017	0.029	0.040	0.468
A. h. (l)	21-Jul-2015	321	0.013	0.007	0.016	0.019	0.118
A. h. (s)	22-Jul-2015	390	0.011	0.075	0.084	0.088	0.128
A. h. (l)	27-Aug-2015	369	0.081	0.014	0.022	0.039	0.775
A. h. (s)	28-Aug-2015	381	0.059	0.083	0.099	0.111	0.686
A. h. (l)	01-Oct-2015	342	0.130	0.030	0.037	0.074	0.908
A. h. (s)	02-Oct-2015	372	0.039	0.082	0.104	0.111	0.542

*The statistics are based on the data of sunny minutes (N) only.

The decline in G_{act} values on cloudy days implies relatively smaller increase in tranmissivity values in summer when transmissivity values are already the lowest. We found comparably high transmissivity values in the case of the larger *A. hippocastanum* at the end of the daily measurement period on the late summer day and the autumn measurement day (*Figure 3*). Accordingly, we got remarkably different median and mean values on these days (median of 0.022 and mean of 0.039 on 27 August, and median of 0.037 and mean of 0.074 on 1 October; *Table 4*). Comparing the transmissivity of the two tree individuals based on their daily medians, we found considerably higher values in the case of the smaller specimen *(Table 4)*, that is, even in the case of adult trees, the dimensional characteristics have a great impact on the shading capacity.

Concerning the differences in standard deviation (*SD*) of the two specimens, almost the same *SD* values were observed in late July (0.013 and 0.011; *Table 4*). At this time of the year the foliage is expected to be fully developed and most dense. In other days, however, the larger individual had considerably higher *SD*. The reason for this can be attributed to the 'regular jump' of the larger tree's transmissivity in the afternoon, which was caused by canopy-structural characteristics (a greater broken off branch).

Discussion and outlook

Planting and maintaining urban tree stands is one of the most obvious ways to fight against heat stress and to create comfortable outdoor places in urban areas. Vegetation mitigates the level of thermal stress most effectively via shading, i.e. by reduction of incoming short-wave radiation (Konarska, J. *et al.* 2014; Kántor, N. *et al.* 2016; Takács, Á. *et al.* 2016a,b). We presented the results of a long-term field measurement series, which covered the whole vegetation period. In line with the primary goal of the study, the analyses focused on the shading capacity of single, mature trees belonging to those species that are frequently planted in Hungarian towns as street or park trees. As a measure, dimensionless transmissivity values were calculated. We were looking for inter-species differences, and examined the effect of dimensional differences on the shading capacity of mature trees. The resulted graphs (*Figures 2* and *3*) revealed that transmissivity is sensitive to the background sky conditions, especially to the rapid changes of sunny and cloudy periods. Therefore, we performed the main descriptive analyses on the basis of clear sky condition values only (*Table 3* and *4*).

Shading efficiency of urban trees and its variation among different species and seasons can provide useful information with

regards to climate sensitive planning and modelling of outdoor thermal comfort in cities (Konarska, J. *et al.* 2014). However, there is still a lack of information in experimental transmissivity data. As an international comparison, *Figure 4* summarizes the outcomes of the available transmissivity studies that have been carried out in different geographical areas. The displayed mean transmissivity values were based on clear (or mostly clear) measurement days in summer – or at least on those days when the investigated trees were fully foliated. (The mean values of the present study were based on the days in *Table 3*). *Figure 4* illustrates great inter-species differences, and evinces the effective shading of *Tilia* and *Aesculus* species.

Besides, similarily to previous investigations (e.g. Cantón, M.A. *et al.* 1994; Konarska, J. *et al.* 2014; Takács, Á. *et al.* 2015a), this study revealed significant annual differences in transmissivity (*Figure 3*), which depend on the species-specific foliation-defoliation cycle. Due to these findings, application of monthly, or at least seasonally transmissivity values would be required in radiation and bio-climate modelling.

Figure 5 offers a graphical summary about the main findings of this study, including the disturbing impact of clouds on the calculated transmissivity values, the dimension-related effects and the inter-species differences. The chart-montage shows the daily graphs of *S. japonica, T. cordata* and the two *A. hippocastanum*s based on the data of four nearby summer days.

The effect of clouds is clearly reflected in the higher and most variable transmitted radiation and thus transmissivity values during the afternoon hours of 21 July (*Figure 5, a*). One reason for that may be that the ratio of diffuse radiation (as part of the global radiation) increases at the expense of direct radiation during cloudy conditions. The foliage, however, is more effective regarding the interception of direct radiation than diffuse radiation (Cantón, M.A. *et al.* 1994; Konarska, J. *et al.* 2014). In cloudy conditions, the actual value of *G* may drop because of the decrease of direct radiation, however, the diffuse part that is less effectively shielded by tree crown is almost the same. This may result in much greater decrease in G_{act} than in G_{trans}, thus an increase in transmissivity.

The frequency of temporary transmittance of direct radiation through the foliage is a species-related attribute depending on canopy-structural characteristics (Shahidan, M.F. *et al.* 2010). Of course, if we put species-specific characteristics in the focus of the inves-

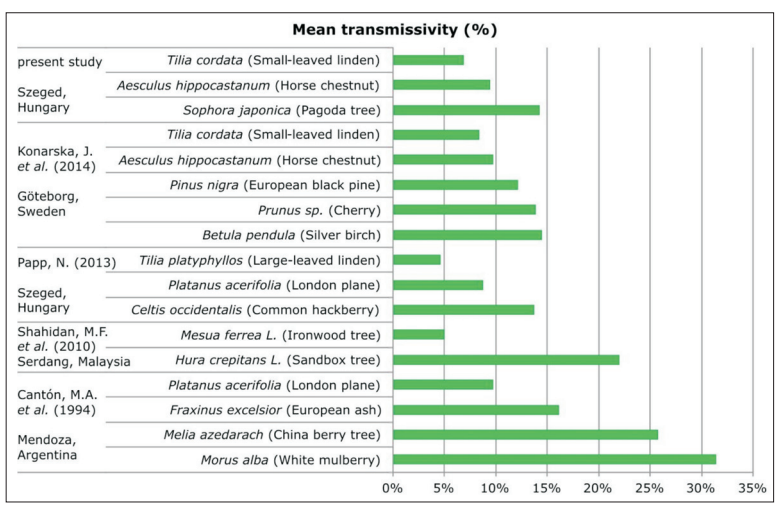

Fig. 4. Comparison of mean transmissivity values found in different experimental studies

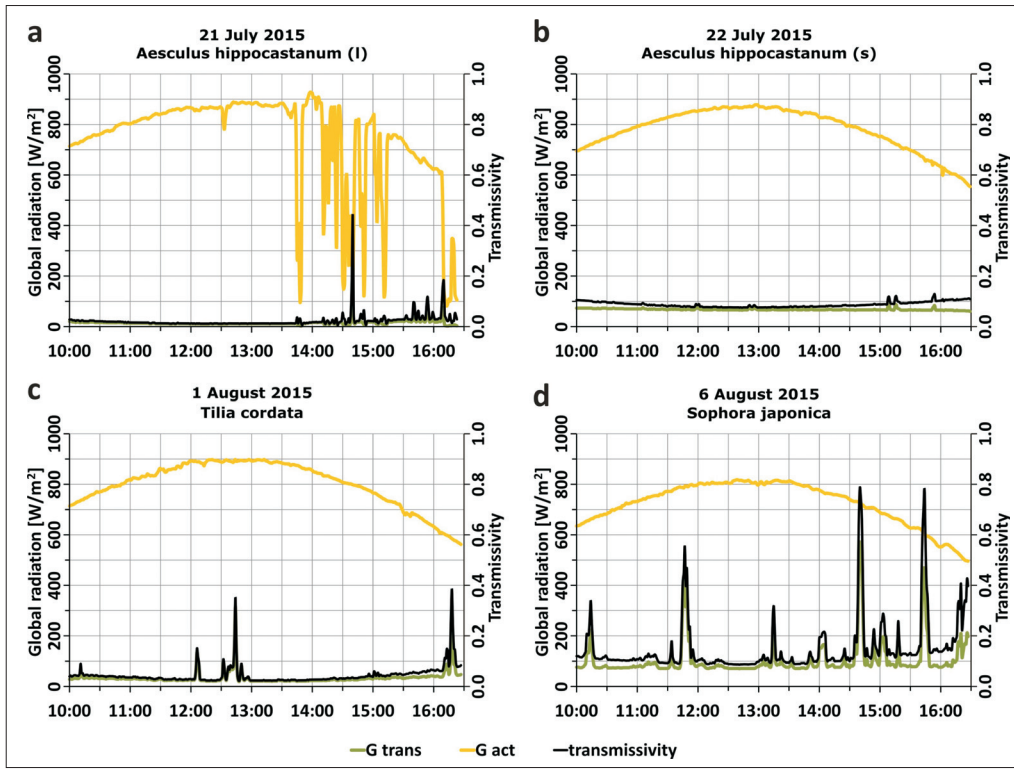

Fig. 5. Transmissivity and the short-wave radiation from the upper hemisphere measured under different shade-trees as well as in a nearby open point. Time is in CET; G_{trans} = transmitted radiation; G_{act} = actual value of global radiation

tigations, it is suggested to analyse a dataset free from the disturbing effect of clouds. Our results confirmed that transmissivity values are more balanced on sunny days, which underpins the necessity of clear days for the more detailed transmissivity investigations focusing on inter-species and canopy-dimensional differences.

The comparison of the results of two *A. hippocastanum* trees provided information on the effect of dimensional differences (*Figure 3; Figure 5, a* and *b*). In the case of the larger individual the lower transmitted radiation values were associated with reduced transmissivity. One reason for this could be the greater crown volume in the large *A. hippocastanum* individual (*Table 1*), which implies a longer distance through the canopy that the direct solar beam has to pass, enhancing the foliage absorption therefore lowering G_{trans}. On the other hand, the greater trunk height of the smaller *A. hippocastanum* specimen (*Table 1*) connotes that larger amount of diffuse radiation may reach the sensor placed under the tree from lateral directions. Thus, both of these dimensional-related differences allow measuring greater G_{trans} under the smaller *A. hippocastanum* at the same time of the year, provided that both individuals are healthy (*Figure 3; Figure 5, a* and *b*). Increased transmissivity values were found in the case of the larger *A. hippocastanum* at the end of the daily measurement period on the investigation days in late summer and autumn (*Figure 3*). This may be the result of lower sun elevation, cloudy conditions or structural deficiencies at certain parts of the tree crown that increased the value of G_{trans} (*Figure 3*).

The remarkable difference between the median and mean values characterizing the transmissivity of the larger *A. hippocastanum* is the consequence of the fact that the arithmetical mean is very sensitive to extremes (*Table 4*) (Andrade, H. and Vieira, R. 2007; Takács, Á. *et al.* 2015a). Since transmissivity may change rapidly and may show some outlier values depending on the slight movements of leaves because of wind as well as the monotonous change in sun elevation and azimuth, we consider it more appropriate to characterize the distribution of transmissivity with the median value.

The obtained inter-species differences (*Figures 2, 4* and *5*) in transmissivity may be explained with the characteristics of canopy structure and leaf density (see also Shahidan, M.F. *et al.* 2010). Due to the dense foliage, there is relatively small and consistent transmitted radiation in the case of *T. cordata,* which results in small transmissivity values. The good shading potential of *Tilia* species was also shown by Papp, N. (2013) in Szeged and Konarska, J. *et al.* (2014) in Gothenburg, Sweden. On the contrary, we found always higher transmissivity values in the case of *S. japonica* due to its sparse canopy allowing direct radiation to reach the instrument more frequently. This attribute is clearly reflected in the fluctuating G_{trans} and transmissitivity values concerning *S. japonica* (*Figure 2; Figure 5, d)*.

We consider that the presented measurement method is suitable for gaining generic information about the shading capacity of trees. According to the resulted transmissivity values, the species can be ranked based on their shading capability, and these information are directly usable in the course of green space planning and in selection of appropriate trees.

The obtained results can be used as input data in microclimate simulations to enable more reliable modelling. For example, from the group of tools designed for the assessment of human thermal comfort conditions, SOLWEIG model allows the users to add or change the transmissivity value of the modelled trees. This means that in the course of outdoor space design the effect of altered transmissivity can be evaluated on a territorial basis.

REFERENCES

Abreu-Harbich, L.V., Labaki, L.C. and Matzarakis, A. 2015. Effect of tree planting design and tree species on human thermal comfort in the tropics. *Landscape and Urban Planning* 138. 99–109.

Andrade, H. and Vieira, R. 2007. A climatic study of an urban green space: The Gulbenkian park in Lisbon (Portugal). *Finisterra* 42. 27–46.

Bajsanski, I.V., Milosevic, D.D. and Savic, S.M. 2015. Evaluation and improvement of outdoor thermal comfort in urban areas on extreme temperature days: Applications of automatic algorithms. *Building and Environment* 94. 632–643.

Bowler, D.E., Buyung-Ali, L., Knight, T.M. and Pullin, A.S. 2010. Urban greening to cool towns and cities: A systematic review of the empirical evidence. *Landscape and Urban Planning* 97. 147–155.

Cantón, M.A., Cortegoso, J.L. and de Rosa, C. 1994. Solar permeability of urban trees in cities of western Argentina. *Energy and Buildings* 20. 219–230.

Coutts, A.M., White, E.C., Tapper, N.J., Beringer, J. and Livesley, S.J. 2016. Temperature and human thermal comfort effects of street trees across three contrasting street canyon environments. *Theoretical and Applied Climatology*, DOI 10.1007/s00704-015-1409-y.

Dimoudi, A. and Nikolopoulou, M. 2003. Vegetation in the urban environment: microclimatic analysis and benefits. *Energy and Buildings* 35. 69–76.

Égerházi, L.A., Kovács, A. and Unger, J. 2013. Application of microclimate modelling and onsite survey in planning practice related to an urban micro environment. *Advances in Meteorology 2013,* Article ID: 251586.

Erell, E., Pearlmutter, D., Boneh, D. and Kutiel, P.B. 2014. Effect of high-albedo materials on pedestrian heat stress in urban street canyons. *Urban Climate* 10. 367–386.

Gál, T. and Unger, J. 2009. Detection of ventilation paths using high-resolution roughness parameter mapping in a large urban area. *Building and Environment* 44. 198–206.

Gulyás, Á., Unger, J. and Matzarakis, A. 2006. Assessment of the microclimatic and human comfort conditions in a complex urban environment: modelling and measurements. *Building and Environment* 41. 1713–1722.

Haase, D., Larondelle, N., Andersson, E., Artmann, M., Borgström, S., Breuste, J., Gomez-Baggethun, E., Gren, A., Hamstead, Z., Hansen, R., Kabisch, N., Kremer, P., Langemeyer, J., Rall, E.L., McPhearson, T., Pauleit, S., Qureshi, S., Schwarz, N., Voigt, A., Wurster, D. and Elmqvist, T. 2014. A quantitative review of urban ecosystem service assessments: concepts, models and implementation. *Ambio* 43. 413–433.

HMS 2015. Climate characteristics of Szeged. http://www.met.hu/eghajlat/magyarorszag_eghajlata/varosok_jellemzoi/Szeged/

Jim, C.Y. and Chen, W.Y. 2008. Assessing the ecosystem service of air pollutant removal by urban trees in Guangzhou (China). *Journal of Environmental Management* 88. 665–676.

Kántor, N. and Unger, J. 2010. Benefits and opportunities of adopting GIS in thermal comfort studies in resting places: An urban park as an example. *Landscape and Urban Planning* 98. 36–46.

Kántor, N. and Unger, J. 2011. The most problematic variable in the course of human-biometeorological comfort assessment – the mean radiant temperature. *Central European Journal of Geosciences* 3. 90–100.

Kántor, N., Kovács, A. and Takács, Á. 2016. Small-scale human-biometeorological impacts of shading by a large tree. *Open Geosciences*, in press (DOI 10.1515/geo-2016-0021).

Kirnbauer, M.C., Baetz, B.W. and Kenney, W.A. 2013. Estimating the stormwater attenuation benefits derived from planting four monoculture species of deciduous trees on vacant and underutilized urban land parcels. *Urban Forestry & Urban Greening* 12. 401–407.

Konarska, J., Lindberg, F., Larsson, A., Thorsson, S. and Holmer, B. 2014. Transmissivity of solar radiation through crowns of single urban trees – application for outdoor thermal comfort modelling. *Theoretical and Applied Climatology* 117. 363–376.

Lee, H., Holst, J. and Mayer, H. 2013. Modification of human-biometeorologically significant radiant flux densities by shading as local method to mitigate heat stress in summer within urban street canyons. *Advances in Meteorology 2013,* Article ID 312572.

Lee, H., Mayer, H. and Schindler, D. 2014. Importance of 3-D radiant flux densities for outdoor human thermal comfort on clear-sky summer days in Freiburg, Southwest Germany. *Meteorologische Zeitschrift* 23. 315–330.

Lelovics, E., Unger, J., Gál, T. and Gál, C.V. 2014. Design of an urban monitoring network based on Local Climate Zone mapping and temperature pattern modelling. *Climate Research* 60. 51–62.

Mayer, H., Holst, J., Dostal, P., Imbery, F. and Schindler, D. 2008. Human thermal comfort in summer within an urban street canyon in Central Europe. *Meteorologische Zeitschrift* 17. 241–250.

Mullaney, J., Lucke, T. and Trueman, S.J. 2015. A review of benefits and challenges in growing street trees in paved urban environment. *Landscape and Urban Planning* 134. 157–166.

Ng, E. 2009. Policies and technical guidelines for urban planning of high-density cities – air ventilation assessment (AVA) of Hong Kong. *Building and Environment* 44. 1478–1488.

Nowak, D.J., Greenfield, E.J., Hoehn, R.E. and Lapoint, E. 2013. Carbon storage and sequestration by trees in urban and community areas of the United States. *Environmental Pollution* 178. 229–236.

Papp, N. 2013. *A városi fás vegetáció hatása a termikus komfortviszonyokra Szeged példáján* (The impact of urban woody vegetation on thermal comfort conditions through the example of Szeged). MS Thesis, Szeged, University of Szeged, 69 p.

Pongrácz, R., Bartholy, J. and Bartha, E.B. 2013. Analysis of projected changes in the occurrence of heat waves in Hungary. *Advences in Geosciences* 35. 115–122.

Shahidan, M.F., Shariff, M.K.M., Jones, P., Salleh, E. and Abdullah, A.M. 2010. A comparison of *Mesua ferrea* L. and *Hura crepitans* L. for shade creation and radiation modification in improving thermal comfort. *Landscape and Urban Planning* 97. 168–181.

Sun, R. and Chen, L. 2012. How can urban water bodies be designed for climate adaptation? *Landscape and Urban Planning* 105. 27–33.

Takács, Á., Kiss, M., Gulyás, Á. and Kántor, N. 2015a. Microclimate regulation potential of different tree species: transmissivity measurements in Szeged, Hungary. 9th International Conference on Urban Climate, Toulouse, 544, 6 p.

Takács, Á., Kiss, M., Kántor, N. and Gulyás, Á. 2015b. A városi fás vegetáció humán bioklimatológiai jelentősége – gyakori szegedi fafajok árnyékhatásának vizsgálata (The human bioclimatic significance of urban woody vegetation – investigation of the shading effect of frequent tree species in Szeged). In *Spring Wind 2015. Conference book.* Ed.: Keresztes, G. Eger–Budapest, Doktoranduszok Országos Szövetsége, 571–587.

Takács Á, Kiss, M., Gulyás, Á., Tanács, E. and Kántor, N. 2016a. Solar permeability of different tree species in Szeged, Hungary. *Geographica Pannonica* 20. 32–41.

Takács, Á., Kiss, M., Hof, A., Tanács, E., Gulyás, Á. and Kántor, N. 2016b. Microclimate modification by urban shade trees – an integrated approach to aid ecosystem service based decision-making. *Procedia Environmental Sciences* 3. 97–109. (Article reference: PROENV3012).

Thorsson, S., Rocklöv, J., Konarska, J., Lindberg, F., Holmer, B., Dousset, B. and Rayner, D. 2014. Mean radiant temperature – A predictor of heat related mortality. *Urban Climate* 10. 332–345.

UN 2014. *World Urbanization Prospects: The 2014 Revision, Highlights (ST/ESA/SER.A/352).* New York, United Nations, 32 p.

Yang, X., Zhao, L., Bruse, M. and Meng, Q. 2013. Evaluation of a microclimate model for predicting the thermal behavior of different ground surfaces. *Building and Environment* 60. 93–104.

Changing Ethnic Patterns of the Carpatho–Pannonian Area from the Late 15th until the Early 21st Century

Edited by: Károly KOCSIS and Patrik TÁTRAI

Hungarian Academy of Sciences, Research Centre for Astronomy and Earth Sciences
Budapest, 2015

This is the third, revised and enlarged edition of the Changing Ethnic Patterns of the Carpatho–Pannonian Area. The work is georeferenced and comes with a CD-appendix. The collection of maps visually presents the ethnic structure of the ethnically, religiously and culturally unique and diverse Carpathian Basin and its neighbourhood, the Carpatho–Pannonian area. The volume – in Hungarian and English – consists of three structural parts. On the main map, pie charts depict the ethnic structure of the settlements in proportion to the population based on the latest census data. In the supplementary maps, changes in the ethnic structure can be seen at ten points in time (in 1495, 1784, 1880, 1910, 1930, 1941, 1960, 1990, 2001 and 2011). The third part of the work is the accompanying text, which outlines ethnic trends in the past five hundred years in the studied area. This volume presents the Carpatho–Pannonian area as a whole. Thus, the reader can browse the ethnic data of some thirty thousand settlements in various maps.

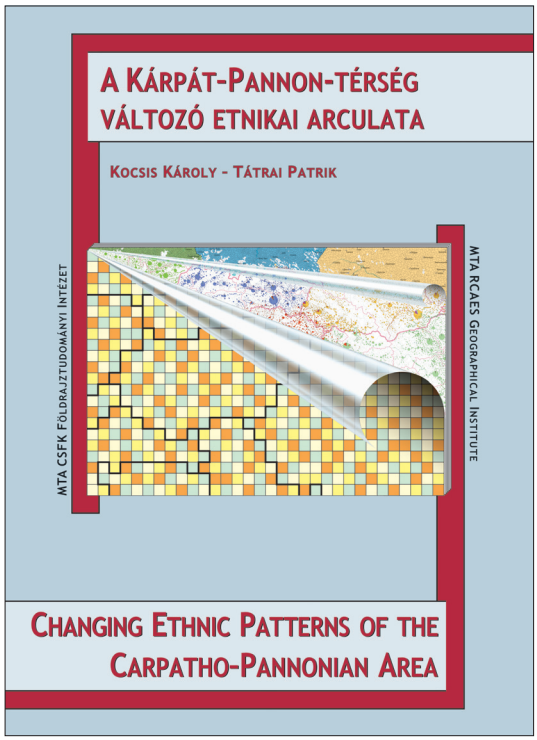

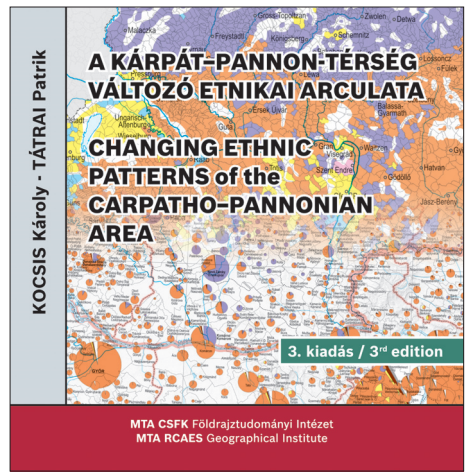

Price: EUR 12.00
Order: Geographical Institute RCAES MTA Library. H-1112 Budapest, Budaörsi út 45.
E-mail: magyar.arpad@csfk.mta.hu

DOI: 10.15201/hungeobull.65.2.7 Hungarian Geographical Bulletin 65 2016 (2) 169–180.

Modelled spatio-temporal variability of air temperature in an urban climate and its validation: a case study of Brno, Czech Republic

Jan GELETIČ[1,2] Michal LEHNERT[3] and Petr DOBROVOLNÝ[1,2]

Abstract

This study compares the results of air temperature model simulations with real temperature measurements in an urban environment. The non-hydrostatic micro-scale model MUKLIMO_3 is used to predict air temperature fields in Brno (Czech Republic). The development of the air temperature fields on three different days was modelled which characterising the radiation-driven weather conditions with high temperature that occurred during the summer of 2015. This analysis demonstrates that the model is able to reproduce the spatial distribution of the air temperature during the day. Statistical tests were applied to establish whether significant differences exist between the modelled and measured air temperatures. Verification of the model results against real temperature measurements was performed at five meteorological stations. The mean absolute differences between the simulated and measured daily mean temperatures were 0.7 °C (4 July), 0.6 °C (18 July) and 0.5 °C (28 August), respectively. This demonstrates that the model overestimated the real values, however, not all the differences were statistically significant. Moreover, there were no significant differences in the variability of the temperatures that were compared. This study also shows that the proper definition of Local Climate Zones and their parameters is critical for more precise model performance.

Keywords: MUKLIMO_3, urban air temperature, Local Climate Zones, GIS, spatial modelling

Introduction

The spatial and temporal variability of the air temperature in urban environments has been studied frequently in recent decades in connection with the formation of Urban Heat Islands (UHIs) (Arnfield, A.J. 2003). With the development of new data sources and new methodological approaches in recent years, research in urban climatology has shifted from identifying UHIs and estimates of UHI intensity to searching for the exact patterns of the spatio-temporal variability of UHIs and temperature fields in urban environments. Given the diversity of urban structure (Bechtel, B. and Daneke, C. 2012; Lelovics, E. *et al.* 2014; Lehnert, M. *et al.* 2015), qualities of relief (Saaroni, H. and Ziv, B. 2010; Bokwa, A. *et al.* 2015) and the variability of synoptic conditions (Gedzelman, S.D. *et al.* 2003; Przybylak, R. *et al.* 2015), it is a fairly complex and challenging task. Contemporary studies of the temperature fields of cities and their surroundings, therefore, impose high demands on the density and quality of the station network and the frequency and range of mobile measurements. At the same time, it appears that the current methods of remote sensing focusing on land surface temperature variability may not provide relevant information about air temperature (Voogt, J.A. and Oke, T.R. 2003). Recently, numerical modelling has come to represent another opportunity leading to more detailed and more accurate

[1] Department of Geography, Faculty of Science, Masaryk University Brno, Kotlářská 2, 611 37 Brno, Czech Republic. E-mails: geletic.jan@gmail.com, dobro@sci.muni.cz
[2] Global Change Research Institute of the Czech Academy of Sciences, Bělidla 986/4a, 603 00 Brno, Czech Republic.
[3] Department of Geography, Faculty of Science, Palacký University Olomouc. 17. Listopadu 12, 771 46 Olomouc, Czech Republic. E-mail: michal.lehnert@gmail.com

information about the spatio-temporal variability of urban air temperatures and UHI parameters.

Because of the progress in exploring the complexity of processes driving the climate system, models designed for application on scale of the city have gradually been developed. The first models demonstrated the differences in the energy balance between the city and its surroundings (e.g. Mills, G. 2009). The current state of the art numerical models make it possible to solve the thermodynamics of the atmosphere and complex relations between variables, such as the height of buildings and the structure of the buildings, materials used, height and the types of vegetation on the scale of the urban environment (Sievers, U. and Zdunkowski, W. 1985; Gross, G. 1989; Baklanov, A. *et al.* 2009). While numerical modelling offers very important information on urban temperature fields, another quite important task is the validation of the model outputs. Hollosi, B. *et al.* (2014) indicate that these results could not be validated as a result of the lack of observations.

The MUKLIMO_3 thermodynamic model developed by Deutscher Wetterdienst (2014) in collaboration with Zentralanstalt für Meteorologie und Geodynamik was used to analyse the main features of air temperature variability in Brno (Czech Republic). The primary aim of this contribution is to validate the MUKLIMO_3 outputs using air temperatures measured at several meteorological stations located in the city of Brno. The comparison is performed for several days that represent typical air temperature (more detail in section Meteorological data) conditions in Brno during the heat waves in the summer of 2015.

Study area

The study area is situated in the south-eastern part of the Czech Republic (*Figure 1*). Brno (49.2N, 16.5E) is the second-largest city in the country (population 400,000, land registry area 230 km^2) and is characterised by a basin position with complex terrain. Altitudes range from 190 m to 479 m a.s.l. with the higher elevations lying largely in the western and northern parts of the region. Lower and flatter terrain is typical of the southern and eastern parts of the study area. There is a water reservoir (area approx. 2.6 km^2) located on the northwest border of the built-up part. The study area lies in one of the warmest and driest regions in the Czech Republic. The mean

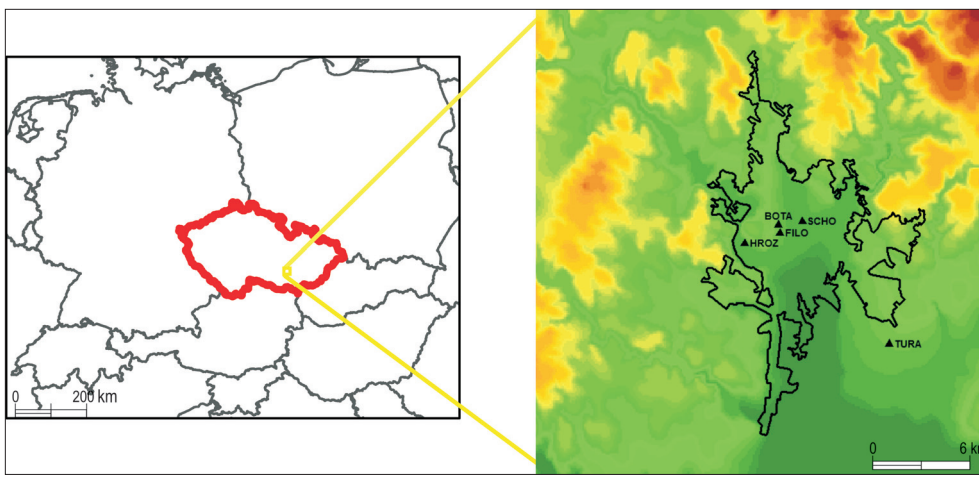

Fig. 1. Elevation in the study area of Brno, position of validation stations and boundary of compact city structure

annual temperature stands at 9.4 °C, while the mean annual precipitation is around 500 mm (1961–2000 reference period).

The highest density of built-up areas occurs in the historical city centre. These are largely residential (20% of the study area). There are several industrial zones and large shopping centres with high percentages of impervious surfaces (almost 14% of the total area). Several large parks are located relatively close to the city centre. Further from the centre, individual land-cover categories form a mosaic of different surface types, such as blocks of flats, gardens, allotments and agricultural fields. Arable land and grasslands cover 34% of the study region and are situated mostly in the south, while forests take up 29% of the region and are to be found largely west and north of the built-up area, at higher elevations.

Methods and data

MUKLIMO_3

MUKLIMO_3 (3D Mikroskaliges Urbanes KLIma MOdel) is a non-hydrostatic microscale model with z-coordinates, which solves the Reynolds-averaged Navier-Stokes equations to simulate atmospheric flow fields in the presence of buildings (Sievers, U. and Zdunkowski, W. 1985; Gross, G. 1989; Sievers, U. 1990, 1995). The thermo-dynamic version of the model includes prognostic equations for atmospheric temperature, relative humidity, wind speed and wind direction (Sievers, U. *et al.* 1983). The model uses high-resolution orography, land use distribution data and the vertical profile of the atmosphere (up to 1 km above ground level). Land use classes were defined on the basis of Local Climate Zones (see below).

For each land use class a set of parameters is defined which describes land use properties and urban structures: building fraction (γ_b), mean building height (h_b), wall area index (w_b), fraction of pavement of the non-built area (v), fraction of tree crown canopy (σ_t) and fraction of low vegetation of the remaining surface (σ_c), height of low vegetation (h_c) (*Table 1*), as well as leaf area index (LAI_c) of the canopy layer, the mean height (h_t) and leaf area index (LAI_t) of the trees, with separate values for the tree trunk and the tree crown area. The model does not include cloud processes, precipitation, horizontal run-off or anthropogenic heat.

MUKLIMO_3 was used to generate the development of the air temperature field in the study area during three selected days. The model simulation for each day was represented with 23 temperature maps with a resolution of 100 m; the time step between two successive modelled fields was 60 minutes. The corresponding modelled and measured temperatures for five localities (stations) were compared with several statistical tests.

Basic statistical tests for testing true difference (t-test) and variance (f-test) were used. A null hypothesis for a two-sample paired t-test is that the true difference in the means is equal to 0. The critical value of the T-distribution is 1.717144. For a two-sample f-test a null hypothesis that the true ratio of the variances is equal to 1 was used. The critical value of the F-distribution is 2.04777.

Local Climate Zones (LCZ)

The scheme of local climatic zones (LCZs) according to Stewart, I.D. and Oke, T.R. has become a standard for the description of the environment in the field of urban climate research. LCZs are defined as regions with a characteristic surface cover, structure and material and human activity that span hundreds of metres to several kilometres on a horizontal scale (Stewart, I.D. and Oke, T.R. 2012). Bechtel, B. and Daneke, C. (2012), furthermore Lelovics, E. *et al.* (2014) subsequently moved the LCZ concept toward a generally recognised regional typology. For this study an LCZ was delimited using a GIS-based method presented by Geletič, J. and Lehnert, M. (2016). The method was based on measurable physical properties of the en-

*Table 1. Parameters for Local Climate Zones in the MUKLIMO_3 model**

Local	Climate Zone	γ_b %	h_b m	w_b	v %	σ_t %	σ_c %	h_t m	h_c m
1	Compact high-rise	0.60	25.00	6.67	1.00	0.00	0.90	0.00	0.10
2	Compact midrise	0.45	16.50	3.42	0.70	0.00	0.90	0.00	0.10
3	Compact low-rise	0.45	9.20	2.40	0.40	0.00	0.80	0.00	0.10
4	Open high-rise	0.30	25.00	7.00	0.20	0.00	0.60	8.00	0.10
5	Open midrise	0.30	18.60	4.40	0.45	0.00	0.80	4.00	0.10
6	Open low-rise	0.30	6.50	2.10	0.40	0.00	0.70	0.00	0.10
7	Lightweight low-rise	0.75	3.00	1.80	0.20	0.00	0.30	0.00	0.10
8	Large low-rise	0.40	6.80	2.00	0.80	0.00	0.80	0.00	0.10
9	Sparsely built	0.15	8.50	2.10	0.45	0.00	0.80	8.00	0.10
10	Heavy industry	0.50	18.00	2.00	0.80	0.00	0.80	0.00	0.10
A	Dense trees	0.00	0.00	0.00	0.00	0.80	0.90	21.00	0.50
B	Scattered trees	0.00	0.00	0.00	0.00	0.40	0.90	14.00	0.50
C	Bush, scrub	0.00	0.00	0.00	0.00	0.40	0.90	2.00	0.50
D	Low plants	0.00	0.00	0.00	0.00	0.00	1.00	0.20	0.50
E	Bare rock or paved	0.00	0.00	0.00	0.95	0.00	0.01	0.00	0.30
F	Bare soil or sand	0.00	0.00	0.00	0.00	0.00	0.01	0.00	0.30
G	Water	0.00	0.00	0.00	-1.00	0.00	0.01	0.00	0.30

*Parameters: building fraction (γ_b), mean building height (h_b), wall area index (w_b), fraction of pavement (v), fraction of tree crown canopy (σ_t), fraction of low vegetation (σ_c), tree height (h_t) and height of the low vegetation (h_c). The fractions γ_b and σ_t are relative to the total grid cell area (1 ha). The fraction v is relative to the area without buildings and trees and σ_c is relative to the remaining surface.

vironment derived from typical values of the geometric and surface cover properties of a particular LCZ as defined by Stewart, I.D. and Oke, T.R. (2012).

The values of the physical properties of the environment were calculated for 100-m pixels on the basis of the ZABAGED vector geo-database and photogrammetric data (3D model of development). The pixels were subsequently classified using a clearly defined decision-making algorithm that had been tested in the Central European environment. Finally, a two-stage majority filter was applied to define the local climate zones in the Brno (*Figure 2*). (For more details see Geletič, J. and Lehnert, M. 2016.)

Meteorological data

As MUKLIMO_3 provides the best results for radiation-driven weather conditions that are characterised by an almost clear sky, minimum cloud cover and weak advection (Hollosi, B. *et al.* 2014), three days in the high summer season of 2015 were used for model validation (4 July, 18 July and 28 August). The maximum daily temperatures exceeded 30 °C and each of these days was the third day of one of the heat waves which affected Brno in the summer season of 2015. A heat wave was defined as at least three consecutive days on which the air temperature reaches over 30 °C (Meteorologický slovník výkladový a terminologický 2016).

Data from five stations was used for the validation of the model outputs (*Table 2*, and see *Figure 1*). Four stations belong to the local meteorological monitoring network, which has been in operation since 2009. These stations represent the specific features of urban weather, because they are located in urban areas among buildings and near the city centre with heavy traffic. The fifth station is a professional station of the Czech Hydro-Meteorological Institute (CHMI), which is located at the airport in Brno-Tuřany (Dobrovolný, P. *et al.* 2012).

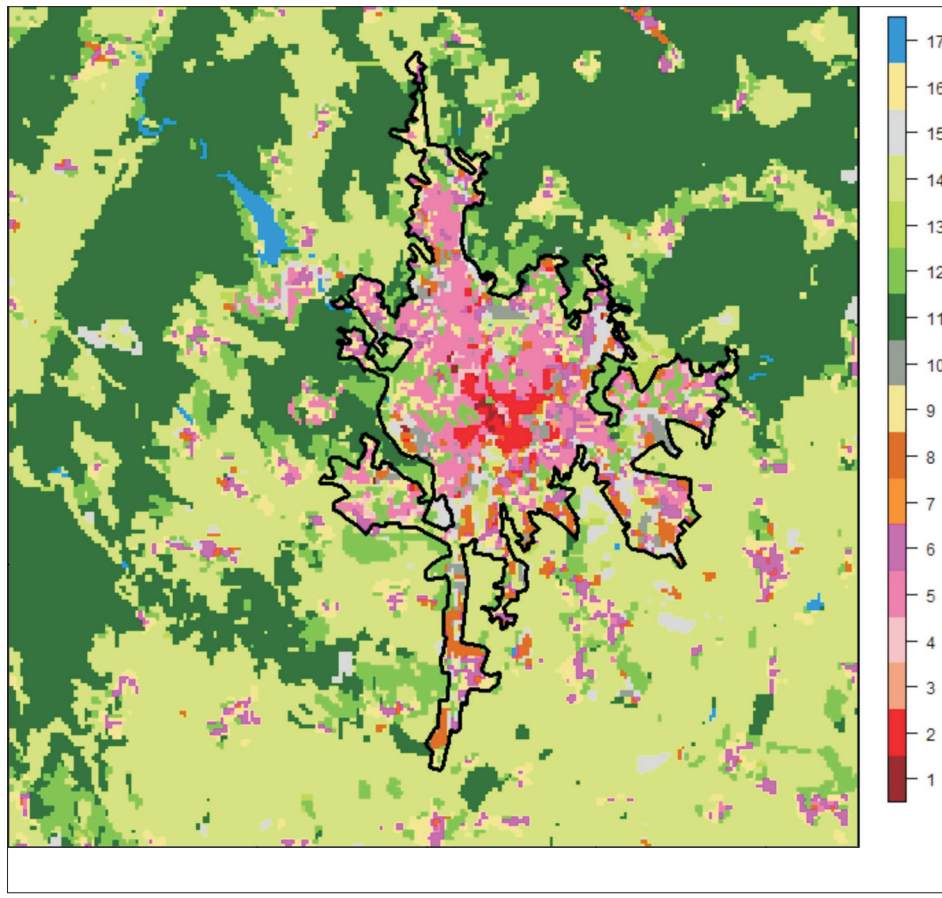

Fig. 2. Local climate zones in Brno and its surroundings (Geletič, J. and Lehnert, M. 2016). The values 11 to 17 correspond with the classes A to G (Coordinate system: S-JTSK / Krovak East North; EPSG: 5514).

*Table 2. Validation stations and their characteristics**

Station ID	Altitude, m	Longitude	Latitude	Exposure	LCZ	NDVI	DENS
BOTA	242	49.20417	16.59639	E	2	0.18	27
FILO	234	49.20028	16.59806	E	5	0.21	39
HROZ	214	49.19361	16.57222	SW	5	0.34	14
SCHO	225	49.20722	16.61389	SW	B	0.31	17
TURA	241	49.15306	16.68889	S	D	0.24	5

*LCZ – LCZ class; NDVI – Normalised Difference Vegetation Index measuring amount of vegetation; DENS – density of buildings (%) in 200 m radius around station.

All the station measurements were performed with a 10-minute frequency and hourly values of the air temperature were used for validation. The meteorological data (air temperature, relative humidity, wind speed and direction) necessary for the operation of the MUKLIMO_3 model were derived from the measurement of vertical profile of the atmosphere up a height of 1 km above surface at the Prostějov station located about 45 km north-east of Brno. In MUKLIMO_3 it is possible to use a minimum of one and a maximum of five layers for the same meteorological elements (Deutscher

Wetterdienst 2014). We used three layers in our vertical profile, at 350, 660 and 980 m. The height of the urban boundary layer can reach approximately 350 m above the ground (Menut, L. *et al.* 2015). Therefore it was supposed that the atmospheric conditions at these heights would probably be the same for Brno and for Prostějov. Meteorological data from the Brno-Tuřany station was used to represent the ground measurements of the study area. For each simulation different vertical profile was used.

The water temperature in the reservoir during the summer season was measured by the Regional Hygienic Station of the South Moravian Region in Brno.

Results

It follows from the model simulations that the places with the lowest air temperatures in the early morning hours before sunrise were located in the deep river valleys in the northern part of Brno *(Figure 3, a)*. Generally, lower air temperatures are typical of LCZ A. After the sunrise the spatial distribution of the air temperature is predominantly influenced by altitude. At 7 a.m. (see *Figure 3, a*) the model forecasts 19 °C for areas with a lower location (particularly the south-eastern part of the area of interest and valleys) and 16 °C for areas with a higher location (particularly the northern and north-western parts of the area).

As the air gets warmer the model gradually generates areas with a higher proportion of LCZs 8, 10 or E that are warmer than their surroundings, including areas located outside the compact urban development. However, the distinct UHI is not formed until 1 p.m. according to the results of the model simulations. At 2 p.m. the UHI is formed over most of the city centre, including areas of LCZs 1 and 2. Higher temperatures were also simulated for smaller settlements with urban development. So-called hotspots were formed in areas with a higher proportion of LCZs 8, 10 or E with air temperatures above 31 °C. On the contrary, relatively cooler spots within the city correspond to larger areas of LCZ B, where air temperatures reach about 29 °C. The lowest temperatures are predicted for forested areas (LCZ A) at higher elevations located in the northern and north-western parts of the area of interest (around 26 °C). Thus the model simulates temperature differences of up to 5 °C between the warmest part of the city and the coolest forests at 2 p.m. (*Figure 3, b*).

The city centre and areas with a higher proportion of LCZs 8, 10 or E are expected to remain slightly warmer than their surroundings until the night hours. Higher temperatures occur around bodies of water (LCZ G). The model, however, forecasts a relatively low intensity of UHI during the evening and night hours. At 9 p.m. the warmest parts of

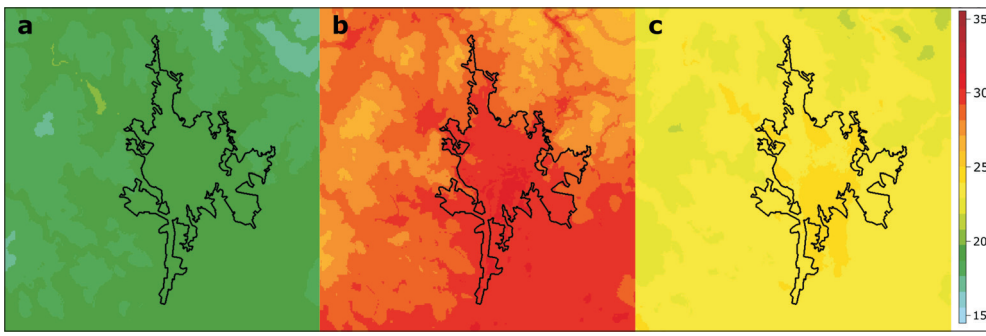

Fig. 3. Modelled spatio-temporal variability of the air temperature (°C) in Brno on 28 August 2015 at 7.00 a.m. (a), at 2.00 p.m. (b) and at 9.00 p.m. (c) CET

the city are only about 1 °C warmer than the agricultural landscape around the city (predominantly LCZ D) and up to 3 °C warmer than the forested areas (*Figure 3, c*).

In general, the MUKLIMO_3 simulations overestimate the real air temperatures on all three of the days that were analysed (*Figure 4*). The simulated mean daily temperatures were, on average, higher by 1.2 °C (4 July), 0.6 °C (18 July), and 0.9 °C (28 August) than the measured temperatures. The temperatures were especially overestimated at the BOTA (LCZ 2) and HROZ (LCZ 5) stations. The minimum absolute difference occurred at the TURA station (0.9 °C) and maximum at the BOTA station (1.2 °C). Clearly higher model temperatures compared to measured ones occurred only on 4 July (in the starting phase of the model) and on 28 August (the model simulation assumes a sharp peak in the daily air temperature curve, whereas the real daily temperature curve showed lower maximum temperatures and simultaneously temperatures remained at relatively higher values for longer intervals). Minimum daily average difference occurred at the TURA station on 4 July (0.8 °C) and maximum at the FILO station on 4 July (1.7 °C).

A comparison of measured and simulated air temperatures for the three selected days demonstrates that the model successfully approximates the temperature variability through day and night at the locations of the individual stations (*Figure 5*). The smallest absolute difference between real and simulated air temperature was found for TURA. Station is located outside the compact urban structure at the international airport (LCZ D). The maximum mean difference is typical of the BOTA station, which is located within a compact city structure (LCZ 2) in a botanical garden inside the built-up area.

The differences between the modelled and measured air temperatures were further evaluated with several statistical tests (*Figure 6*). It allows evaluate the statistical significance of the differences that had been found between measurements and model outputs. The results of the t-test confirm that most model

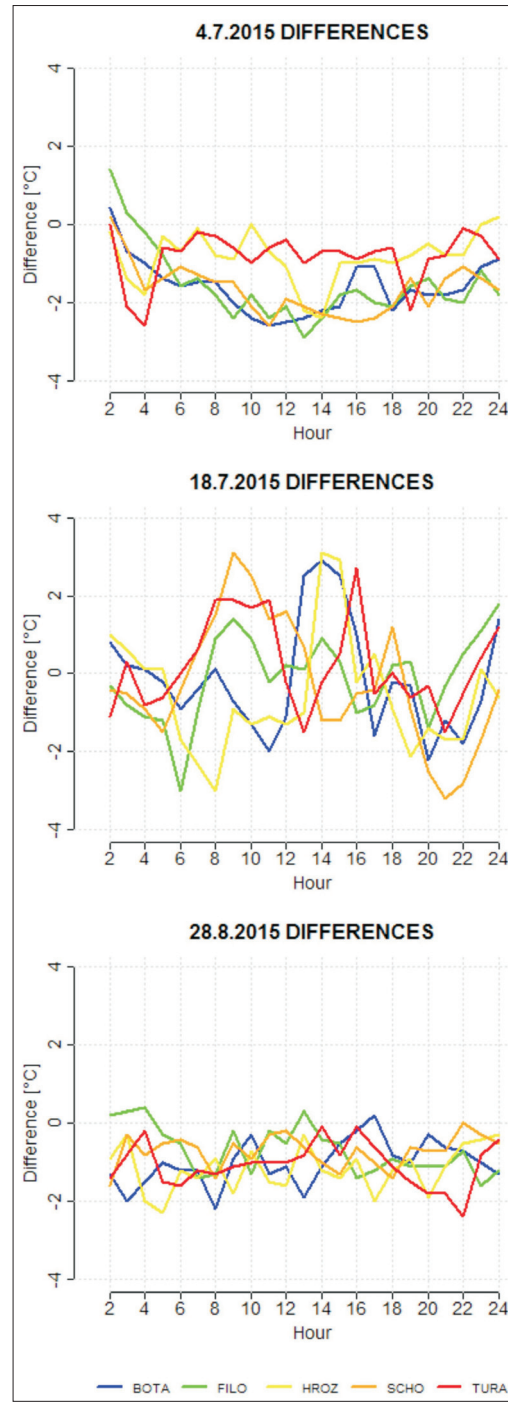

Fig. 4. Differences between real measurements and model outputs

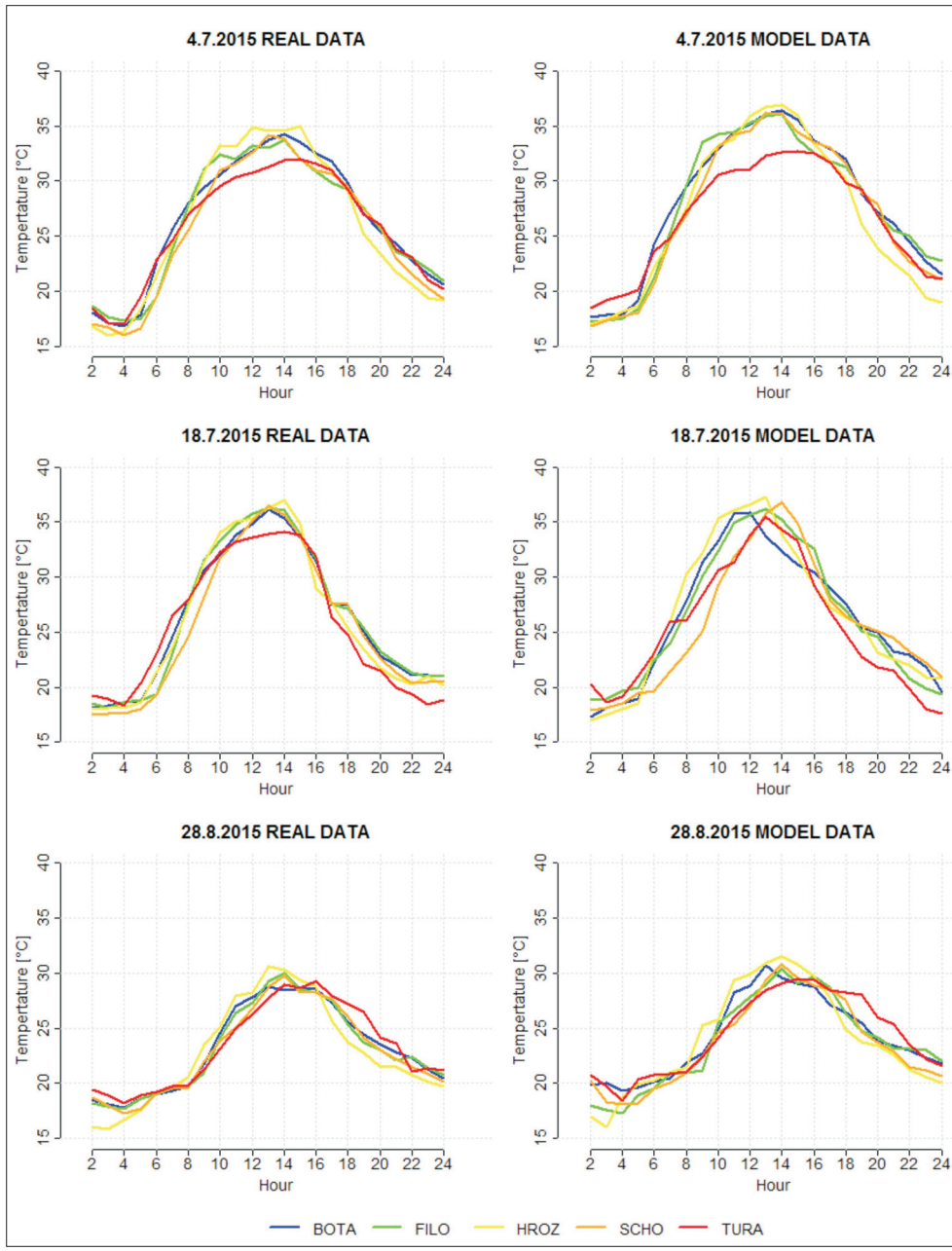

Fig. 5. Comparison between real measurements (left) and model outputs (right)

outputs are overestimated for all stations. While the mean daily modelled temperatures were significantly higher than the measured ones at all five stations on two of the days that were analysed (4 July, 28 August), there were no significant differences on 18 July ($p >$

0.05 for all stations except HROZ). Moreover, there were no significant differences in the temperature variability according to the F-test ($p >> 0.05$) at any of the stations on all three days that were analysed.

Discussion

The comparison of the real station measurements and MUKLIMO_3 simulations in Brno and its surroundings shows that the model is able accurately to simulate the daily cycles of the air temperature at the five selected locations and to take into account some of the specific local features. The model corresponds best with the situation on 28 August 2015 (see *Figure 4*); this may be related to more stable atmospheric conditions very close to climatological autumn. Individual problems with the accuracy of the model simulation were primarily related to the starting phase of the modelling (esp. on 4 July 2015; see *Figure 4*). This problem may be related to the interaction of the 1D and 3D models. The 1D model starts before the 3D model and prepares the atmospheric conditions for the 3D model (Deutscher Wetterdienst 2014). In our case it starts 24 hours before the 3D model. This may be too far in advance. The correct settings of the Land Use Table parameter may also be responsible (see below).

At times when the surface displays a negative energy balance MUKLIMO_3 frequently assumes a sharp drop in the temperature earlier than the measurements (for example at the TURA station on 4 July) or steady decline rather than a sharp drop after sunset (at all stations on 18 July). This could largely be due to the complexity of the relief in Brno and its surroundings and the related local circulation systems.

The spatial patterns of the simulated temperature field correspond to the theoretical expectations in those periods when there is a positive energy balance.

The first hotspots were formed in the morning in LCZs 8, 10 and E, which indicates the beginning of UHI formation. In the early afternoon hours (1–3 p.m.) the central part of the Brno area was about 1-2 °C warmer compared to suburban areas and up to 4 °C warmer than the surrounding forests, according to the model outputs. The air temperature of a large part of the urban areas was not higher than in the areas where there was an agricultural landscape with a predominance of fields (LCZ D). This is in agreement with the findings of several other studies which indicated that the daily measurements of air temperatures in LCZ D may be higher than the temperatures measured in some types of compact built-up areas (e.g. LCZs 5 or 9; Houet, T. and Pigeon, G. 2011; Lehnert, M. *et al.* 2015).

At night during the period of negative energy balance MUKLIMO_3 assumed a temperature that was just 1 °C higher in the centre of the city than in the suburbs and temperature that was 3 °C higher in the city centre than in the coldest forests. This may be compared to the results of mobile measurements in the Brno area (Dobrovolný, P. and Krahula, L. 2015). These authors claim that during the first half of the night in summer the city centre is almost 2 °C warmer compared to the suburbs and almost 5 °C warmer than the surrounding rural areas. The actual comparison of the model results and station measurements does not refer to an underestimation of the intensity of the UHI effect. The differences in the average daily minimum temperatures between the stations that were analysed here, because of the absence of a reference station located in a cool area, smaller than measured Dobrovolný, P. *et al.* (2012). The surroundings of the city may actually be cooler than the model expects.

The analysis of the spatial patterns of the simulated temperature field shows that the MUKLIMO_3 model primarily reflects the effect of altitude. This is especially evident in the late afternoon and evening hours and during the night. The model predicts globally higher temperatures at lower altitudes. It can be considered as a simplification (Bokwa, A. *et al.* 2015). On the other hand, the model does not reflect the extent of the variability of building density (i.e. the amount and effect of accumu-

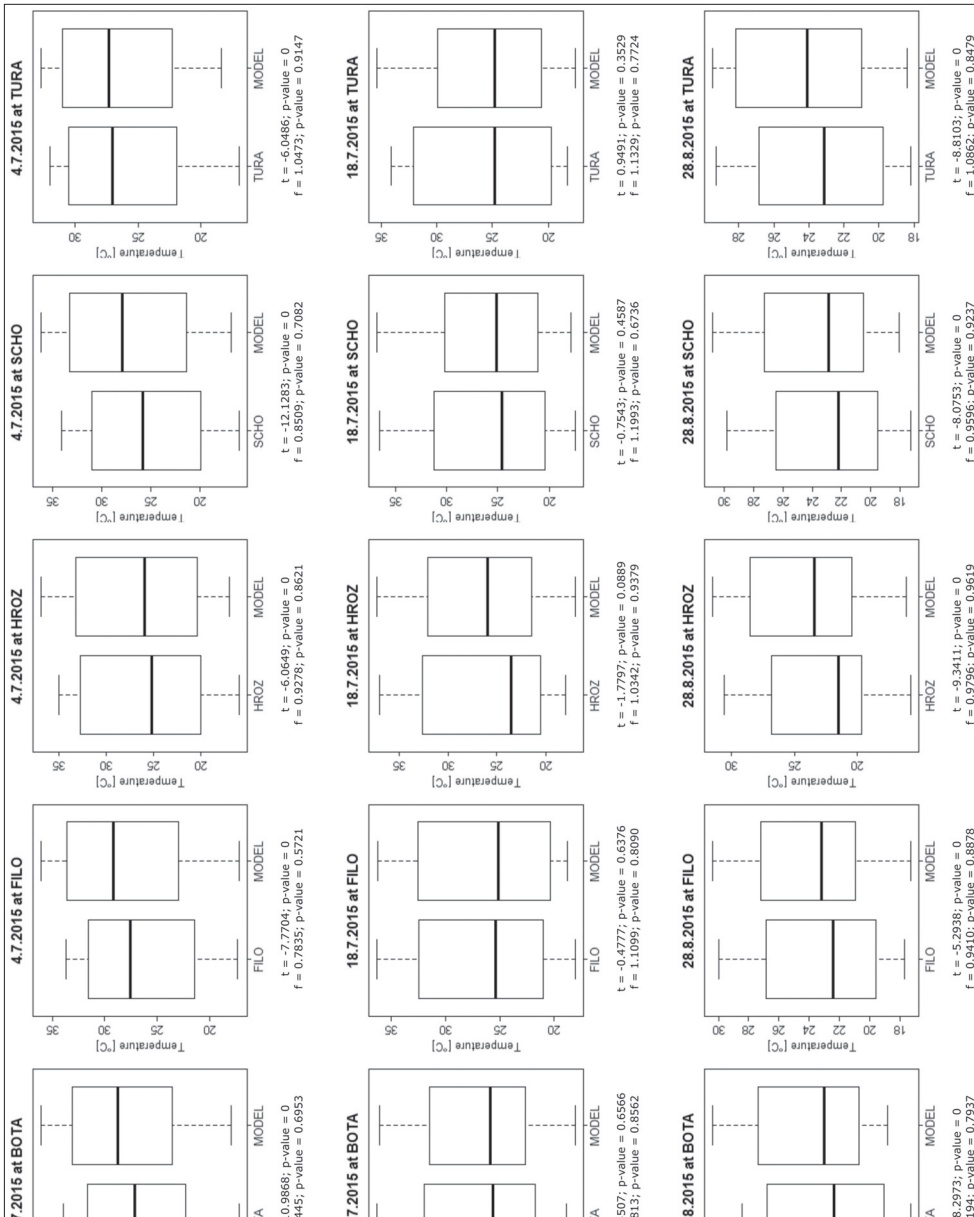

Fig. 6. Boxplots of air temperature measurements at the stations, model outputs and results of statistical tests (paired t-test and f-test)

lated heat). It is anticipated that for more accurate simulation of the spatio-temporal temperature field it is necessary to focus attention on a Land Use Table. Moreover, it is possible that the concept of local climate zones (LCZ) is too general for modelling on a detailed level. It may cause incorrect settings of the thermal capacity of individual surfaces.

Conclusion

Using numerical models for the prediction of air temperature on a local scale represents progress in urban climatology. Although the MUKLIMO_3 simulations showed a number of uncertainties and customisation which must be improved (e.g. the classification of local climate zones seems to be too general as input for the Land Use Table), the model showed good performance in its approximation of the daily courses of air temperature in different urban environments. The degree of imprecision is highly dependent on the quality (e.g. representatives of meteorological measurement) and degree of generalisation (e.g. spatial resolution) of the input data. The model outputs may be used to study the development of the air temperature field in high temporal resolution (e.g. 60 minutes) but also for quantification of the effect of relief, land cover/use and weather conditions on local (urban) climate. The model is also useful to analyse UHIs. To reach a better performance the model must be validated in various cities with different landscape structures throughout the moderate climate zone. Therefore, it is necessary to continue to study the model settings and try to prepare optimal inputs for better results.

Acknowledgments: This contribution was prepared within the project "Urban climate in Central European cities and global climate change" of the International Visegrad Fund's Standard Grant No. 21410222 and the project "UrbanAdapt – Development of urban adaptation strategies using ecosystem-based approaches to adaptation", supported by grant EHP-CZ02-OV-1-036-2015 from Iceland, Liechtenstein and Norway.

REFERENCES

Arnfield, A.J. 2003. Two decades of urban climate research: a review of turbulence, exchanges of energy and water, and the urban heat island. *International Journal of Climatology* 23. 1–26.

Baklanov, A., Grimmond, S., Alexander, A. and Athanassiadou, M. 2009. *Meteorological and air quality models for urban areas***.** Heidelberg, Springer Berlin, 183 p.

Bechtel, B. and Daneke, C. 2012. Classification of local Climate Zones based on multiple Earth Observation Data. *IEEE Journal of Selected Topics in Applied Earth Observations and Remote Sensing* 5. (4): 1191–1202.

Bokwa, A., Hajto, M.J., Walawender, J.P. and Szymanowski, M. 2015. Influence of diversified relief on the urban heat island in the city of Kraków, Poland. *Theoretical and Applied Climatology* 122. (1–2): 365–382.

Deutscher Wetterdienst 2014. *User's Guide MUKLIMO_3 Thermodynamik Version***.** Department of climate and environment consultancy. Offenbach am Main, 59 p.

Dobrovolný, P. and Krahula, L. 2015. The spatial variability of air temperature and nocturnal urban heat island intensity in the city of Brno, Czech Republic. *Moravian Geographical Reports* 23. (3): 8–16.

Dobrovolný, P., Řezníčková, L., Brázdil, R., Krahula, L., Zahradníček, P., Hradil, M., Doleželová, M., Šálek, M., Štěpánek, P., Rožnovský, J., Valášek, H., Kirchner, K. and Kolejka, J. 2012. *Klima Brna. Víceúrovňová analýza městského klimatu***.** Brno, Masarykova univerzita. 200 p.

Gedzelman, S.D., Austin, S., Cermak, R., Stefano, N., Partridge, S., Quesenberry, S. and Robinson, D.A. 2003. Mesoscale aspects of the urban heat island around New York City. *Theoretical and Applied Climatology* 75. (1–2): 29–42.

Geletič, J. and Lehnert, M. 2016. Towards standardized mapping of local climate zones: the case of medium-sized Central European cities. *Moravian Geographical Reports* (in review).

Gross, G. 1989. Numerical simulation of the nocturnal flow systems in the Freiburg area for different topographies. *Beiträge zur Physik der Atmosphäre* 62. 57–72.

Hollosi, B., Zuvela-Aloise, M. and Koch, R. 2014. Daily simulations of urban heat load in Vienna for 2011. *EGU General Assembly Conference Abstracts* 16. 6287.

Houet, T. and Pigeon, G. 2011. Mapping urban climate zones and quantifying climate behaviours – An application on Toulouse urban area (France). *Environmental Pollution* 159. (8–9): 2180–2192.

Lehnert, M., Geletič, J., Husák, J. and Vysoudil, M. 2015. Urban field classification by "local climate zones" in a medium-sized Central European city: the case of Olomouc (Czech Republic). *Theoretical and Applied Climatology* 122. (3): 531–541.

Lelovics, E., Unger, J., Gál, T. and Gál, C.V. 2014. Design of an urban monitoring network based on Local Climate Zone mapping and temperature pattern modelling. *Climate Research* 60. 51–62.

Menut, L., Flamant, C. and Pelon, J. 1999. Urban boundary layer height determination from lidar measurements over the Paris area. *Applied Optics* 38. (6): 945–954.

Meteorologický slovník výkladový a terminologický 2016. ČMeS, eMS 1.3, version 2/2016, available at: http://slovnik.cmes.cz.

Mills, G. 2009. *Luke Howard, Tim Oke and study of urban climates*. 89th American Meteorological Society Annual Meeting, Eighth Symposium on the Urban Environment 10–16.10. 2009.

Przybylak, R., Uscka-Kowalkowska, J., Araźny, A., Kejna, M., Kunz, M. and Maszewski, R. 2015. Spatial distribution of air temperature in Toruń (Central Poland) and its causes. *Theoretical and Applied Climatology* 10.1007/s00704-015-1644-2

Saaroni, H. and Ziv, B. 2010. Estimating the urban heat island contribution to urban and rural air temperature differences over complex terrain: application to an arid city. *Journal of Applied Meteorology and Climatology* 49. 2159–2166.

Sievers, U. 1990. Dreidimensionale Simulationen in Stadtgebieten. Umwelt-meteorologie, Schriftenreihe Band 15: Sitzung des Hauptausschusses II am 7. und 8. Juni in Lahnstein. Kommission Reinhaltung der Luft im VDI und DIN, Düsseldorf. 92–105.

Sievers, U. 1995. Verallgemeinerung der Stromfunktionsmethode auf drei Dimensionen. *Meteorologische Zeitschrift* 4. 3–15.

Sievers, U. and Zdunkowski, W. 1985. A numerical simulation scheme for the albedo of city street canyons. *Boundary-Layer Meteorology* 33. 245–257.

Sievers, U., Forkel, R. and Zdunkowski, W. 1983. Transport equations for heat and moisture in the soil and their application to boundary layer problems. *Beiträge zur Physik der Atmosphäre* 56. 58–83.

Stewart, I.D. and Oke, T.R. 2012. Local Climate Zones for urban temperature studies. *Bulletin of American Meteorological Society* 93. (12): 1879–1900.

Voogt, J.A. and Oke, T.R. 2003. Thermal remote sensing of urban climates. *Remote Sensing of Environment* 86. (3): 370–384.

DOI: 10.15201/hungeobull.65.2.8 Hungarian Geographical Bulletin 65 2016 (2) 181–193.

Projection of intra-urban modification of night-time climate indices during the 21st century

Nóra SKARBIT and Tamás GÁL[1]

Abstract

The present paper evaluates the alteration of certain night-time climate indices namely warm nights ($T_{min} \geq 17$ °C) and tropical nights ($T_{min} \geq 20$ °C) during the 21st century in the city of Szeged. This examination was performed within the framework of a project founded by International Visegrad Fund, where the change of more climate indices were examined in several Central European cities. In this study the MUKLIMO_3 microclimatic model was used, which ensured the modelling of the local scale processes in the examined area. In the model for the land use we applied the Local Climate Zone (LCZ) system. In order to analyze longer periods the cuboid method was applied, which is a dynamical-statistical downscaling technique. We calculated the indices for 1981–2010 based on measurements and for 2021–2050 and 2071–2100 from the EURO-CORDEX datasets. In this study we present the results of Representative Concentration Pathways (RCP) scenarios namely RCP 4.5 and RCP 8.5. Our results show that highest values appear in the city centre and the number of the days clearly increases in the 21st century especially according to scenario RCP 8.5. The values depend on the built-up types and there are more days towards to the densely built-up LCZs. Moreover, considering the relative changes of the zones, larger values appear in sparsely built-up zones and natural surfaces.

Keywords: climate indices, Szeged, MUKLIMO_3, Local Climate Zones, EURO-CORDEX

Introduction

By the end of the 21st century the global mean temperature increase likely exceeds 1.5 °C compare to period 1850–1900 (Stocker, T.F. *et al.* 2013). Global climate change affects the environment at regional and local scale as well. Beside the global problems caused by this phenomenon the regional or local consequences are neither negligible. The rate of the urban population continuously increases thus more and more people live in urbanized area. Nowadays, half of the human population is affected by the unfavourable conditions of the city life. The most important climate impacts are air pollution, increased heat load and thermal stress in cities.

In case of summer heat waves, the increased nocturnal temperature might be very stressful, because of the lack of night-time recreation is harmful for the human well-being and health. It raises the question: what awaits us in the future if it is already a huge problem. Furthermore, it is also an important question how the temperature change varies according to the different built-up types. The crucial question is how possible to mitigate climate change at local scale using urban planning actions and which built-up types are preferable? Using the Local Climate Zone (LCZ) system developed by Stewart, I.D. and Oke, T.R. (2012) it is possible to carry out appropriate assessments and modelling. Furthermore, the results may be simple enough to apply or adapt globally in the frame of urban planning.

This study is a part of an international cooperation concentrating on five Central European cities aiming to predict the change

[1] Department of Climatology and Landscape Ecology, University of Szeged, H-6722 Szeged, Egyetem u. 2. E-mails: skarbitn@geo.u-szeged.hu, tgal@geo.u-szeged.hu

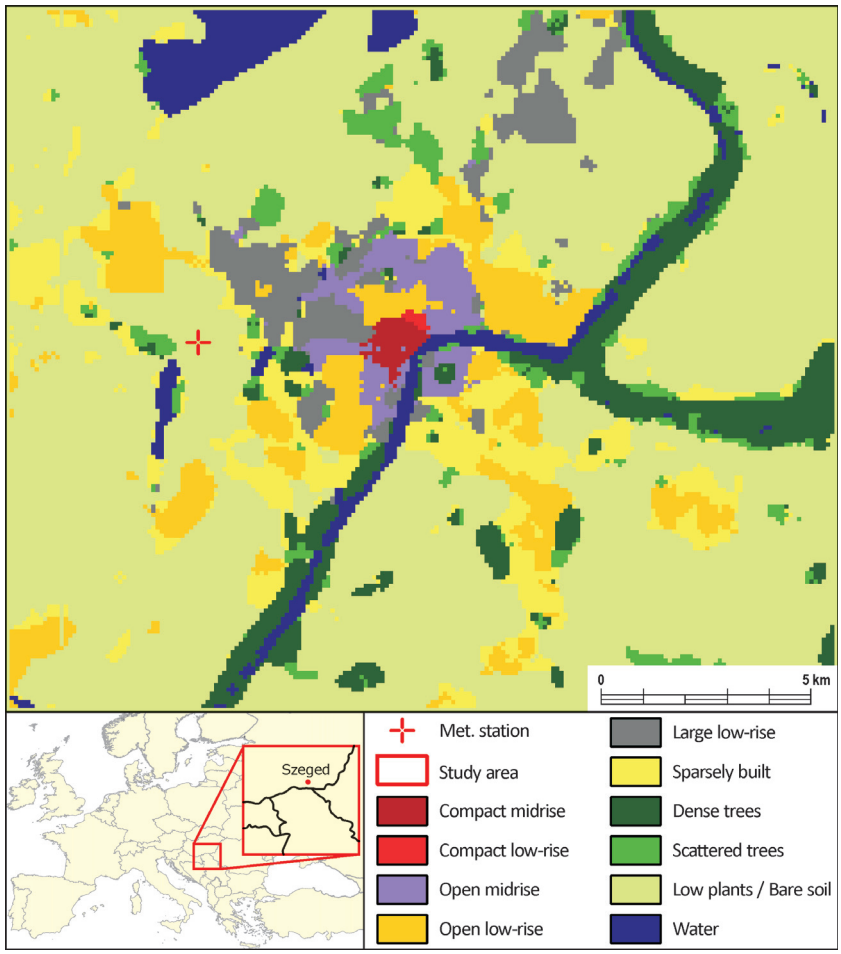

Fig. 1. Study area and the Local Climate Zones in Szeged

of several climate indices in this century (Bokva, A. *et al.* 2015). In case of urban areas, the nocturnal thermal features are the most important therefore we present those indices which characterize the night-time conditions. The indices using daily minimal temperature are appropriate to describe the nocturnal urban-rural thermal differences, thus we examined the average number of warm nights ($T_{min} \geq 17$ °C) and tropical nights ($T_{min} \geq 20$ °C) (Früh, B. *et al.* 2011b).

The aim of this study is to present the change of the number of warm and tropical nights during the 21st century. The spatial pattern of these climate indices was evaluated in the examined area in 1981–2010 as a reference period and the future deviation from this period. This evaluation is extended by the average values for each Local Climate Zone. Furthermore, inter-zone comparisons were carried out based on relative changes from the reference period.

Study area

Szeged is located in the Carpathian Basin in Central Europe *(Figure 1).* It is a medium-

sized city in the south-eastern part of Hungary. According to Köppen climate classification system the climate of Szeged is moderately warm with rather uniform annual distribution of precipitation (Cfb) (Kottek, M. *et al.* 2006). The population of the city is approximately 170,000. The average altitude is 80 m and the city is located on a nearly flat terrain. The urbanized area covers approximately 40 km^2 of the city. River Tisza divides the city into two parts and the road network has a regular avenue-boulevard structure. The structure of the city has few characteristic districts: a densely built centre, blocks of flats in the northern part, family houses in the outskirts and warehouses mostly in western part (Unger, J. *et al.* 2001).

Applied data and methods

Local climate zones

In the modelling process we applied the Local Climate Zone (LCZ) classification (Stewart, I.D. and Oke, T.R. 2012) as the basis of land use/land cover data. Originally it was designed for the classification of urban measurement sites, but several different applications are possible. One of the most important opportunities is to use this system as an input data for urban climate modelling to represent better the urban landforms. The application of this system is advantageous because the classification is based on the thermal characteristics of the urban and rural surfaces. Furthermore, it can be connected to the urban heat island phenomenon, which is the most important modification in the urban areas. Nowadays several LCZ mapping methods are known (Lelovics, E. *et al.* 2014; Bechtel, B. *et al.* 2015; Lehnert, M. *et al.* 2015).

In this study, we used Bechtel-method, which is a simple method for LCZ mapping. This method applies free-access satellite imagines and open-source software. For this method two software programs are necessary (Google Earth and SAGA-GIS) and it applies Landsat satellite images as input (Bechtel, B. *et al.* 2015). *Figure 1* presents the obtained LCZs for Szeged. It can be seen that four LCZ classes are absent in Szeged: LCZ 1 (compact high-rise), LCZ 4 (open high-rise), LCZ 7 (lightweight low-rise) and LCZ 10 (heavy industry). Compact midrise (LCZ 2) and compact low-rise (LCZ 3) are located in the centre of the city. Open midrise (LCZ 5) is located near to the city centre in the North and in the South. The most common classes are open low-rise (LCZ 6) and sparsely built (LCZ 9). The north-western part of the city includes large low-rise (LCZ 8). The dominant land cover types around the city are bare soil and low plants. These areas temporarily change within a year because of their agricultural use thus these two LCZ categories were merged. Since multiple satellite images of different dates were used to classify the different LCZs, the merging of the two zones simplifies the classification.

MUKLIMO_3

In this study the microclimatic model MUKLIMO_3 was used (Sievers, U. 1995). It was developed by the German and Austrian weather services (DWD and ZAMG). The model is non-hydrostatic and the precipitation is not implemented. The horizontal resolution is 100 m, while the vertical one alters from 10 to 100 m. The vertical grid distance is lower so the resolution is larger towards the surface. Several parameters are necessary for the description of buildings, for instance building density, wall area for a given volume and mean building height (Früh, B. *et al.* 2011a). The initial conditions are ensured by a 1D profile from a reference station.

The interactions between the atmosphere and the vegetation are simulated by a 3-layer model and between the soil and the atmosphere by a 15-layer model. The land use categories distinguished by MUKLIMO_3 are buildings, trees, open country and water. The outputs of the model are the spatial patterns of air temperature, humidity, wind speed and direction for every hour in a 24-hour period (for details see Sievers, U. 2012).

Cuboid method

In order to calculate the mentioned climate indices the so-called cuboid method was used (Früh, B. *et al.* 2011a). This is a dynamical-statistical downscaling technique, which provides the spatial pattern of the climate indices for a 30-year period. The benefit of this method is the reduction of the computations using a tri-linear interpolation scheme. *Figure 2* shows the concept of the cuboid. The method assumes that the urban heat load can occur in a specific combination of meteorological parameters and it can be characterized by three of them: temperature (t), relative humidity (rh) and wind speed (ws). These parameters represent the dimensions of the cuboid, while the limit of favourable situations represents the corners of the cuboid. With the MUKLIMO_3 model we simulated these corners for two prevailing wind direction: Northeast and Northwest. In addition to these simulations, a 30 year daily data series is needed, which was measured near the study area or obtained from a climate model.

Meteorological data

As reference station the observatory of Hungarian Meteorological Service *(Figure 1)* was used. This station ensured the initial conditions for the modelling and the 30 year daily dataset for the reference period (1981–2010) in the cuboid method. Air temperature, humidity, wind speed and direction data were utilized.

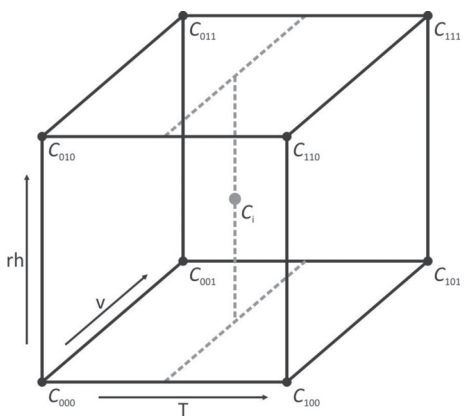

Fig. 2. The concept of the cuboid method (for details see Zuvela-Aloise, M. *et al.* 2014)

EURO-CORDEX simulations

We analyzed the 21st century through two periods: 2021–2050 and 2071–2100. For these periods we used temperature, humidity, wind speed and direction datasets from EURO-CORDEX model simulations (Jacob, D. *et al.* 2014). The resolution of the simulations is 0.11° (approximately 12 km) and they use the latest Representative Concentration Pathways (RCP) scenarios. These scenarios express the change in radiative forcing and are not directly based on socioeconomic factors. 15 simulations (5 global climate models and 3 regional climate models) were used where the necessary climate data for the cuboid method (temperature, relative humidity, wind speed and direction) was available. Among them there are one simulation for RCP 2.6 and seven simulations for RCP 4.5 and RCP 8.5. The simulations for the last two scenarios were averaged. In order to show the outcomes of more model simulations, we present the averaged results of scenarios RCP 4.5 and RCP 8.5.

Results

Warm nights

Thirty year averaged number of warm nights in period of 1981–2010 range from 1 day to 73 days in the entire model domain *(Figure 3).* In the central part of the city, in a relatively smaller area, the number of days is over 60, but generally it exceeds 40 days in the whole city centre and it is over 20 days in other urban parts. In the downtown (where compact mid- and low-rise zones are located) most of the values are between 42 and 57 days (*Figure 3).* In the surrounding areas (mostly open mid- and low-rise categories) the number of warm nights is between 12 and 40 days. In

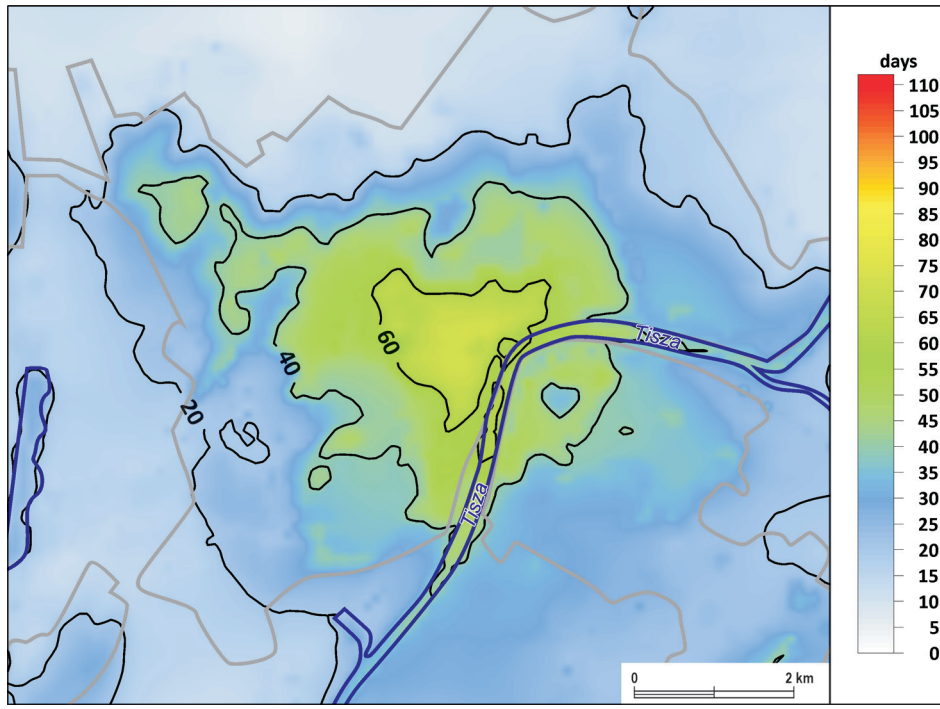

Fig. 3. Average number of warm nights ($T_{min} \geq 17$ °C) in period of 1981–2010. Grey lines = border of built-up areas; blue lines = border of water surfaces

western part of the city where the large low-rise class is typical, the values are about 13 to 23 days. In the perimeter of the city where the typical category is sparsely built, the values are between 12–21 days. In non-urban areas the value of warm nights is below 15 days except at larger water surfaces.

The 30-year mean number of warm nights based on RCP 4.5 and RCP 8.5 scenarios for period 2021–2050 is presented on *Figure 4*. In this period there is no significant difference between the two examined scenarios and the deviation from period 1981–2010 is minimal in both cases. Consequently, their features can be described together. In this period the values range from 1 to 80 days in the whole examined area. The most conspicuous change is the outspread of the area with values over 20 days. This tendency can be observed along the border of the city in northeast and southwest. Around the city centre all of the isolines spread towards the suburbs especially in case of the 40 days, but is notable in case of the 60 days also.

Considering the LCZs, in the areas of the compact zones in the inner city, the average number of warm nights is between 46 and 65 days. The mean values for the open zones which appear in more different parts of the city are about 14–39 days. In the sparsely built and large low-rise zones, which are more typical in the outskirts, the average number of warm nights is approximately between 14 and 28 days, but near to the city centre values over 40 days appear also. Most of the natural surfaces have less than 20 days in this period, but especially near the Western city border and in the water surfaces the number of warm nights is over 20 days.

For the period 2071–2100, significant changes are taking place, especially in case of RCP 8.5 compared to the reference period

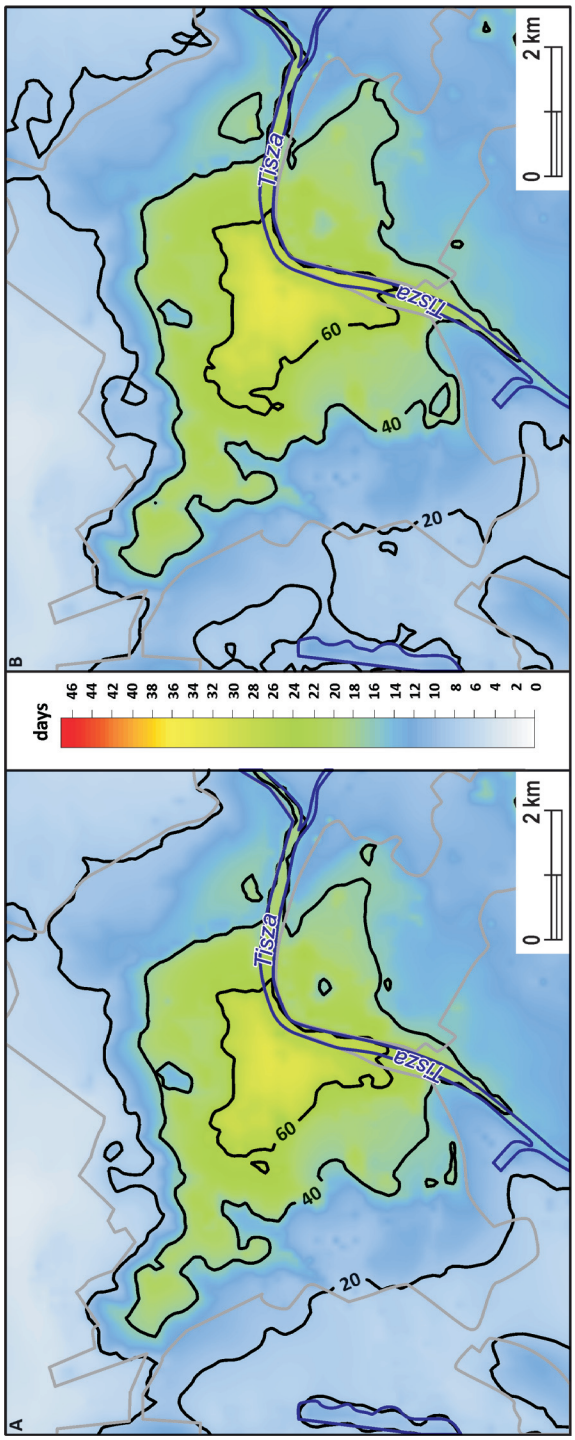

Fig. 4. Average number of warm nights ($T_{min} \geq 17$ °C) in period of 2021–2050 based on scenario RCP 4.5 (A) and RCP 8.5 (B). Grey lines = border of built-up areas; blue lines = border of water surfaces

(Figure 5, A). In the entire model domain, the minimum value for RCP 4.5 is 2 days and the maximum is 88 days, while in case of RCP 8.5 the values range from 12 to 111 days. In case of RCP 4.5, aside from the north-northeast region, the number of warm days is over 20 days in the examined area. It can be noted that the area of days over 40 around the city extends significantly. Moreover, spatial extent of the number of days over 60 stretches from the city centre towards the external areas.

In the inner-city values over 80 days become typical. In the compact zones the number of warm nights is between 60 and 80 days. In case of the open zones, there is larger difference between mid-rise and low-rise areas, while in the first case the values are approximately 50 to 77 days, in low-rise these numbers are 30 to 60 days. In the large low-rise and sparsely built zones the values are between 20 and 60 days can be found. In the natural and water surfaces, the number of warm nights is 20–30.

In case of RCP 8.5, the number of warm nights has a similar spatial distribution, but the values are higher by approximately 20 days *(Figure 5, B).* Almost in the entire study area the number of warm days is over 40 days, and values over 60 days appear in rural areas as well. Significant changes take place in the city centre which is surrounded by the isoline of 60 days. In the inner areas, values over 80 days are typical, while in the city centre the number of warm nights exceeds 100 days in a substantial area.

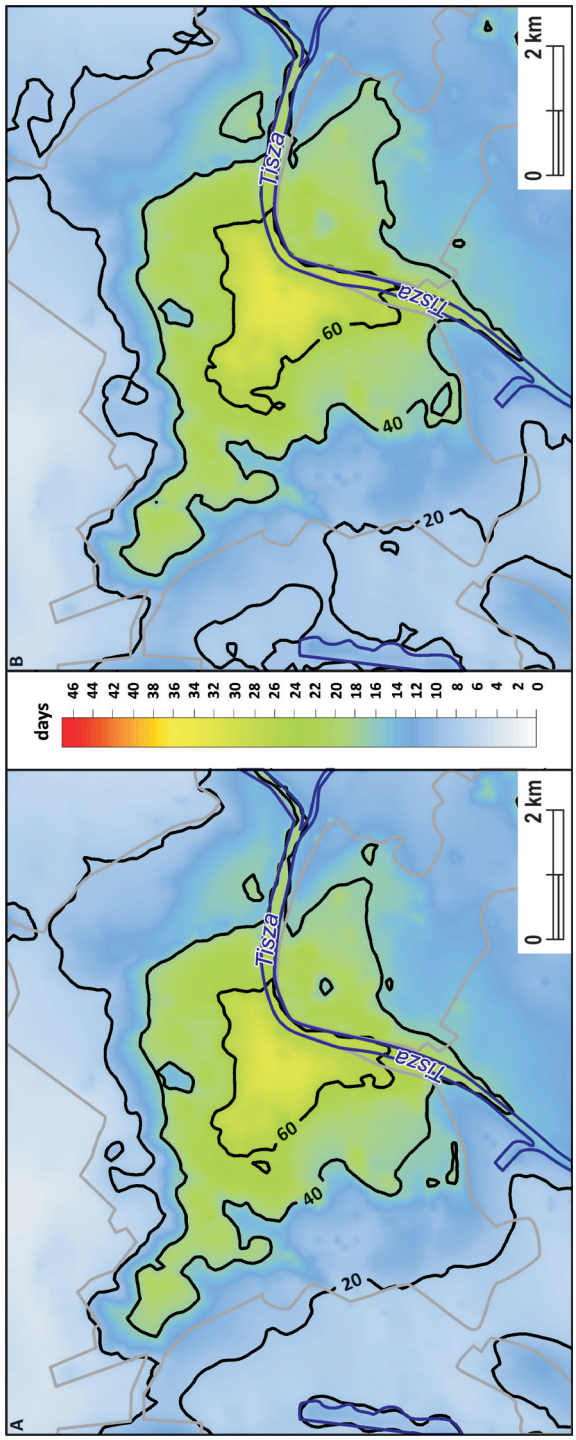

Fig. 5. Average number of warm nights (T_{min} ≥ 17 °C) in period of 2071–2100 based on scenario RCP 4.5 (A) and RCP 8.5 (B). Grey lines = border of built-up areas; blue lines = border of water surfaces

Considering the local climate zones the typical values for the compact zones are between 80 and 110 days. In the open midrise zone the number of warm days is also high, approximately 75–95 days, while in open low-rise this is 52–80 days. In the outskirts (large low-rise and sparsely built) the values are between 50 and 90 days. The natural surfaces also have large values, of 43 to 58 days.

Evaluation of the average number of warm nights as well as the absolute and relative change from 1981–2010 compared to each examined future periods and scenarios in the typical LCZ areas helps to analyse how the LCZ classes are exposed to the climate change *(Table 1).* In period 2021–2050 the greatest relative change appears in sparsely built zone at both scenarios. It is followed by the open zones and the large low-rise zone. In case of RCP4.5 the changes in compact midrise and low-rise is marginal while in case of the natural surfaces there is no average change at all. The order is the opposite in case of RCP 8.5, where the change is the smallest in compact midrise and low-rise zones. In the natural surfaces this number is almost the same.

In period of 2071–2100 the greatest change also appears in sparsely built areas in case of both scenarios *(Table 1).* The natural surfaces follow this zone as the second most changed areas. This zone is followed by open midrise, low-rise and large low-rise, where open low-rise has the largest value. The smallest relative changes appear in compact midrise and low-rise.

Table 1. Number of warm nights and their absolute and relative change compared to the measured values in 1981–2010 in LCZ areas of Szeged at different time periods and RCPs

Time period	RCPs	Compact-midrise	Compact low-rise	Open midrise	Open low-rise	Large low-rise	Sparsely-built	Natural surfaces
1981–2010	Measured	71	67	41	37	42	12	18
2021–2050	RCP 4.5	75	72	47	42	47	15	18
		4	5	6	5	5	3	0
		6	7	15	14	12	25	0
	RCP 8.5	78	74	49	44	49	17	20
		7	7	8	7	7	5	2
		10	10	20	19	17	42	11
2071–2100	RCP 4.5	86	82	58	53	58	22	26
		15	15	17	16	16	10	8
		21	22	41	43	38	83	44
	RCP 8.5	110	107	85	81	85	49	51
		39	40	44	44	43	37	33
		55	60	107	119	102	308	183

Tropical nights

High numbers of tropical nights ($T_{min} \geq 20$ °C) are relatively uncommon in this climate and the model calculations also confirmed this in case of 1981–2010 *(Figure 6)*. The values range from 0 to 12 days. It can be noted that the values do not exceed 5 days except in the densely built areas. However, the number of tropical nights exceeds 10 days in the inner city core.

Considering the number of tropical nights through the different LCZs, there are no significant difference between the zones. Most of the values range from 4 to 11 days

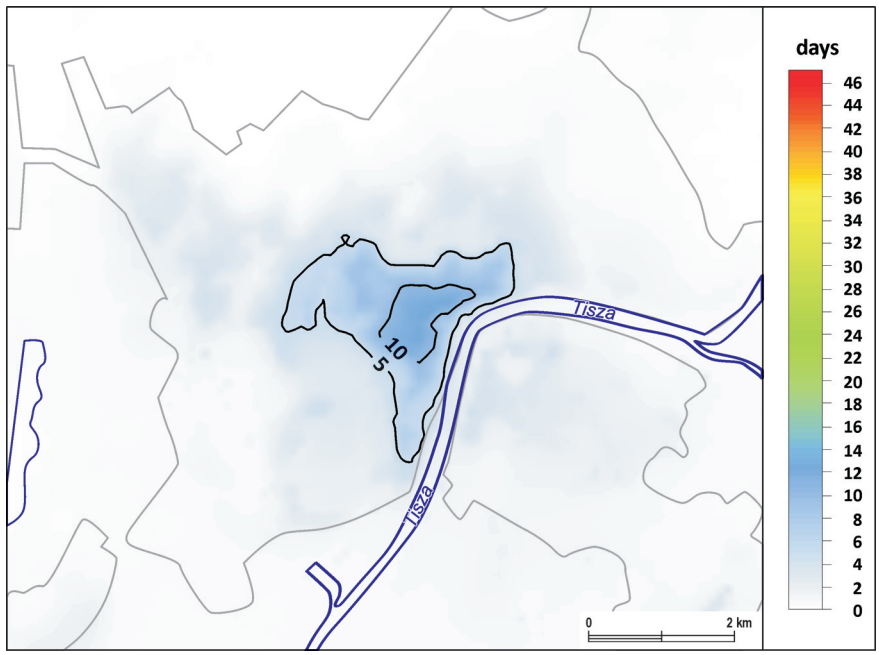

Fig. 6. Average number of tropical nights ($T_{min} \geq 20$ °C) in period of 1981–2010. Grey lines = border of built-up areas; blue lines = border of water surfaces

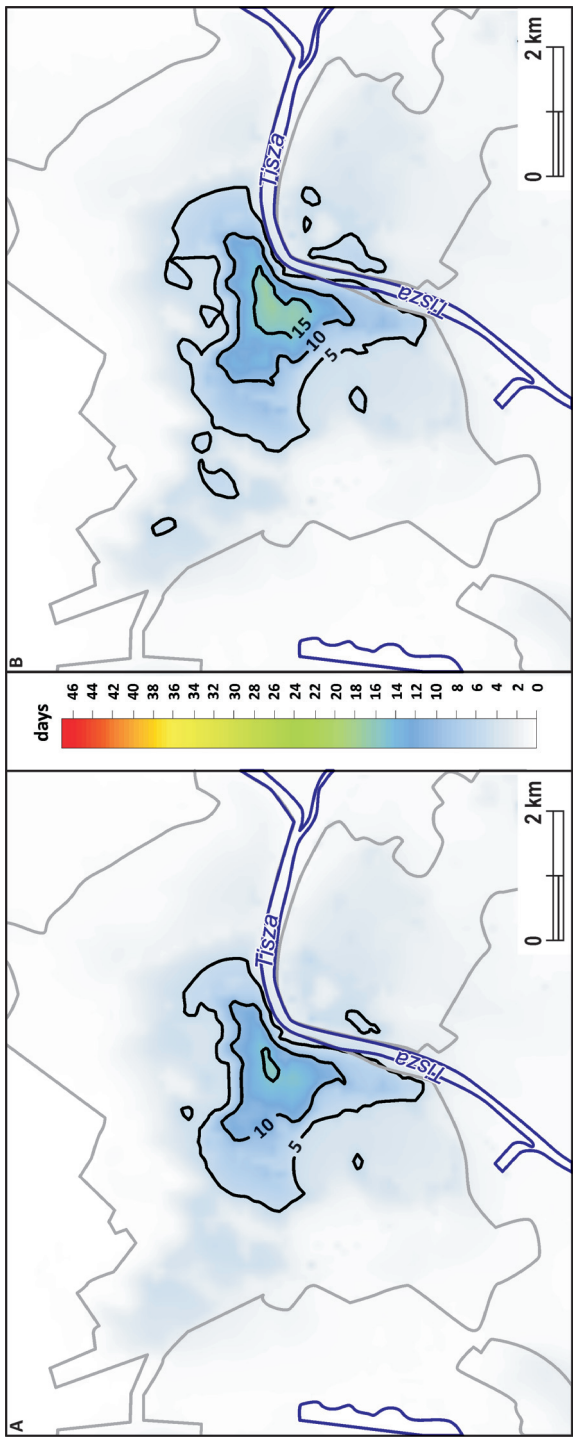

Fig. 7. Average number of tropical nights (T_{min} ≥ 20 °C) in period of 2021–2050 based on scenario RCP 4.5 (A) and RCP 8.5 (B). Grey lines = border of built-up areas; blue lines = border of water surfaces

in compact midrise and from 6 to 11 days in compact low-rise. In the open midrise zone the number of tropical nights exceeds 5 days in the inner city. In case of large low-rise and sparsely built, most of the values range from 0 to 3 days, while in case of open midrise from 0 to 5 days. In the natural and water surfaces, the majority of the values is around 0.

The change from period of 1981–2010 is not significant in case of both scenarios and the difference between them is minimal *(Figure 7).* The minimum value is 0 day for each scenarios, the maximums are approximately 16–17 days. In both cases, the areas with over 5 days increase in the city centre and in addition they appear scattered in other regions. In case of RCP 8.5, the mentioned change is more spectacular and the number of the affected regions is larger. The isoline of 10 days spreads also, especially into north-western and north-eastern direction. The other important change is the appearance of values over 15 days in the city centre. It is minimal in case of RCP 4.5, but in case of RCP 8.5, the area with values over 15 days covers a significant part of the inner city.

Considering the LCZs slightly greater change can be observed in case of compact midrise and compact low-rise. Most of the values range from 5 to 14–16 days depending on the scenarios in compact midrise. For compact low-rise, the average number of tropical nights varies from 10 to 13–14 days. In case of open midrise

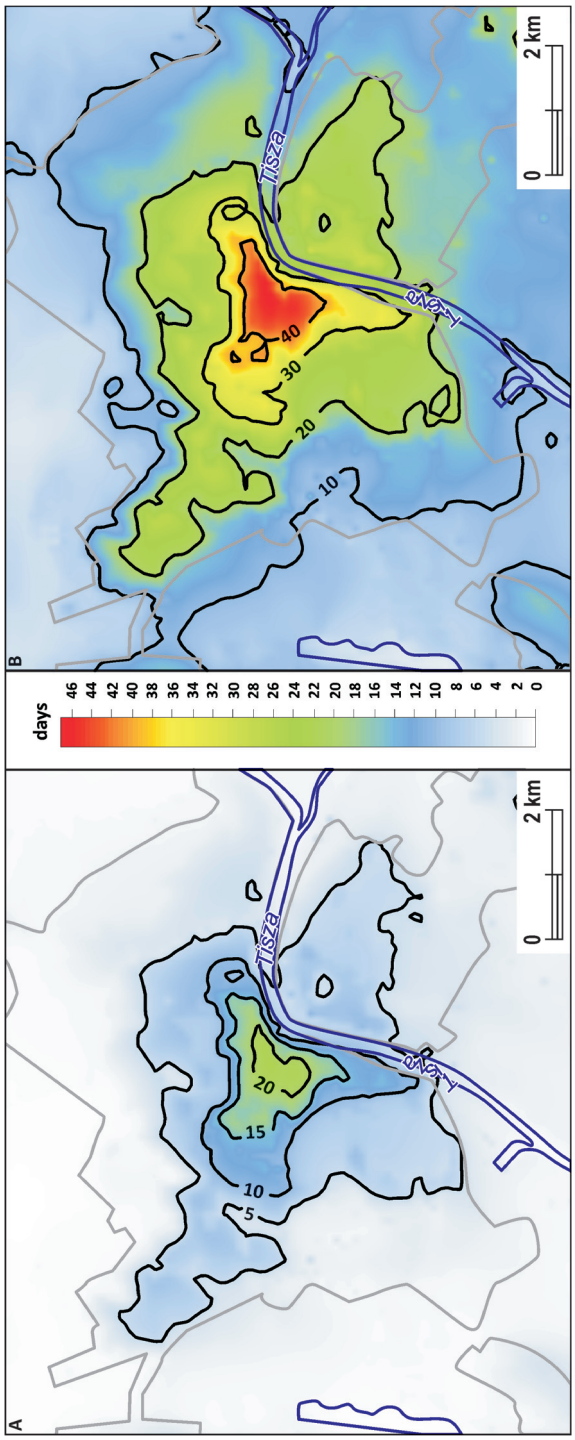

Fig. 8. Average number of tropical nights ($T_{min} \geq 20$ °C) in period of 2071–2100 based on scenario RCP 4.5 (A) and RCP 8.5 (B). Grey lines = border of built-up areas; blue lines = border of water surfaces

and low-rise, the change is minimal. The change is not noticeable in large low-rise and sparsely built, and neither in the natural and water covered surfaces.

At the end of the century (2071–2100) the difference between the two scenarios is remarkable *(Figure 8).* The minimal value for RCP 4.5 is 0 day, the maximum is 23 days, while these numbers for RCP 8.5 are 1 day and 47 days. While in case of scenario RCP 4.5, the change from period 2021–2050 is minimal, in RCP 8.5, the changes are enormous and spectacular. Based on the first scenario *(Figure 8, A)* the area with values over 5 days continues to grow and stretches to the East side of the Tisza and north-western direction from the city centre. In the centre the areas with values more than 10 and 15 days also increase. Another change is that values over 20 days appear in the city.

Considering the LCZs in case of RCP 4.5, the change compared to the reference period is the largest in the compact zones. In these zones most of the values range from 16 to 21 days. In the other zones the change is less remarkable; generally, the increase is below 2 days. In the natural and water surfaces the average change is only 1 day from the reference period like in period 2021–2050.

The results of scenario RCP 8.5 give a very different picture *(Figure 8, B).* The number of tropical nights is over 5 days. On the East side of the Tisza values over 10 days are typical and in a larger area the number of tropical nights is over 20 days.

The urban areas are outlined by the isoline of 15 days. In the densely built up areas the number of tropical nights is over 30 days and in the city centre it exceeds 40 days.

The average values for compact zones are between 35 and 45 days. In case of open midrise, most of the values are between 20 and 30 days. In open low-rise the values vary from 10 to 30 days. In case of large low-rise and sparsely built the typical number of tropical nights ranges from 10 to 30 days and from 10 to 25 days, respectively. In areas of natural surfaces the change is 7–8 days on average compared to the reference period.

Table 2 presents the average number of tropical nights in every LCZ type and their absolute and relative change compared to 1981–2010 in the examined periods based on the two applied scenarios. It should be noted that since the number of tropical nights in LCZ 9 is 0 day in the reference period thus the relative change in the future periods cannot be calculated. In period 2021–2050 the relative changes are the highest in open mid-rise. In case of RCP 4.5 the second large change appears in open low-rise. The values of compact low-rise and large low-rise are almost the same. Compact midrise follows these zones. In the natural surfaces, there is no change compared to period 1981–2010. In case of RCP 8.5 large low-rise is the second largest changed zone. This zone is followed by open low-rise and midrise. Similar to RCP 4.5 compact midrise is the least changed among the build-up zones.

The most noticeable changes also appear in open midrise in the period 2071–2100 in both scenarios. In case of RCP 4.5, it is followed by open low-rise again. The difference is similar in large low-rise. In compact midrise and low-rise, this value is slightly smaller. According to this scenario, the relative change in the natural surfaces is still zero percent. In case of RCP 8.5 the second largest change is in open low-rise. However, the relative change in the natural surfaces becomes also high and exceeds the value of large low-rise. The least changed zones are compact midrise and low-rise.

Conclusions

This study presented the changes in the number of warm and tropical nights during the 21st century compared to period of 1981–2010 in Szeged. We examined the spatial distribution of these indices and the number of days and their change through the different local climate zones. Furthermore, the difference between the relative changes of the zones was also investigated.

Our results show the substantial increasing tendency for both indices. The spatial

Table 2. Number of tropical nights and their absolute and relative change compared to the measured values in 1981–2010 in LCZ areas of Szeged at different time periods and RCPs

Time period	RCPs	Compact midrise	Compact low-rise	Open midrise	Open low-rise	Large low-rise	Sparsely built	Natural surfaces
1981–2010	Measured	12	10	2	2	3	0	1
2021–2050	RCP 4.5	14	13	4	3	4	0	1
		2	3	2	1	1	0	0
		17	30	100	50	33	–	0
	RCP 8.5	16	14	5	3	5	0	1
		4	4	3	1	2	0	0
		33	40	150	50	67	–	0
2071–2100	RCP 4.5	21	19	8	6	8	1	1
		9	9	6	4	5	1	0
		75	90	300	200	167	–	0
	RCP 8.5	45	42	25	21	26	8	9
		33	32	23	19	23		8
		275	320	1150	950	767	–	800

pattern shows that most of the days appear in the city centre stretched to the Northwest direction and values decrease towards to the natural surfaces. In period of 2021–2050, the change compare to the reference period and the difference between the two scenarios is not significant. In contrary, for the end of the century the increase is more significant and the two scenarios predict completely different spatial patterns.

The results also show that high values appear at compact LCZs in case of both indices. It is also noticeable that the increase of the number of days is higher in the less built LCZs, however the differences between LCZs do not change significantly. In case of warm nights, the largest relative change appears in sparsely built zone, followed by the natural surfaces and open zones while the smallest values are in the compact zones. For tropical nights the order is slightly different because the most changing zone is open midrise.

This study intended to highlight the interaction between urban climate effects and global climate change. The results clearly prove that global or regional scale climate predictions without urban climate interactions do not have enough information for urban planners or local authorities. In addition, the results can be used as a good example for the demonstration of the expected changes of the climate of 21th century. Using these results the presentation of climate change in urban scale to wider audience is easier. The increasing number of tropical nights can be used to express the change of unfavourable and stressful conditions until the end of the century. The number of tropical nights will be almost the same in rural areas at the end of the century as today in the city centre. Furthermore, in the most urbanized areas one month of this extreme heat stress may become a natural part of every summer. This is a crucial problem because if the minimum temperature exceeds 20 °C then a significant increase of the relative number of deaths can be observed.

Hopefully, these results help to draw attention of urban planners and local governments or local decision makers for this problem and based on the model results for different LCZs it may be helpful to find the optimal built-up characteristics for urban areas in order to mitigate the effect of climate change.

***Acknowledgements*:** The study was supported by the International Visegrad Fund, Standard Grant No. 21410222, by the Hungarian Scientific Research Fund (OTKA K-111768) and the second author was supported by the János Bolyai Research Scholarship of the Hungarian Academy of Sciences. We acknowledge the CORDEX project for producing and making available their model output. Special thanks to Boudewijn van Leeuwen for the language revision of the manuscript.

REFERENCES

Bechtel, B., Alexander, P.J., Böhner, J., Ching, J., Conrad, O., Feddema, J., Mills, G., See, L. and Stewart, I. 2015. Mapping local climate zones for a worldwide database of the form and function of cities. *ISPRS International Journal of Geo-Information* 4. (1): 199–219.

Bokwa, A., Dobrovolny, P., Gál, T., Geletič, J., Gulyás, A., Hajto, M.J., Hollósi, B., Kielar, R., Lehnert, M., Skarbit, N., Stastny, P., Svec, M., Unger, J., Vysoudil, M., Walawender, J.P. and Zuvela-Aloise, M. 2015. Modelling the impact of climate change on heat load increase in Central European cities. In *International Conference on Urban Climate (ICUC 9.* Extended abstracts, 5 p.

Früh, B., Becker, P., Deutschländer, T., Hessel, J.D., Kossmann, M., Mieskes, I., Namyslo, J., Roos, M., Sievers, U., Steigerwald, T., Turau, H. and Wienert, U. 2011a. Estimation of climate change impacts on the urban heat load using an urban climate model and regional climate projections. *Journal of Applied Meteorology and Climatology* 50. (1): 167–184.

Früh, B., Kossmann, M. and Roos, M. 2011b. *Frankfurt am Main im Klimawandel – Eine Untersuchung zur stadtischen Warmebelastung. Berichte des Deutschen Wetterdienstes 237*. Offenbach am Main, Selbstverlag des Deutschen Wetterdienstes, 68 p.

Jacob, D., Petersen, J., Eggert, B., Alias, A., Christensen, O.B., Bouwer, L., Braun, A., Colette, A., Déqué, M., Georgievski, G., Georgopoulou, E., Gobiet, A., Menut, L., Nikulin, G., Haensler, A., Hempelmann, N., Jones, C., Keuler, K., Kovats, S., Kröner, N., Kotlarski, S., Kriegsmann, A., Martin, E., Meijgaard, E., Moseley, C., Pfeifer, S., Preuschmann, S., Radermacher, C., Radtke, K., Rechid, D., Rounsevell, M., Samuelsson, P., Somot,

S., Soussana, J.-F., Teichmann, C., Valentini, R., Vautard, R., Weber, B. and Yiou, P. 2014. EURO-CORDEX: new high-resolution climate change projections for European impact research. *Regional Environmental Change* 14. 563–578.

Kottek, M., Grieser, J., Beck, C., Rudolf, B. and Rubel, F. 2006. World Map of the Köppen-Geiger climate classification updated. *Meteorologische Zeitschrift* 15. (3): 259–263.

Lehnert, M., Geletič, J., Husák, J. and Vysoudil, M. 2015. Urban field classification by "local climate zones" in a medium-sized Central European city: the case of Olomouc (Czech Republic). *Theoretical and Applied Climatology* 122. (3): 531–541.

Lelovics, E., Unger, J., Gál, T. and Gál, C.V. 2014. Design of an urban monitoring network based on Local Climate Zone mapping and temperature pattern modeling. *Climate Research* 61. (1): 51–62.

Sievers, U. 1995. Verallgemeinerung der Strom-funktionsmethode auf drei Dimensionen. *Meteorologische Zeitschrift* 4. 3–15.

Sievers, U. 2012. *Das kleinskalige Strömungsmodell MUKLIMO_3 Teil 1: Theoretische Grundlagen, PC-Basisversion und Validierung*. Offenbach am Main, Berichte des Deutscher Wetterdienst, 136 p.

Stewart, I.D. and Oke, T.R. 2012. Local Climate Zones for urban temperature studies. *Bulletin of the American Meteorological Society* 93. 1879–1900.

Stocker, T.F., Qin, D., Plattner, G.-K., Tignor, M., Allen, S.K., Boschung, J., Nauels, A. Xia, Y., Bex, V. and Midgley, P.M. 2013. *Climate Change 2013: The Physical Science Basis. Contribution of Working Group I to the Fifth Assessment Report of the Intergovernmental Panel on Climate*. Cambridge and New York, Cambridge University Press, 1535 p.

Unger, J., Sümeghy, Z., Gulyás, Á., Bottyán Z. and Mucsi, L. 2001. Land-use and meteorological aspects of the urban heat island. *Meteorological Applications* 8. 189–194.

Zuvela-Aloise, M., Koch, R., Neureiter, A., Böhm, R. and Buchholz, S. 2014. Reconstructing urban climate of Vienna based on historical maps dating to the early instrumental period. *Urban Climate* 10. (3): 490–508.

Geography in Visegrad and Neighbour Countries

Regional Socio-Economic Processes in Central and Eastern Europe – 20 Years in Transition and 2 Years in Global Economic Crisis

Edited by
Ágnes Erőss and Dávid Karácsonyi

Geographical Research Institute Hungarian Academy of Sciences
Budapest, 2011. 169 p.

During the last twenty years the erstwhile Soviet bloc countries in Central and Eastern Europe (CEE) have taken distinct routes in post-socialist development, wherein the national trends and internal regional processes proved to be in deep contrast. Responses to the challenges of the global economic crisis also varied, repeatedly brought to the surface long existing regional issues, structural problems and ethnic conflicts. Human geographers are divided in the assessment of the shifts that occurred during the past twenty years and the exchange of experience is vital for finding adequate answers to the new challenges. In order to provide a forum for discussion the Geographical Research Institute Hungarian Academy of Sciences with the generous support of the International Visegrad Fund Small Grant Programme organized a conference in order to induce the revival of contact between the institutes of geography of Visegrad Countries and their Western and Eastern neighbours. Present volume is a selection of presentations aiming to provide a deeper insight in socio-economic processes and their

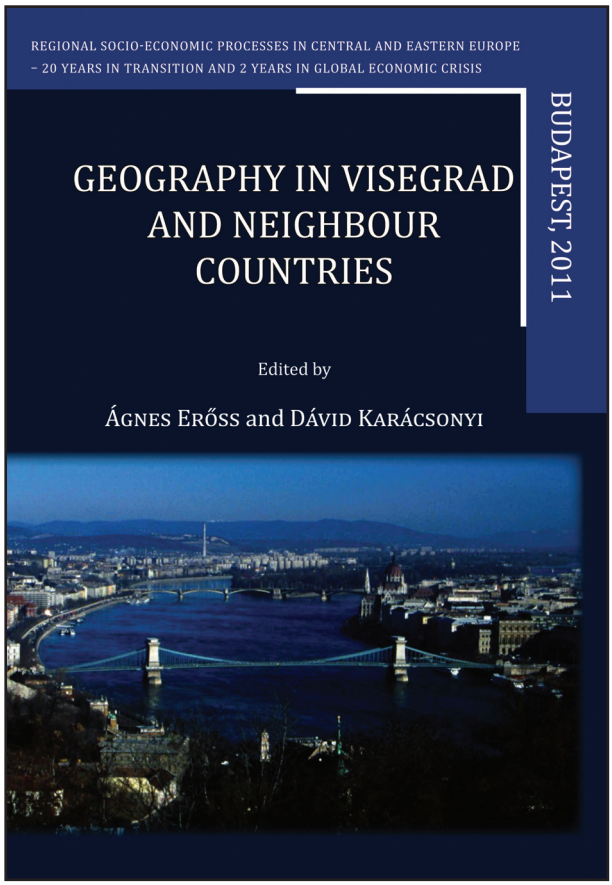

Price: EUR 10.00
Order: Geographical Institute RCAES MTA Library, H-1112 Budapest, Budaörsi út 45.
E-mail: magyar.arpad@csfk.mta.hu

BOOK REVIEW

Kuttler, W., Miethke, A., Dütemeyer, D. Barlag, A.-B.: Das Klima von Essen / The Climate of Essen. Hohenwarsleben, Westarp Wissenschaften, 2015. 249 p.

The artificial environmental circumstances in the cities (e.g. complex surface structures, different heat capacity and run-off properties of human-made materials) result in changes of climatic and air quality conditions in urban areas. The Urban Heat Island (UHI), the degradation of the water supply, changes of the ventilation and increasing air pollution are some of the most frequently mentioned and most extensively examined modifying effects of the cities. The main principles of these phenomena are similar, but every city has its peculiarities and develops its own characteristic climate. There is a growing interest in urban climate research especially due to the strongly deteriorating macroclimatic conditions combined with negative changes in land use. Urban environment (and the billions of people living in it) is exposed to greater stress due to climate change. To achieve more efficient environmental protection and mitigation of the negative impacts of climate change we have to understand the climatic characteristics of cities thoroughly. Works like "The Climate of Essen" contribute to this need.

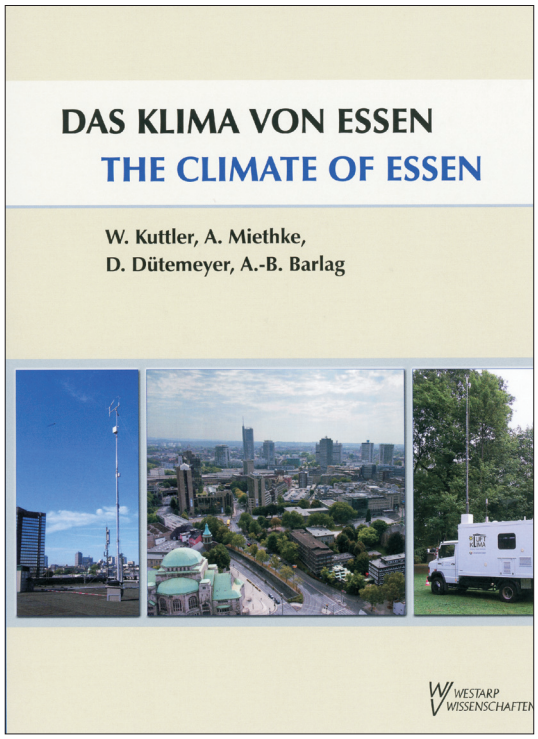

This book is a "classic" monograph on the urban climatology (the overview of climatic and air quality conditions) of Essen, which summarises the results achieved over 30 years at the Department of Applied Climatology at the University of Duisburg-Essen. This department was a dominating centre of German urban climate research until its activity was finally finished in February 2015. The research in Essen examined the thermal and humidity conditions and air quality of the urban environment at both the levels of basic and applied research focusing on the effects of climatic change. The latest directions of research included VOCs, NO, NO_2 and O_3 pollution in the urban atmosphere (e.g. Melkonyan, A. and Kuttler, W. 2012; Wagner, P. and Kuttler, W. 2014), and many aspects of urban thermal comfort in the light of climate change (Dütemeyer, D. *et al.* 2013; Müller, N. 2013). Besides presenting the assessment of observation data reaching back about 100 years, the book also gives a detailed analysis of data recorded at fixed stations and during mobile measurements between June 2012 and May 2013 in 33 stations over the city.

Essen was temporarily the most important, and presently is the second largest, city of the Ruhr area (the so called "Ruhrgebiet", one of the great industrial, especially coal and steel industry agglomerations of the 19th and 20th centuries in Europe) and the seventh largest in Germany. While Essen had over 700,000 inhabitants in the 1960s, there is a significant decrease of the population in the last decades (583,000 inhabitants in 2015). This phenomenon can be explained with the decreasing importance of, and job opportunities offered by, coal mining. The last mine (Zollverein Coal Mine Industrial Complex) was closed in 1986 and it is today a World Heritage site. Nowadays, the tertiary sector dominates the economy. Considerable changes of land use and corresponding changes of emission structure formed the urban climate observable today.

The volume presents the typical urban-climatological methodology, and gives an overview of climatic features (trends of air temperature, relative humidity, precipitation, wind conditions etc.) and

air quality (emission of particular matter and gases) of the region and the city of Essen, and also shows data from state-of-the-art investigations like energy flux measurements.

Chapter 1 and Chapter 2 describe the main geographical features and land use characteristics of the city. The urban climate phenomena cannot be understood without the background macroclimatic conditions. Therefore, Chapter 3 describes these features of the Essen region based on a long-term dataset (1881-2009). Although the basic climatic conditions are similar to those of Hungary, there is moderate continentality, thus less climatic extremism in the region. The analysis shows significant increasing trends in air temperature, in the number of summer and hot days, but decreasing trends in the number of frost days and wind speed (for the period 1935–2012). Because of the large industrial emissions in the 1960s, dust, SO_2, CO and NO_x caused the most air pollution problems and there was frequent occurrence of sulphurous smog. Recently, air quality has improved a lot, but the annual mean tropospheric ozone concentrations are still high (in context with air pollution caused by traffic).

Furthermore, the third part of Chapter 3 deals with projections of the air temperature and precipitation in Essen for the near (2041–2050) and far (2091–2100) future in comparison with the current situation (the decade from 1991 to 2000) according to four climate change models. The results indicate clear trends. The temperature is forecasted to rise by 1.6 to 2.9 K from the near to the far future, which seems to be a moderate change, but could lead to significant increases of the extreme values and thermal stress (especially in summer times). According to the calculations 9 percent annual precipitation increase is expected by for the near and 4 percent for the far future.

In the longest chapter of the book (Chapter 4, 120 pages) a very detailed analysis of a one-year-long dataset (measured between 2012 and 2013) is presented in two main sections. The first section deals with the general assessment of the data, while the second discusses selected aspects of the urban climate (including urban heat island, urban moisture excess, turbulent heat flux and carbon dioxide flux density).

The climatic overview shows that the characteristics (such as global radiation, radiation balance, temperature precipitation, precipitation, and air quality) follow a "classic" structure. UHI and the thermal stress are particularly important data for researches on the effects of climate change. In the chosen year, the maximum UHI is nearly 6 K (in Szeged, Hungary, the highest value measured is more than 8 K). The extent of this difference is similar, thus, the observations and data analysis made in Essen and described in detail in this chapter could be interesting for researchers studying Hungarian cities, especially those with a subject area located in Western Hungary. Because of the heterogeneous topography of Essen, the spatial distribution of the UHI is also not homogenous. It becomes less pronounced from the city centre to the suburb, but is interrupted by smaller cooler areas (parks, gardens). In Chapter 4.2.3 there is an interesting analysis about the "Urban moisture excess" (UME), which is particularly significant in Essen. This might be for a variety of reasons, for example (i) local precipitation events, (ii) differences between the times when changes in vapour pressure, which are caused by advection, started at the different stations, or (iii) the impact of temperature inversion at measurement stations (located at different elevations).

Chapter 4 also contains a microclimatic (ENVI-met) simulation for a city area that was earlier used as a supermarket site, to show the effect of land use changes, and to optimise the climatic conditions of this location. Such studies provide very useful data for the development of climate-conscious urban planning methodology, to locate thermally sensitive areas and improve the thermal comfort (also in Hungary).

Not only is the dataset interesting, the obtained results are also compared with other national and international studies in Chapter 5. Thus, a solid analysis in the field of meteorological parameters and human comfort is presented here. The urban climatic features of Essen are compared with other German and European cities, providing informative datasets for professionals.

Finally, Chapter 6 deals with the methods used for the collection and the analysis of the data recorded at stationary and mobile measurements. Useful tips and professional advices are presented especially for data processing (data gaps, measurements set-up, data quality control, etc.) and the widely used eddy covariance method.

The book contains 120 figures and 40 tables. Besides shedding light on the most important principles, these informative presentations can also be used for educational purposes. Because of this, the way of the presentation of the data collection and analysis methods is even more important. The book is published as a two-language edition helping to generate wider international interest.

This work can be most useful to everyone who is interested in urban climatology due to professional reasons (meteorologists, climatologists, geographers, environmental scientists, architects, and urban planners), university students who just started to learn about this scientific discipline as well as decision-makers who would like to learn more deeply about the climatic problems and phenomena arising especially in cities.

Ágnes Gulyás[1]

[1] University of Szeged, Szeged.
E-mail: agulyas@geo.u-szeged.hu

REFERENCES

Dütemeyer, D., Barlag, A.-B., Kuttler, W. and Axt-Kittner, U. 2013. Measures against heat stress in the city of Gelsenkirchen, Germany. *Die Erde* 144. 181–201.

Melkonyan, A. and Kuttler, W. 2012. Long-term analysis of NO, NO_2 and O_3 concentrations in North Rhine-Westphalia, Germany. *Atmospheric Environment* 60. 316–326.

Müller, N. 2013. Stadtklimatische *Adaptationsmassnahmen in Oberhausen vor dem Hintergrund des globalen Klimawandels.* Essen, Essener Ökologische Schriften, Band 33. 235 p.

Wagner, P. and Kuttler, W. 2014. Biogenic and anthropogenic isoprene in the near-surface urban atmosphere – A case-study in Essen, Germany. *Science of the Total Environment* 475. 104–115.

Lenzholzer, S.: Weather in the City: How Design Shapes the Urban Climate. Rotterdam, nai010 publishers, 2015. 224 p.

The author, Sanda Lenzholzer, had two clear and conscious goals with this book, to close the gap between the area of meteorology and urban design, and to do so while reaching for a wider audience but still maintaining scientific background. The volume was written by an architect who has a hands-on knowledge on the practical considerations of the planning and construction of buildings. Her interesting aspect is that she does not consider the weather as a stress factor on built structures but as a stress factor on the people living in and around the buildings. The work was previously published in Dutch, and in its time, it gained a lot of media attention. Later on, the author was persuaded into rewriting it for an international audience in English, resulting in this volume. Judging by the contents, it was a worthy decision.

Most books on urban climate and weather have a special topic regarding extreme weather events, e.g. storm water management or heatwaves. One can also find works about specific technologies such as the green roofs, or using renewable energy technologies in buildings. Some other studies are about mitigation of, or adaptation to, climate change or about the vulnerability of city systems and residents to climate change. However, a collection of weather effects on cities and urban neighbourhoods is lacking, especially the one understandable for people outside the scientific community. This book is a perfect choice for all, including policymakers, who wish to understand the need for urban meteorology and conscious urban planning. The volume is easy to read, but at the same time, it requires some natural scientific interest.

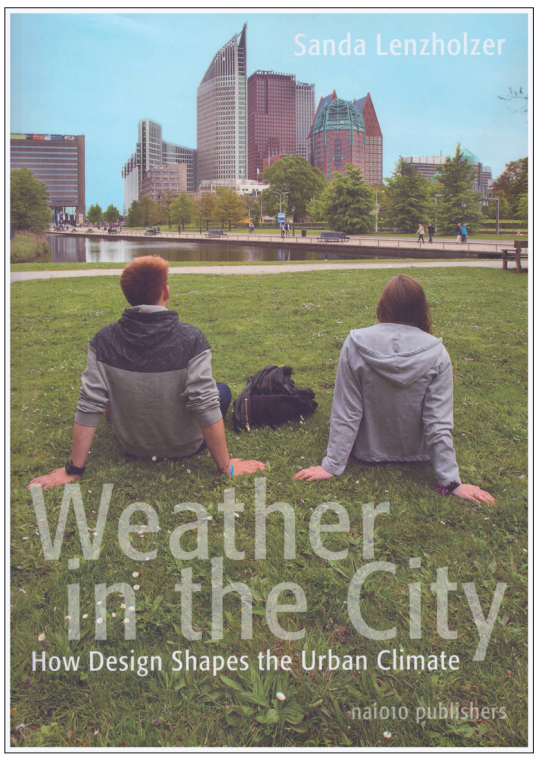

The focus of the book goes from large-scale to micro-scale. It has to be noted that the features included in the volume pertain mostly to cities with temperate climate. The first chapter is a general introduction to how we experience the physical and psychological factors of urban microclimate. Of all the physical factors, special emphasis is put on the role of temperature and wind. Though other factors are noted as well, the clearly important effects of solar radiation, relative humidity and ventilation are the key issues throughout the book. In the first chapter, where the impact of heat stress and wind nuisance on residents and on their activities is considered, we get a glimpse of the mind of an architect.

The second chapter breaks down into units that present each factor determining the urban climate from a more scientific point of view. The radiation effect is not only shown as a heat source but also as how the altitude angle of the sun affects incoming radiation and shadowing. Also from an architectural perspective, the thermal properties (reflection, heat storage and conductivity) of building materials are introduced. Naturally, from radiation the author proceeds to temperature and to the urban heat island effect, but does not go into details about the latter, since that is the main target in most studies. These issues are followed by the description of the wind effect. This is a more detailed part of the chapter and contains a lot of interesting findings based on measurements and modelling. Perhaps the most interesting topic is, from at least a meteorologist's point of view, the formation of typical wind patterns in the urban environment. The author shows how the direction, height and width ratio of a slab-like building affects wind direction and speed, and how they create wind tunnels, downwashes and windbreaks around the buildings, which have a great effect on pedestrians and on their day-to-day behaviour. Especially in this part of the book, the figures are most helpful. Since the phrasing aims for a wide readership, the author omits some physical explanations, but the figures can be further discussed, e.g. in university classes with background knowledge on fluid dynamics.

This chapter also discusses the perception of buildings from a thermal comfort view as well.

The third chapter tackles the question of mapping and categorisation methods of physical properties of a city, from a microclimate forming perspective, e.g. heat emission or wind nuisance. By creating such maps, urban climate related problematic areas can be identified in a city. One presented method is the determination of different 'climatope' areas – urban areas with typical microclimatic characteristics (e.g. parks, garden cities, and commercial districts). The other method is the creation of urban maps based on in-situ and satellite measurements.

The shortest chapter of the book (Chapter 4) introduces general methods that can be implemented in city planning in order to reduce the adverse effect of cities on weather. It shows general methods to reduce heat stress, creating ventilation between and within districts, and their possible implementation in planning practices.

The fifth chapter is about mapping the microclimate at a building scale. Analyses of physical microclimate experience are introduced using shadow simulations, educated guesses about wind patterns, wind tunnel tests, computational fluid dynamic simulations and combined versions of observation and simulations. In addition, the method of mapping the psychological aspects of microclimate experience based on interviews and the observation of the behaviour of residents is presented.

The sixth chapter embraces half of the content of the entire volume, it is also the most practical part, containing information on special urban designs. These range from different techniques for shadowing through building materials to the positioning of buildings. In order to avoid a simple enumeration, these architectural designs are grouped along their capacity to influence sun and shade, reflection, emissivity and heat conductivity, and evaporation, to slow or avoid wind, to improve ventilation, to protect against precipitation and to consider psychological aspects of microclimate experience. For each design the author provides general description and refers to issues of effectiveness, advantages and disadvantages, construction problems, costs and maintenance fees. The general description explains the theoretical background and purpose of each design, and employs informative photographs or schemes. The description of the effectiveness, advantages and disadvantages of a given design is usually short but straightforward and critical. Cost estimates are only approximate ones, as the market value depends on the availability of a construction material and on general economic conditions. At the end of the book, a table summarises the goals and target location of each architectural design.

The topics, illustrations and descriptions make one wonder about their own urban environment. After reading the book, I often find myself looking at buildings from a climate responsive design point of view and I can even recognise the drawbacks of certain architectural designs, though I have no such background. One can also use the design examples to improve the comfort of their own home.

The book itself has an up-to-date look, with a paperback cover. The high quality figures are both informative and simple, not overpowered by design. The figures are understandable for the general audience, but they can be employed even in higher education. Photographs are mostly real life illustrations. Interestingly, the pages are colour coded based on which climatic factors they mostly concern, what can help the readers in finding what they are looking for. Since all the topics in the book are relevant to temperate climates, every aspect is valid and can be used in the Central European region, from the theoretical background to the architectural designs. The price of the book also indicates that the aim is not to provide a comprehensive, physical equation based, urban planning content, but to reach a wider, even non-academic audience. At a mere price of 30€ the book is a bargain for all interested readers.

Hajnalka Breuer[1]

[1] Eötvös Loránd University, Budapest.
E-mail: bhajni@nimbus.elte.hu

Johnson, C., Toly, N. and Schroeder, H. (eds.): The Urban Climate Challenge: Rethinking the Role of Cities in the Global Climate Regime (Cities and Global Governance). London–New York, Routledge, 2015. 258 p.

Urbanisation is a hot topic: the urban population has already exceeded the world's rural population for the first time in our history, and the number and ratio of people living in cities are projected to increase further. This growth is mostly expected to occur in the developing world. The increase of urban population is accompanied with the increasing demand for clean air, water, land, and other essential services. As cities are major emitters of greenhouse gases (GHGs), mitigation, adaptation, and sustainability of cities have also become pressing global priorities.

The volume is built up from five parts and includes 12 chapters in total, bringing together articles written by researchers working on climate change, sustainability, global governance, and political science. The case studies were carried out with the contribution of acknowledged local experts from North America, Latin America and India. Chapter 9 and 11 are freely available as Open Access PDF from the publisher. The book is part of the current Routledge series 'Cities and Global Governance', launched in 2014, which makes an attempt to describe the role and influence of the city in global governance.

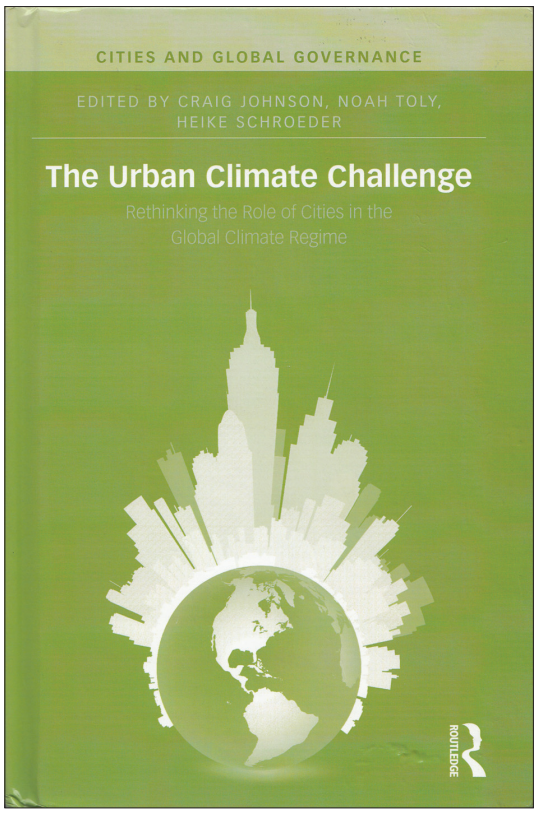

The book focuses on the following questions from theoretical, geographical, and political perspectives: How are cities incorporating climate change into urban planning and policy? What is the impact of international climate change norms on urban and national climate policies? How cities and urban networks are positioned in global climate governance politics? What are the implications for the study of international relations and global climate governance?

Part 1 explores the theoretical dimensions of urban and global climate governance Chapter 1 serves as an introduction to the book, written by the editors. They formulate the importance of the urban climate challenge, review recent state of the role of cities in climate governance, then guide the reader through the content of the book.

Saskia Sassen argues in Chapter 2 for bringing cities into the global climate network. Even though global governance regimes as Kyoto Protocol or the United Nations Framework Convention on Climate Change do not include cities, they are on the stage – as goals on this scale are more easily achievable than on the global scale. Cities are part of the problem, but can be part of the solution, too, as they can set more ambitious goals than national governments due to their practical engagement. The author sketches the strategy to maximise urban capacities, use science and technology to transform negative links into positive ones between cities and biosphere, and implement environmental measures that engage the legal system and profit logics to achieve advances towards environmental sustainability.

Chapter 3 focuses on cities as systems, and articulates why it can be misleading to build cities from scratch instead of re-thinking our existing systems. In her opinion, a paradigm shift is needed, a transition from 'open' to 'closed' resource flows, together with an other from 'closed' to 'open' urban space governance. The chapter introduces interactions in cities as complex adaptive systems, and discusses what happens if the equilibrium between production and consumption is disturbed. After presenting the complexity of the city, two structures of sets, the 'tree' and the 'semi-lattice' are shown, and the disadvantages of tree-like structures in urban systems are discussed. The difference between the two is in the number and position of connections. In the tree structure no overlap occurs, while the semi-lattice represents a more complex, ambiguous

structure, which is more natural, and thought to be more resistant for harmful events. Therefore, in semi-lattice structures there are much more connections between people, and between different parts of the city as well. Consequently, the amount and size of isolated neighbourhoods, which exist independently from their surroundings and where people live, work and shop in a somewhat artificial and closed circle, is much smaller. It is a well-explained and interesting chapter even for the layperson, and makes the reader think about sustainability of cities and relevance of the ready-made eco-city gigaprojects.

Part 2 looks at cities as parts of international networks. Chapter 4 describes the history and improvement in city-climate governance since the early 1990s, the first and second wave of transnational city networks, like ICLEI (International Council for Local Environmental Initiatives) and C40 Cities Climate Leadership Group. The latter is the main focus of the chapter. These networks put climate change on the local agenda, try to engage the municipalities with the issue of sustainability, and held regular summits to exchange experience. The authors explain the discursive, tactical, and organizational strategies of legitimation at the cities' disposal.

Chapter 5 considers the interactions between cities and multinational companies (MNCs) from the climate governance perspective. As cities are competing to become the most eco-friendly, sustainable, climate proof etc., but sometimes lack knowledge how to achieve that, MNCs happen to advise or assess climate policies (e.g. from creating solutions in transport to reduce carbon footprint). But they do so on a purely market-based approach. The chapter therefore critically examines the link between the two parties, and ask the question, if 'techno-fixes' will make cities more sustainable. The answer is probably no, as without questioning the way of living it just exports the pollution and emission elsewhere, since it treats the symptoms, not the causes. On the other hand, these actions can help in raising awareness, or increase efficiency, but one has to be careful to set up long term, city-wide, or even global goals to achieve a climate friendly city and sustainable lifestyle for its citizens.

Part 3 turns to the national level, comparing the ways in which interactions with national policy institutions have influenced governance processes and outcomes in different urban policy settings in Brazil, Canada, India and the USA.

Chapter 6 provides the example of São Paulo's efforts to reduce GHG emissions, adapt and mitigate climate change since 2005. Transnational activity was key to introduce the issue of climate change at the local level (which made São Paulo one of the first cities in the world to address climate change), but lost its importance at the implementation stage of the climate change policy due to the discrepancy between local and national level policies and interests.

Chapter 7 shows a case study for four cities in British Columbia, Canada. In the chapter the authors state that the difference between adaptation and mitigation is over-emphasised, as integrating them into a broader sustainability framework could have been the way to 'change our lens'. Instead of considering responding to climate change a stressor only, we could start to look at it as an opportunity to improve our environment. The four selected cities represent a diverse sample on the spectrum of responses and levels of integration in community climate change planning. The work reveals that an integrated sustainability approach is prevalent amongst 'leading' communities, which can help optimising efforts to reach both climate targets and local political priorities.

Chapter 8 is about adaptation in Mumbai, India, to the reoccurring flood events. It can be clearly seen that climate change governance is still an issue for the national elite, where the challenges of adaptation are exacerbated by the viewpoint on historical responsibility, by inequality, lack of resources, and of administrative origin (i.e. infrastructural deficiencies, waste management problems). Further analysis is needed therefore to foster adaptation, and help the municipality and the government to find access to international 'adaptation funds'.

Chapter 9 describes the case study of Portland, Oregon, thus, how a logging town has transformed into a successful leader in urban responses to climate change since the early 1990s. Aylett's analysis shows that significant systemic transformations (e.g. changing the focus from technocratic to holistic, replacing isolated agencies by collaborative ones, capitalising on the synergies between different groups of actors or subject areas, like emission reduction and health) in the municipal structures could make this happen, and that building internal networks within departments is an effective strategy in governance.

Part 4 offers a regional and comparative perspective on the politics of urban climate governance (p. 17.). It looks at urban responses in Latin America and East Africa. Chapter 10 and 11 show the differences and similarities between cities of the 'Global South'. Some problems they face are the fragmented institutional structures, the lack of power, budget, and human resources in defining climate issues and response strategies, and the fact that scientific information is sometimes disconnected from needs, therefore, it has little contribution to policy-making. When urban population growth and economic growth are disconnected, it creates another source of tension. However, there are some success stories as well, as some of these cities are acting and has a willingness to act to respond climate change.

The final section concludes with a chapter from the editors to highlight the central topics of the book and identifies the direction for future research. At the end of the book one can find the biography of

its authors, and an index which makes it easier to look for definitions or concepts covered inside. The importance of the book is emphasised by the fact that although it was released only a bit more than a year ago, it is already cited in the literature. The chain of chapters appearing in the volume gives the reader a wide spectrum of climate governance issues. Some main ideas are repeated in the introductory part of different chapters, with different focal points and slightly different opinions, however, as they could stand as independent papers, it is not distracting at this level.

After an overall assessment the book discusses the current state of climate policy around the world, which helps the readers put into context their own experiences, and helps to avoid administrative and political mistakes or failures (including never-realised plans and disintegrated institutional systems) already explained in the literature. The diversity of the displayed cities helps to understand both the different and common challenges they are facing with. This makes it a useful reading for scholars from Central and Eastern Europe despite the fact that no European example is discussed in the volume. The book will be of interest to scholars and practitioners of urban climate policy, global environmental governance and climate change. Adaptation, mitigation and sustainability issues are present in the urban climate change literature. This volume puts them in a different context and shows these topics from a political and social science perspective, in the practical chapters using mostly the interview method. I found it interesting to see, how the results of science can, or in some cases cannot, get incorporated into the decision-making processes.

The book is written in meticulous scientific language. At the end of each chapter one can find the notes and bibliography, which helps the reader to navigate through the related literature. It is accessible for a broad public, as not only the hardcover, but an electronic version is available for a moderate price.

Ildikó Pieczka[1]

[1] Eötvös Loránd University, Budapest.
E-mail: pieczka@nimbus.elte.hu

Solarz, M.W.: The Language of Global Development. A misleading geography. London–New York, Routledge, 2014. 181 p.

In the last few decades an intensive scientific discourse has emerged about the meaning, notion and measuring of the process of development. The term itself is rather problematic to define, and there are many theoretical questions related to studying development that need deeper knowledge to be deconstructed. One of them focuses on the various spatial terms used by scientists and politicians to describe and divide the world according to the social, cultural and economic differences between countries. No doubt that these topics are considered very relevant nowadays.

We are living in a world with huge and, in some sense, even growing inequalities, where powerful spatial metaphors like developing and developed countries, North and South, First, Second and Third World are used to describe these differences and the spatial pattern of inequalities. As Alberto Vanolo mentioned in his analysis on geographical representations of the world system (2010), these terms play a fundamental role in shaping our knowledge and building our personal imageries. Paraphrasing the language of J. Baudrillard (1983), these 'hyper-realities' (representations) are often more determining than 'hard facts' in influencing our actions. Some use these terms as synonyms, however, not bearing in mind that they comprise different theories and have been embedded in the discourse on development due to various historical events and in different political contexts. That is why the subtitle of the book is very suggestive and signs the existence of debates about world development and its interpretations. To go further, illustrating these issues on world maps with a mass of labels often results in different explanations.

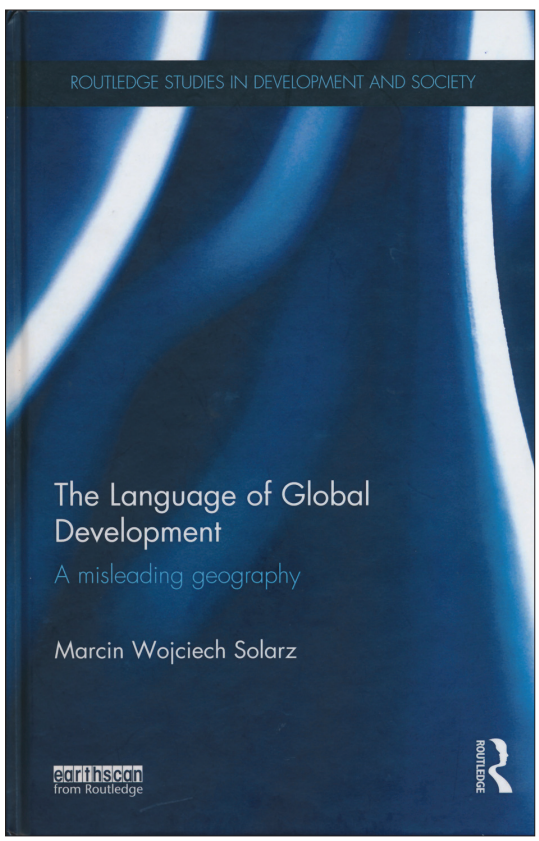

As Solarz's book clearly shows, the practice of how to classify and label the regions of the world is complex, difficult and challenging, and has been changing over time. The author who is associate professor at the Faculty of Geography and Regional Studies at the University of Warsaw, clearly, coherently and critically looks at the origins and meanings of the different terms and notions that have surrounded the global development discourse over the past few decades. The book consists of five main chapters, where the first four are about the roots and explanations of the different spatial terminologies discussed above.

Chapter 1 reviews the main discourses about the origins of the main concepts on the global divisions of development. Furthermore, it follows a chronological line from the early historical periods to the latest century and its 'Big Bang' (the author's words) in the terminology of spatial development. Yet, this chapter differs from the following ones, since it mainly focuses on differences of development in the world in an historical perspective rather than the genealogy of the terms used to label various countries and country groups. Solarz traces back the history of world development to the Palaeolithic Age, where the control of fire "was the first real, substantive global divide in terms of differences in development levels" (p. 6.). In the author's interpretation there were two universal warps that determined world history, thus, the global development of society. These were the Agricultural and the Industrial Revolutions. But he also emphasises that the early divisions of development resulted in atomised, local 'nano-worlds' and a fragmented world community, the exact locations of which in the world map we have no precise knowledge about. Still in the first chapter Solarz

discusses the changing developmental divisions from the Industrial Revolution to nowadays. At first he refers to the GDP estimates of Angus Maddison to demonstrate how the developed and underdeveloped parts of the world have changed over the past centuries.

Another important issue is to compare through maps how historically and recently used terms and concepts have divided the world, and to what extent they correspond to each other. While soon after the Industrial Revolution the dynamics of industrialisation as process marked the centres of development, then divisions were not identical with contemporary ones. Despite the socio-economic differences in the nineteenth century, some scholars, mostly with a postcolonial viewpoint, link the process of underdevelopment to the process of colonisation, arguing that colonial dependence has negatively influenced the development of these areas.

These theories had much influence on the development discourse, which they dominated through the 1960s and 1970s. Still in the first chapter Solarz discusses the main historical events of the twentieth century that have shaped the classification and labelling of the countries of the world. The end of World War II, the rise and spread of communism, the rivalry between the USA and the Soviet Union, and the emergence of new independent countries led to new classifications of the world system. (Solarz calls this phenomenon 'the terminological Big Bang', p. 50.) However, it was never unambiguous how to attribute the countries to various groups. The Second World, for example, which the author gives an extensive portrayal of, was rather a political than a socio-economic category from the very beginning. While it was a part of the tripartite division of the world system, it kept its political character. It was identified with the countries of the Eastern bloc and was never referred to as a less developed category than the First World. (As Solarz puts it: "the communist world also wanted to be regarded as a highly developed community […]" p. 37.) Later on, as the notion of development has become globally problematised, and the meaning of development has changed, many international organisations, such as the IMF, World Bank and UNDP, prepared their own divisions based on different criteria.

The longest part of Solarz's book (Chapter 2 and 3) is about the origins and meanings of the 'Third World', and it presents a critical debate on the concept. Since its introduction by Alfred Sauvy in 1952, the explanation of the term has not been unproblematic. At the beginning it was considered a political label referring to the non-aligned countries during the Cold War rivalry between the USA and the Soviet Union. ('Third World' was, thus, a synonym for 'third force' or 'third way' based on the notion of the 'third estate' in the French Revolution). To demonstrate the complexity of variable meanings, Solarz argues in the second chapter that the term appeared in literature and journalism at the end of the nineteenth century with a completely different meaning from those used after World War II. The underlying concept and the term itself, however, were centrepiece of keen scientific debates, especially in the 1960s and 1970s. For the category 'Third World' started to be used in another way associated with the 'underdeveloped' or 'backward' world. Solarz discusses clearly and in great detail how the concept has changed over time, and what critiques it evoked almost immediately after its birth.

Some critics argued for rejecting the concept itself, because in their view it suggested the existence of a single, unique and cohesive World, while ignoring its diverse character and content. Thus, the relevance of the 'Third World' as a large aggregate was put into question. Other scholars suggest, however, that if we wanted to reject the term because of its diversity, than, as the author mentions, we would also have to remove all other generalising concepts from the language of geography, saying that "terms such as 'Third World', as every general category, will always distort and simplify reality" (p. 91.).

As mentioned before, some scholars connect the term to the process of decolonisation, putting equal sign between the former colonies and the colonial legacy on the one hand, and the Third World on the other hand. But this is misleading if we think on Thailand or Ethiopia, where colonisation was never complete, or on Canada and the United States, which were colonies at one stage or another in their history. As the author underscores in a separate subchapter ("Is the term still valid and useful?"), another important and relevant problem with the concept is that according to many, the end of the Cold War has made the term irrelevant, since with the collapse of the Soviet Union and the fall of socialism the former Second World does not exist anymore. While this kind of argument for the disappearance of the term could be valid, Solarz argues that the rumours about the end of the concept are exaggerated. In the titles of journals and books and the names of institutions one can still find the expression 'Third World'. But the fact is that nowadays the term is mainly analogous with the underdeveloped, backward, and least developed countries. Therefore, when we are talking about it, we usually join it to socio-economic characteristics.

The last two chapters of the book contain an historical and critical overview of the 'challengers' ('developing countries' and 'North–South divide') of the former, often-used categories. Solarz argues that 'developing countries' seemed to be a positive category suggesting progress and improving situation, but in fact these countries showed the lowest level of development over time. Another explanation for the emergence of the term 'developing' was given by Gunnar Myrdal, the Swedish Nobel laureate economist and

sociologist, whose work was connected mainly to economic and social theory. According to him, the shift to 'developing' from 'underdeveloped' was an outcome of 'diplomacy by language'. This means that 'underdevelopment' is not a flattering description of the situation of poor countries, while the term 'developing' is much more positive and politically feasible. Besides, the concept of 'developing countries' was connected to certain trends in economic thought throughout the decades. In the lens of modernisation theory, which interpreted development as a linear, irreversible process universal for all countries of the world, developing countries must follow the path of developed countries. In other words, developed countries were claimed responsible for navigating and controlling developing ones. In this theory, developing countries were linked to the concept of 'underdevelopment', which neglected the optimism radiated by the term 'developing'.

Later on, in the early 1980s the concept of a North–South opposition has emerged due to the former German Chancellor Willy Brandt. Although this categorisation had more controversies than others do, in the last 30 years "it has been reproduced in numerous publications … with only minor changes, if any", as Solarz puts it while discussing the usefulness and popularity of the term. Although terminological innovation has shown less dynamics since the 1980s than before, new categories and terms have still appeared to replace the already existing notion of the three 'worlds'. Labels like 'emerging markets', 'newly industrialised countries', 'Fourth' or 'Fifth World' and 'BRIC countries' are still in use nowadays, and according to Solarz this present situation will continue in the foreseeable future. There will always be supporters and opponents, terms will be used and criticised, and new categories will appear. As inequalities still exist between the countries of the globe, geography will always need generalised labels to describe them. But in my view, we need to use these terms carefully, we need to look behind them and explore their theoretical and historical backgrounds, and see them in a global context.

That is why Marcin W. Solarz's treatise is very impressive and suggestive. It gives a comprehensive and all-embracing overview of the main questions concerning global disparities of development during the last centuries, while discussing in detail the historical and conceptual framework of much used terminologies. The book is illustrated with several maps, which help the reader localise the mentioned 'worlds' and follow the main concepts and how they again and again regionalised the world in new ways. In my opinion, this work is addressed to and definitely required by those interested in the geographies and economies of global development.

For those who are interested in the aforementioned issues, Solarz's book might seem different to contemporary geographical works from Anglophone countries, since it tries to capture rather the practical than the theoretical questions and problems of global development. Furthermore, the volume examines these issues from an East Central European point of view, also referring to many authors from this region. Thus, it provides much space for relevant concepts and views barely present in international literature on the topic. It can serve as a useful tool in university teaching in all subjects related to these problems. It can help students understand how we regionalise the world, why we are doing it the way we are, why we use these labels, and how these concepts are related to development theories. With the multilingual and multidisciplinary bibliography one can find the most important and relevant sources on global development and spatial terminology. Students and teachers in the fields of geography, development studies, politics or history can be the main public of this book, but with its easily comprehensible content and readability it is offered for everyone interested in these issues.

Máté Farkas[1]

REFERENCES

Baudrillard, J. 1983. Simulations. New York, Semiotexte.

Vanolo, A. 2010. The border between core and periphery: Geographical representations of the world system. *Tijdschrift voor Economische en Sociale Geografie* 101. (1): 26–36.

[1] Hungarian Central Statistical Office, Budapest. E-mail: mate.farkas@ksh.hu

GUIDELINES FOR AUTHORS

Hungarian Geographical Bulletin (formerly Földrajzi Értesítő) is a double-blind peer-reviewed English-language quarterly journal publishing open access **original scientific works** in the field of physical and human geography, methodology and analyses in geography, GIS, environmental assessment, regional studies, geographical research in Hungary and Central Europe. In the regular and special issues also discussion papers, chronicles and book reviews can be published.

Manuscript requirements

We accept most word processing formats, but MSWord files are preferred. Submissions should be single spaced and use 12pt font, and any track changes must be removed. The paper completed with abstract, keywords, text, figures, tables and references should not exceed **6000 words**.

The Cover Page of the article should only include the following information: title; author names; a footnote with the affiliations, postal and e-mail addresses of the authors in the correct order; a list of 4 to 8 keywords; any acknowledgements.

An abstract of up to **300 words** must be included in the submitted manuscript. It should state briefly and clearly the purpose and setting of the research, methodological backgrounds, the principal findings and major conclusions.

Figures and tables

Submit each illustration as a separate file. Figures and tables should be referred in the text. Numbering of figures and tables should be consecutively in accordance with their appearance in the text. Lettering and sizing of original artwork should be uniform. Convert the images to TIF or JPEG with an appropriate resolution: for colour or grayscale photographs or vector drawings (min. 300 dpi); bitmapped line drawings (min.1000 dpi); combinations bitmapped line/photographs (min. 500 dpi). Please do not supply files that are optimized for screen use (e.g., GIF, BMP, PICT, WPG). Size the illustrations close to the desired dimensions of the printed version. Be sparing in the use of tables and ensure that the data presented in tables do not duplicate results described elsewhere in the article.

REFERENCES

Please ensure that every reference cited in the text is also present in the reference list (and vice versa).

Reference style

Text: In the text refer to the author's name (small capitals with initials) and year of publication. References should be arranged first chronologically and then further sorted alphabetically if necessary. More than one reference from the same author(s) in the same year must be identified by the letters 'a', 'b', placed after the year of publication.
Examples: (Ridgewell, A.J. 2002; Maher, B.A. *et al.* 2010) or Ridgewell, A.J. (2002); Maher, B.A. *et al.* (2010)

Journal papers:
Aagaard, T., Orford, J. and Murray, A.S. 2007. Environmental controls on coastal dune formation; Skallingen Spit, Denmark. *Geomorphology* 83. (1): 29–47.

Books:
Pye, K. 1987. *Aeolian Dust and Dust Deposits.* Academic Press, London, 334 p.

Book chapters:
Kovács, J. and Varga, Gy. 2013. Loess. In: Bobrowsky, P. (Ed.) *Encyclopedia of Natural Hazards.* Springer, Frankfurt, 637–638.

Submission

Submission to this journal occurs online. Please submit your article via geobull@mtafki.hu.

All correspondence, including notification of the Editor's decision and requests for revision, takes place by e-mail.